# CARDIAC LIPOPROTEIN LIPASE FUNCTION FOLLOWING DIABETES IS REGULATED BY CARDIOMYOCYTES AND ENDOTHELIAL CELLS

by

Ying Wang

M.Sc., Wuhan University, China, 2008

A THESIS SUBMITTED IN PARTIAL FULFILLMENT OF

THE REQUIREMENTS FOR THE DEGREE OF

DOCTOR OF PHILOSOPHY

in

THE FACULTY OF GRADUATE AND POSTDOCTORAL STUDIES

(Pharmaceutical Sciences)

THE UNIVERSITY OF BRITISH COLUMBIA

(Vancouver)

March 2014

## Abstract

In diabetes, when glucose consumption is restricted, the heart adapts to use fatty acid (FA) exclusively. The majority of FA provided to the heart comes from breakdown of circulating triglyceride, a process catalyzed by lipoprotein lipase (LPL) located at the vascular lumen. Transfer of LPL from cardiomyocytes to the coronary lumen requires liberation of LPL from the myocyte surface heparan sulfate proteoglycans (HSPGs) with subsequent replenishment of this reservoir. We examined the contribution of coronary endothelial cells (EC) and cardiomyocytes towards regulation of LPL function following diabetes. To induce acute hyperglycemia, diazoxide (DZ), a selective ATP-sensitive $K^+$ channel opener was used. For chronic diabetes, streptozotocin (STZ), a β-cell specific toxin was administered at doses of 55 (D55) or 100 (D100) mg/kg to generate moderate and severe diabetes, respectively. Cardiac LPL processing into active dimers and breakdown at the vascular lumen was investigated. Following acute hyperglycemia and moderate diabetes, more LPL is processed into an active dimeric form, which involves the endoplasmic reticulum chaperone calnexin in cardiomyocytes. Severe diabetes results in increased conversion of LPL into inactive monomers at the vascular lumen, a process mediated by FA-induced expression of angiopoietin-like protein 4. On exposure of bovine coronary artery EC to high glucose, both latent and active heparanase were released into the medium, termed ECCM. ECCM liberated LPL from the myocyte surface, in addition to facilitating its replenishment. Of the two forms of heparanase secreted from EC in response to high glucose, active heparanase released LPL from the myocyte surface, whereas latent heparanase stimulated reloading of LPL from an intracellular pool via HSPG-mediated RhoA activation. Latent heparanase can be also taken up by cardiomyocytes, converted into active heparanase in lysosomes, and its nuclear entry

likely to modulate gene expression. Results from this study advance our understanding of how the cross-talk between EC and cardiomyocytes facilitate LPL secretion and how diabetes influences coronary LPL maturation and turnover. Pharmaceutical manipulation of these pathways could potentially provide an additional strategy to limit FA delivery to the heart, and prevent cardiomyopathy seen with chronic diabetes.

## Preface

All of the work presented in Chapter 2, 3 and 4 was conducted in Faculty of Pharmaceutical Sciences at the University of British Columbia.

Parts of these chapters have been published in the following manuscripts:

1. [**Wang Y**, Puthanveetil P, Wang F, Kim MS, Abrahani A, and Rodrigues B. Severity of diabetes governs vascular LPL by affecting enzyme dimerization and disassembly. Diabetes. 2011.] I was the first author responsible for generation of the ideal, and collecting and analyzing most of data. My supervisor Brian Rodrigues and I designed the experiment and wrote the manuscript. Puthanveetil P (Figure 7), Wang F (Figure 9*D*), Kim MS (Figure 1), and Abrahani A (Figure 3*C*) helped me in obtaining some of the data.

2. [**Wang Y**, Zhang DH, Chiu AP, Wan A, Neumaier K, Vlodavsky I and Rodrigues B. Endothelial heparanase regulates heart metabolism by stimulating lipoprotein lipase secretion from cardiomyocytes. Arterioscler Thromb Vasc Biol. 2013.] I conceived and designed the experiments, obtained most of the data, analyzed and interpreted the results, as well as wrote the major part of manuscript. Zhang DH (Figure 16), Chiu AP (Figure 18), Wan A (Figure 18), and Neumaier K (Figure 21*C*) contributed to acquiring some of the data. Vlodavsky I assisted with valuable suggestions and the preparation of highly purified latent and active heparanase. Brian Rodrigues helped with writing the manuscript.

The investigation conforms to the guide for the care and use of laboratory animals published by the US National Institutes of Health and the University of British Columbia, and was approved by the Animal Care Committee in the University of British Columbia (Certificate No. A13-0098).

# Table of Contents

## List of Tables

## List of Figures

## List of Abbreviations

| | |
|---|---|
| AMPK | AMP-activated protein kinase |
| Angptl-4 | Angiopoietin-like protein 4 |
| bCAECs | Bovine coronary endothelial cells |
| CHX | Cyclohexamide |
| CPT-1 | Carnitine palmitoyltransferase |
| DAPI | 4,6-Diamidino-2-phenylindole |
| DZ | Diazoxide |
| EC | Endothelial cells |
| ECCM | Endothelial cell conditioned medium |
| EGFR | Epidermal growth factor receptor |
| ER | Endoplasmic reticulum |
| ERK-1 | Extracellular signal-regulated kinase |
| FA | Fatty acid |
| GPI | Glycosylphosphatidyl inositol |
| GPIHBP1 | Glycosylphosphatidylinositol-anchored high density lipoprotein-binding protein 1 |
| HAT | Histone acetyltransferase |
| HG | High glucose |
| HS | Heparan sulfate |
| HSPGs | Heparan sulfate proteoglycans |
| IRE-1 | Inositol-requiring kinase 1 |
| LMF1 | Lipase maturation factor 1 |
| LPL | Lipoprotein lipase |
| MMP-9 | Matrix metalloproteinase 9 |
| NEFA | Nonesterified fatty acid |
| PA | Palmitic acid |
| PDH | Pyruvate dehydrogenase |
| PFK | Phosphofructokinase |
| PHPLA | Post-heparin plasma LPL activity |
| PKC | Protein kinase C |
| PKD | Protein kinase D |
| PPAR | Peroxisome proliferator-activated receptor |
| RAOEC | Rat aortic endothelial cells |
| ROS | Reactive oxygen species |
| SREBP-1 | Sterol regulatory element binding protein-1 |
| STZ | Streptozotocin |
| T1D | Type 1 diabetes |
| T2D | Type 2 diabetes |
| TCA | Trichloroacetic acid |
| TG | Triglyceride |
| UCP3 | Uncoupling protein 3 |
| UPR | Unfolded protein response |
| VLDL | Very-low-density lipoprotein |

## Acknowledgements

To begin with I would like to express my sincere gratitude to Dr. Brian Rodrigues, without whom I would have never been "whipped" into such a shape. It was Dr. Rodrigues who gave me the opportunity to taste the flavor of real science and generously teaches me everything he knows. I am thankful for his dedication to the students, the time he spent with us. His support has accompanied me throughout the past four years. Every word in this thesis reflects his contribution to my career.

I would definitely like to thank my committee members Dr. Roger Brownsey, Dr. James Johnson, Dr. John Hill, and chair Dr. Urs Hafeli. Your intelligence and experience have broadened my view and strongly encouraged me to pursue perfection. Those valuable suggestions you provided means a lot to me. I give my special thanks to Dr. Israel Vlodavsky who kindly shared his resources and expertise with us.

During my work in the lab, there are always been people guiding me on the way. I would like to thank Mr. Ashraf Abrahami, Ms. Bahira Hussein, Dr. Minsuk Kim, Dr. Fang Wang, and Dr. Prasanth Puthanveetil for training me with technical skills and inspiring me with good ideals. Much appreciation goes to Dahai Zhang, Amy Chiu, Katharina Neumaier, Andrea Wan, as well as Fulong Wang and Nathaniel Lal for every small little things you helped. I am also thankful to our secretary Rachel Wu for always being there.

Thanks for all my friends who pushed me to the top when I was down.

I would like to express my thanks to CDA for their financial support during my graduate program.

## Dedication

*To my family and friends who understand and support me without asking for anything. Sometimes it is just enough to have you around.*

# Chapter 1: Introduction

## 1.1 Diabetic cardiomyopathy

Diabetes is a global disease that currently affects 371 million of people worldwide. The prevalence of this disease is estimated to rise to 552 million by 2030[1]. According to the International Diabetes Federation Atlas, diabetes mellitus caused 4.8 million deaths in 2012. Approximately 6.8% of Canadians were diagnosed with diabetes, contributing to nearly 30% of the total deaths in the country from 2008 to 2009[2]. For both Type 1 diabetic (T1D) and Type 2 diabetic (T2D) patients, cardiovascular disease, predominantly associated with atherosclerosis, is the most prevalent cause of this mortality[3]. Nevertheless, deterioration of cardiac function can also occur in the absence of coronary heart disease, termed "diabetic cardiomyopathy". Initially, diabetic cardiomyopathy is characterized by prolonged diastolic relaxation time and increased stiffness of the left ventricular wall, leading to subsequent systolic dysfunction and heart failure. Myocardial fibrosis, small vessel disease, cardiac autonomic dysfunction, and metabolic disturbances have all been implicated in the pathogenesis of diabetic cardiomyopathy[4].

With metabolism, the heart is capable of using a broad spectrum of substrates, including fatty acids (FA), glucose, and to a lesser extent lactate and ketone bodies[5]. Normally, hearts derive about 70% of their energy from FA metabolism[6], with glucose (20%) and lactate (10%) making up the remaining part. After diabetes, several major factors restrict glucose utilization in the heart. These include a lack of glucose transporters at the sarcolemmal membrane, and inhibition of key enzymes that control glycolysis (eg., phosphofructokinase, PFK) and glucose oxidation (eg., pyruvate dehydrogenase complex, PDH) in the mitochondria[4]. As a result, hearts require more FA to generate ATP. This could be achieved

by switching on its FA delivery machinery. Compared to albumin-bound free FA, triglyceride (TG)-rich lipoproteins are the preferred source of FA[7, 8]. This would require hydrolysis of plasma TG to release free FA at the luminal side of the endothelium, a reaction catalyzed by lipoprotein lipase (LPL)[9]. Following 2 weeks of streptozotocin (STZ) injection, LPL activity is significantly higher at the coronary lumen of diabetic rats compared to control, which increased the rate of TG-lipoprotein breakdown[10]. Interestingly, LPL activity can be turned on within 4 h after diabetes[11], suggesting a prominent role in rapidly modulating heart metabolism. The adaption to use FA is beneficial to the heart in the short term as energy production is maintained in the presence of impaired glucose oxidation. However, chronic reliance on FA metabolism is detrimental to heart function. As the cardiomyocyte has a limited capacity for storing FA, the substrate influx has to tightly match its oxidation in the mitochondria to generate ATP. Beta-oxidation is the primary pathway for FA catabolism in the heart[12]. It generates reducing equivalents to create an electrochemical gradient across the mitochondrial inner membrane that drives ATP synthesis, a process called oxidative phosphorylation. However, reactive oxygen species (ROS) are also produced when electrons leak out of the oxidative phosphorylation process. In *db/db* mice hearts, oxidative phosphorylation capacity failed to increase coordinately with elevated fatty acid and beta-oxidation, which leads to excess ROS generation[13]. Cardiac contractile function is disturbed as ROS affect calcium homeostasis by damaging ion channels[14]. Excess ROS also destabilize mitochondria membranes, triggering cell death[15]. Increased FA influx that overwhelms mitochondria oxidation capacity would cause accumulation of lipid intermediates such as ceramide, diacyglycerol, and acyl-CoA, which further inhibit glucose utilization and promote cell death[16, 17]. FA are considered endogenous ligands for

peroxisome proliferator-activated receptor alpha (PPAR α) in the heart. Activation of PPAR α not only boosts gene expression of carnitine palmitoyltransferase (CPT-1) to facilitate acyl-CoA entry into the mitochondria, but also enzymes involved in beta-oxidation[18, 19]. Ironically, FA also increases uncoupling protein 3 (UCP3) expression in the heart through PPAR α[20]. By exporting free fatty acid anions from the mitochondrial, overexpression of UCP3 dissipates the electrochemical gradient across the mitochondrial membrane, thereby uncoupling beta-oxidation and ATP synthesis in STZ-induced T1D hearts [13, 21]. In T1D rat model, depressed mitochondria respiration rate was observed 4 weeks following injection of STZ[22]. Hence, chronic exposure of cardiomyocytes to FA ultimately reduces metabolic efficiency. Although not demonstrated in the heart, overexpression of LPL in skeletal muscle induced UCP3 expression in this tissue by promoting TG-derived FA intake[23], suggesting that LPL could potentially cause mitochondrial uncoupling. In heart studies, because PPAR α activation favors FA utilization, mice with cardiac-specific overexpression of PPAR α (MHC-PPAR) showed phenotype features similar to diabetic hearts[24, 25]. Strikingly, deletion of LPL reduced myocyte TG accumulation, and rescued cardiac function in these animals[26], implicating LPL in a pivotal role in diabetic cardiomyopathy.

## 1.2 Lipoprotein lipase

### 1.2.1 Gene transcription

Lipoprotein lipase (LPL) belongs to the lipase family. Its gene is located on 8p22 encoding for a 475 amino acid protein with a 27 amino acid signal peptide[27, 28]. A large number of variants have been identified in the LPL gene, and some of them are known to influence LPL function. For example, most patients with Familial Chylomicronemia

Syndrome carry homozygous or compound heterozygous mutations in LPL gene that abolish the activity of the enzyme[29]. These includes substitution of G—A at nucleotide position 680 which replaces glutamic acid for glycine at amino residue 142[30]; a missense mutation resulting in substitution of an alanine for a threonine at residue 176[31]; and mutation 207, the most prevalent LPL gene mutation among French Canadians[32]. Due to LPL deficiency, patients manifest hypertriglyceridemia and fasting chylomicronemia. LPL HindIII polymorphism is associated with risk of coronary artery disease by affecting binding site of a transcription factor to regulate LPL gene expression[33]. Gene transcription of LPL is regulated by multiple cis-acting elements in the promoter region. In humans, a TATA box at -46, a CCAAT motif that binds transcription factor NF-Y, and octamer motif interacting with Oct-1 accounts for the basal promoter activity[34, 35]. In 3T3-L1 adipocytes, cholesterol depletion stimulated LPL transcription by binding sterol regulatory element binding protein-1 (SREBP-1) to the sterol regulatory element 2 site in the LPL promoter[36], whereas estrogen suppressed promoter activity via an AP-1-like element[37]. Reduced binding of transcription factor Sp1 and Sp2 to LPL promoter is responsible for Interferon γ-mediated inhibition of LPL transcription in macrophages[38]. Tumor necrosis factor α also decreased LPL promoter activity by inhibition of NF-Y binding to the CCAAT motif[39]. The discovery of Peroxisome proliferator-activated response element in the promoter region could explain the tissue-specific gene modulation effect of PPAR activators on LPL. As PPAR γ is more restricted to adipose tissue, thiazolidinedione can induce LPL expression, but had no effect on liver[40], whereas fibrates selectively increased mRNA level of LPL in the liver by activating the predominant PPAR isoforms-PPAR α in this tissue[41]. LPL expression is also regulated at translational level. Insulin increased LPL activity in adipocytes probably by stabilizing LPL

mRNA[42]. Epinephrine inhibits LPL translation in adipocytes possibly due to activation of protein kinase A (PKA). PKA forms a complex with A kinase anchoring protein (AKAP) 121/149 and binds to the 3'-untranslated region of LPL mRNA to prevent translation[43]. Because AKAP121/149 is more abundant in white adipose tissue than in muscle and brown adipose tissue, the inhibitory effect of epinephrine is not significant in these tissues[44]. Despite the above regulation, LPL function is largely controlled in a post-translational manner.

### 1.2.2 Maturation inside the endoplasmic reticulum

Although LPL hydrolyzes TG-rich lipoproteins at the coronary lumen, it is not expressed by endothelial cells, but originates from cardiomyocytes[45]. In cardiomyocytes, as newly synthesized LPL protein enters the endoplasmic reticulum (ER), it undergoes glycosylation by attaching oligosaccharide chains to the asparagine residues (Asn43 and Asn359)[46]. At this stage, LPL is present as an inactive monomer. The oligosaccharide chains are subsequently trimmed by Glucosidase I and II, exposing a structure recognized by ER-resident chaperones calnexin/calreticulin. Association of calnexin/calreticulin with nascent LPL is part of the "quality control" for most glycosylated proteins. It allows nascent LPL folding into a proper tertiary structure qualified for dimerization[47]. This step is indispensable for LPL processing into active enzyme as folding/dimerization of human LPL in transfected sf21 cells is only promoted when calreticulin is co-expressed[48]. Using castanospermine to inhibit glucosidase-mediated trimming of the oligosaccharide chains, the interaction between LPL monomers with chaperones was hindered, thereby decreasing active LPL[49]. The two inactive monomeric LPL are then assembled noncovalently in a head-to-tail fashion to form a catalytically functional enzyme[50-52]. LPL dimerization relies on lipase maturation factor 1

(LMF1)[53, 54]. LMF1 is a five transmembrane protein localized in the ER, and its highly conserved domain DUF1222 is essential for physically interacting and maturation of LPL as well as hepatic lipase[55]. Mutations of *lmf1* that result in truncations of DUF1222 domain are responsible for combined lipase deficiency in both mice and human[56]. Patients with this disorder demonstrate decreased LPL and hepatic lipase activity with concomitant hypertriglyceridemia. Notably, only dimeric LPL is active and competent to exit the ER[47, 57].

### 1.2.3 Secretion to cardiomyocyte surface

So far, there is limited information regarding how LPL is further processed and sorted into secretion vesicles in the Golgi. Recently, protein kinase D (PKD) has emerged as a crucial factor in the formation of LPL secretion vesicles[58]. By phosphorylating phosphatidylinositol-4 kinase IIIbeta (PI4KIII-β), it activates the lipid kinase activity of PI4KIII-β to stimulate fission of vesicles from the trans-Golgi network[59]. PKD is also known to direct secretory vesicles to the plasma membrane with its partner vesicle associated membrane protein (VAMP), a soluble NSF attachment protein receptor (SNARE) localized on the vesicle membrane serves as docking proteins for exocytosis[60]. In the trans Golgi network, LPL can also be captured by SorLA (sortilin-related receptor) that would route LPL to endosomes, and ultimately lysosomes for degradation[61]. It is suggested that up to 80% of newly synthesized LPL in the adipocytes is degraded in the lysosomes instead of being secreted[62]. However, details of intracellular turn-over of this enzyme in the heart remain to be elucidated. For LPL-containing vesicles destined for secretion, they require polymerization of actin cytoskeleton to build a "bridge" from the Golgi to the plasma membrane[63]. The secreted LPL is sequestered by heparan sulfate proteoglycans (HSPGs) on the cardiomyocyte membrane. Depolymerization of the actin cytoskeleton by cytochalasin D reduced LPL

activity on the myocyte surface[63]. The Rodrigues' lab has reported an increased intracellular trafficking of LPL from Golgi to the myocyte surface after diabetes which is driven by the energy sensor AMP-activated protein kinase (AMPK)[64]. In STZ-induced T1D rats, AMPK is activated at an early stage possibly because impaired glucose utilization caused a rapid energy deficiency[65]. As a result, heat shock protein 25 (Hsp25) was phosphorylated, dissociated from actin monomers and PKC γ, leading to actin cytoskeleton polymerization and PKD-mediated vesicle formation, respectively[58]. In this way, more intracellular LPL is moved to the myocyte surface after diabetes.

### 1.2.4 Release from the cardiomyocyte surface

Myocyte surface HSPGs serve as a temporary docking site for LPL. The core proteins of HSPGs are attached to the cell surface either through a transmembrane domain in case of the syndecan family, or via glycosylphosphatidyl inositol (GPI) anchor as observed with glypican[66, 67]. The core protein is decorated with heparan sulfate (HS) side chains covalently attached to specific serine residues on the ectodomain[68]. The HS side chains are polymers of repeating disaccharides (glucurionic acid and N-acetylglucosamine) modified via deacetylation, sulfation, and epimerization, which introduces heterogeneity to the structure. These modifications also create negatively-charged residues that allow the HS to interact with multiple ligands through their heparin-binding domain, including antithrombin, fibroblast growth factor, and LPL[69-71]. In fact, LPL is bound to HSPGs on the myocyte surface through ionic interaction, which is important for maintaining LPL activity[72]. HS has been suggested to be a putative extracellular chaperone, retaining LPL activity as it translocates from synthesizing sites to the endothelium[73].

For its onward secretion towards the endothelium, cleavage of myocyte surface HSPGs is required. When endothelial cell conditioned medium (ECCM) was given to adipocytes, LPL activity was released from adipocyte surface, suggesting that factors required to cleave HSPGs arise from the endothelium[73]. Heparanase, an endoglucuronidase synthesized in the endothelial cells (EC) could be the factor mediating this cross-talk. It is synthesized in the EC as a latent 65 kDa precursor, secreted and bound to EC surface HSPGs before being internalized into lysosomes[74]. There it is cleaved into a 50 kDa active form that can digest the HS into 7~8 kDa fragments[74], oligosaccharides that are capable of carrying LPL, and preserving its bioactivity. For example, lysophosphatidylcholine-treated endothelial cell medium can release LPL activity from the adipocytes, and it has been shown that more heparanase is secreted from the basolateral than the apical side upon stimulation, suggesting its role in LPL trafficking from parenchymal cell rather than detaching LPL from the vascular lumen[73]. Secretion of heparanase from EC was also increased in the presence of high glucose, and heparanase was found infiltrated into the interstitial space between EC and cardiomyocytes in hearts from diabetic animals[75]. In addition, high glucose also upregulates heparanase gene expression in EC[76], an effect inhibited by insulin[77]. In fact, heparanase level in the plasma was directly correlated with that of blood glucose in T2D patients[78]. It is tempting to suggest that diabetes may liberate more LPL from the myocyte surface HSPGs as a result of increased heparanase secretion from EC. As these liberated LPL translocate to the coronary lumen, more FA will be delivered to the heart. In this way, EC can possibly control cardiomyocyte metabolism. Besides releasing HSPG-bound ligands from extracellular matrix and cell surface, heparanase also has other biological effects. Studies on cancer biology suggested that tumor cells might change the phenotype of surrounding cells by

"feeding" them heparanase that is capable of modulating gene transcription. Nuclear entry of active heparanase stimulated differentiation of esophageal keratinocyte by cleaving heparan sulfate in the nucleus[79]. It also reduced the nuclear content of syndecan-1, a type of HSPGs that inhibits histone acetyltransferase (HAT) activity, and hence promoted certain gene expression in CAG human myeloma cells, including vascular endothelial growth factor (VEGF) and matrix metallopepetidase 9 (MMP-9)[80]. In addition, heparanase is known to regulate gene expression by controlling histone H3 methylation patterns[81]. Whether heparanase in the heart would affect LPL gene expression remains unclear.

### 1.2.5 Translocation from cardiomyocyte towards the apical side of EC

The mechanism by which LPL is transported across the interstitial space, vascular basement membranes, and to ultimately its functional site at the vascular lumen remained a mystery for a long time. However, a deficiency in extracellular collagen XVIII, a HSPG present in vascular basement membranes decreased LPL activity at the vascular lumen in humans[82], suggesting the importance of extracellular matrix HSPGs for LPL migration. Digestion of HSPGs on the basolateral side of EC also hindered the transcytosis of LPL[83, 84]. At the apical side of EC, HSPGs were considered binding sites for LPL which also mediate the internalization and recycling of LPL inside EC[85, 86]. However, HSPGs are ubiquitously expressed in many cell types and do not bind LPL specifically. So far, no evidence has shown that genetic deletion of any type of HSPGs *in vivo* is associated with hypertriglyceridemia. On the other hand, a newly discovered molecule, glycosylphosphatidylinositol-anchored high density lipoprotein-binding protein 1 (GPIHBP1) was identified as a unique LPL receptor located on the luminal face of the capillary endothelium, docking LPL to break down triglyceride[87]. It is distributed in LPL-

expressing tissues including heart, adipose tissue, and skeletal muscle, and unlike HSPGs, it does not bind to any other member of the lipase family[88]. In addition, transcytosis of LPL across the EC requires GPIHBP1 shuttling. LPL captured by GPIHBP1 at the subendothelial space is transported in vesicles to the vascular lumen in a caveolin-1-independent manner[89, 90]. Thus, GPIHBP1 knockout mice manifest severe hypertriglyceridemia in accordance with a dramatic reduction in LPL activity at the vascular lumen[91]. The C-terminus portion, especially amino acids 403-407 (a region different from the principal heparin-binding domain) of LPL is responsible for interacting with GPIHBP1[92]. For GPIHBP1, both the amino-terminal acidic domain and the lymphocyte antigen 6 motif are important for binding and transport of LPL[93]. Mutations that disturb protein structure of these regions could lead to chylomicronemia in human[94, 95]. Expression of GPIHBP1 in EC is rapidly regulated by nutrition status and PPAR $\gamma$[96]. Notably, GPIHBP1 expression depends on factors released from parenchymal cells as primary EC lost GPIHBP1 expression after a single passage[96]. The role of GPIHBP1 in LPL function after diabetes has yet to be studied. It should be noted that GPIHBP1 can also serve as a "platform", permitting the simultaneous binding of both LPL and lipoproteins at the vascular lumen, enabling lipolysis[90].

### 1.2.6 Turnover at the vascular lumen

LPL activity is also regulated at the vascular lumen. Previously, we have shown an increase in coronary LPL activity in animals made diabetic with 55 mg/kg STZ (D55). Intriguingly, on increasing the dose to 100 mg/kg (D100), LPL activity was "turned-off"[97]. Compared to D55, D100 animals had a more profound reduction in circulating insulin which also made these animals hyperlipidemic. In this situation, FA could possibly decrease coronary LPL in multiple ways: a) FA displace LPL from its endothelial cell surface binding

sites for degradation in the liver[98], b) direct inactivation of LPL enzyme activity[99], and c) FA impair LPL vesicle trafficking to the myocyte surface through caspase-3-mediated inactivation of PKD[100]. A decade ago, two angiopoietin-like proteins, Angptl-3 and Angptl-4, drew attention as deficiency of either protein caused elevation of post-heparin plasma LPL activity (PHPLA) in transgenic mice (representing whole body LPL activity released from the vascular lumen)[101]. Both Angptl-3 and Angptl-4 are composed of a NH2-terminal coiled-coil domain and a C-terminal fibrinogen-like domain, and the coiled-coil domain is sufficient to interact and inactivate LPL[102]. Though sharing similar structures, the two angiopoietin-like proteins work in different ways. Expression of Angptl-3 is mainly restricted to the liver. Its action is possibly through promotion of LPL cleavage via proprotein convertases, leading to dissociation of LPL from both HSPGs and GPIHBP1 binding sites[103]. Its expression is driven by the liver X receptor and is mainly active in the fed state[104]. However, in humans, the level of Angptl-3 is not related to that of PHPLA and plasma triglyceride[105]. Angptl-4 is widely expressed in various tissues including white adipose tissue, liver, heart, and skeletal muscle[106]. In these cells, it forms oligomers through disulfide linkage, and after secretion, is cleaved at a canonical proprotein convertase cleavage site that separates the N- and C-terminal domain[107]. The N-terminal coiled-coil domain remains oligomerized, a feature that is essential for its stability and LPL inhibitory effect[108]. The secreted N-terminal oligomers function in the circulation, converting dimeric LPL at the vascular lumen into inactive monomers[109]. Interestingly, long chain FA, through activation of PPAR δ, increased transcription of muscle-derived Angptl-4[110]. Change in Angptl-4 expression is rapid as in adipose tissue, down-regulation of its mRNA was observed within 6 h after refeeding fasted animals, which is consistent with elevated LPL activity in this tissue[109]. *ANGPTL4* variants

E40K and T266M with defective Angptl-4 function lowered fasting triglyceride levels in patients with a T2D background[111], suggesting a potential therapeutic value of Angptl-4 blocker in treating dyslipidemia after diabetes. The effect of Angpt-4 in cardiac LPL is not well-studied. It is possible that in D100 animals showing hyperlipidemia, LPL could be "turned-off" when FA stimulates Angptl-4 expression in the heart.

### 1.3 Hypothesis and research objectives

Cardiac LPL is of crucial importance for maintaining normal heart function. My hypothesis is that coronary LPL activity following diabetes is regulated by multiple factors derived from both cardiomyocytes and endothelial cells (Figure 1).

The objectives of my research proposal were to:

1. Investigate the impact of cardiomyocyte chaperones and angiopoietin-like proteins on LPL dimerization and disassembly.
2. Determine the mechanisms by which EC, through its secretion of heparanase, regulates cardiomyocyte LPL.

Gaining further insight into these mechanisms should allow the identification of novel targets for therapeutic intervention, to prevent or delay cardiac failure following diabetes.

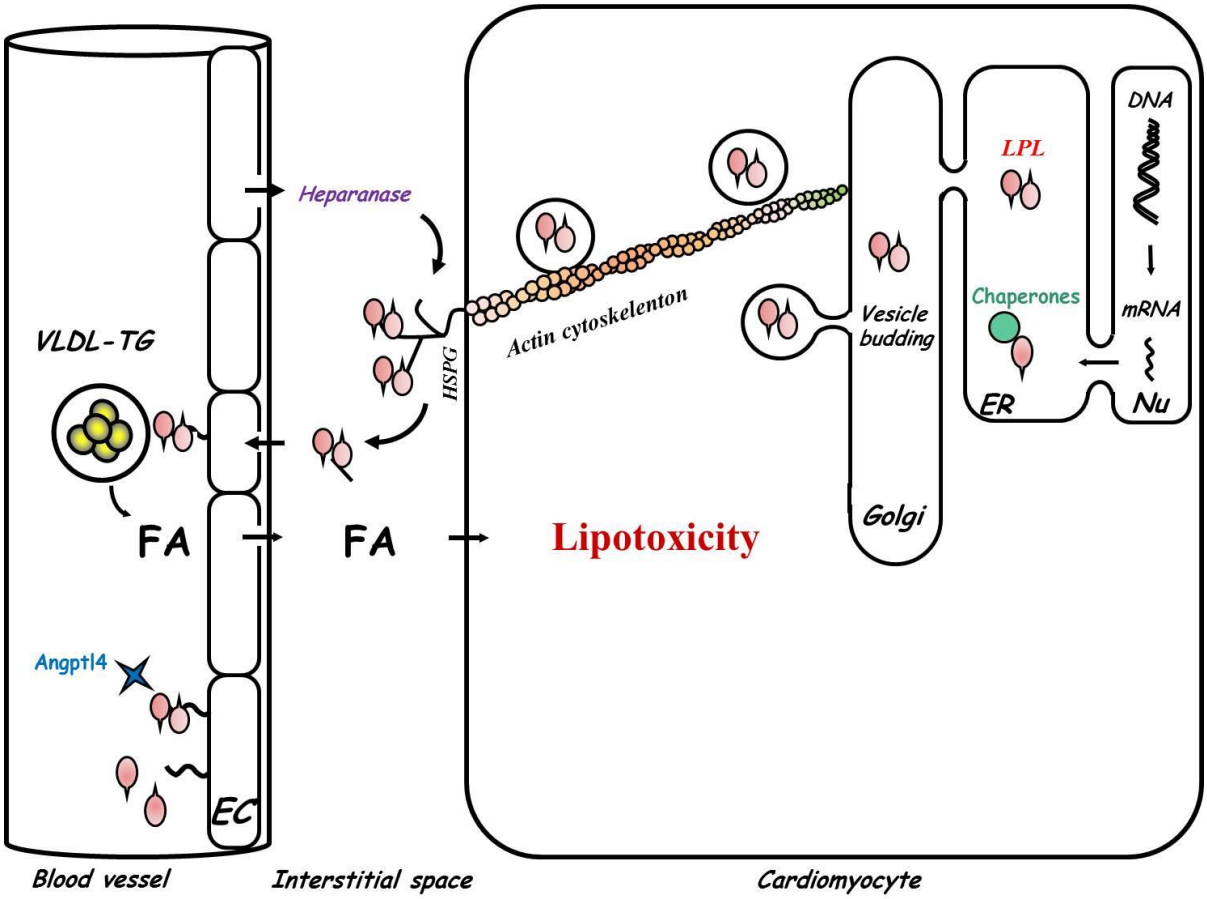


**Figure 1 Coronary LPL activity following diabetes is regulated by multiple factors derived from both cardiomyocytes and endothelial cells.**

Following gene transcription, LPL mRNA is translated as a monomer. The inactive monomer undergoes maturation with the help of chaperones to form the functional dimer in the endoplasmic reticulum (ER). Dimerized LPL then moves to the Golgi for further processing. The fully processed LPL is sorted into vesicles that are targeted for secretion. These secretion vesicles transport LPL to the myocyte surface via actin cytoskeleton. On the myocyte surface, LPL is sequestered by HSPGs. Heparanase secreted from endothelial cells (EC) in response to glucose can cleave myocyte HSPGs side chains, thereby liberating LPL for ongoing secretion. LPL released into the interstitial space is then transported towards the

apical side of EC to bind to luminal binding sites (HSPGs and GPIHBP1), where they break down triglyceride lipoprotein such as VLDL-TG, providing fatty acid (FA) to cardiomyocytes. Dimeric LPL can be dissembled into inactive monomers by Angptl-4. Augmented LPL function following diabetes would bring overwhelming amounts of FA to the heart, which leads to lipotoxicity in the long term. Nu: nucleus.

# Chapter 2: Methods

## 2.1 Materials

Rat aortic endothelial cells (RAOEC) were obtained from Cell Applications. Bovine coronary artery endothelial cells (bCAECs) was from Clonetics. Diazoxide (DZ), streptozotocin (STZ), palmitic acid (PA), castanosperimine (Cs) and cyclohexamide (CHX), lysophosphatidic acid (LPA), cytochalasin D, Y-27632, Gö6976, phorbol 12-myristate 13-acetate (PMA), filipin, genistein, and chloroquine were obtained from Sigma. Heparin (HEPALEAN, 1000 U/ml) was from Organon, Canada. PKC β inhibitor was obtained from Calbiochem. It inhibits PKC βI and PKC βII with $IC_{50}$ of 21 and 5 nM, respectively. Heparinase III (IBEX techonologies) was purified from recombinant *Flavobacteriumheparinum*. Heparanase inhibitor SST0001 was kindly provided by Sigma Tau Research (Switzerland S.A., Mendrisio, CH). [$^3$H]-triolein was purchased from Amersham Canada. Purified human Angptl-4 protein (Genway Biotech) is a human recombinant and 100% homologous to the 26-229 amino acid sequence of human Angptl-4. Purified active and latent heparanase were prepared as described[112]. Anti-calnexin antibody was from Stressgen Canada. Anti-LPL 5D2 antibody was a kind gift from Dr. J. Brunzell, University of Washington, Seattle. It is a monoclonal antibody recognizing LPL from different species, but not related lipases like hepatic lipase[113]. Anti-heparanase antibody mAb 130 was from InSight (Rehovot, Israel), which recognizes both the active (50 kDa) and latent form (65 kDa) of heparanase. Anti-rabbit True Blot was from eBioscience. All other antibodies were obtained from Santa Cruz. The RhoA activation G-LISA assay kit and F-actin/G-actin assay kit were obtained from Cytoskeleton (Denver, CO). HTRF heparanase

activity assay kit was obtained from Cisbio. To measure free fatty acid released from VLDL-TG breakdown, an NEFA-C assay kit was purchased from Wako.

### 2.2 Experimental animals

The investigation conforms to the Guide for the Care and Use of Laboratory Animals published by NIH and the University of British Columbia (UBC). Adult male Wistar rats (250–320 g) were used. To induce acute hyperglycemia, diazoxide (DZ), a selective ATP-sensitive $K^+$ channel opener was administered intraperitoneally at 100 mg/kg. DZ causes a rapid decrease of insulin secretion within 1 h, and the animals remain hyperglycemic for 4 h[114-116]. 4 h after DZ, animals were killed and hearts removed. For chronic diabetes, streptozotocin (STZ), a β-cell specific toxin was administered as a single dose intravenously to more closely mimic Type 1 diabetes[58, 100]. STZ was given at doses of 55 (D55) or 100 (D100) mg/kg. STZ animals were kept for 4 days before hearts were removed for every experiment. With D55, animals are insulin deficient, but do not require insulin supplementation for survival (moderate diabetes). Unlike D55, D100 animals also develop hyperlipidemia and are not able to survive beyond 4 days without insulin supplementation (severe diabetes).

### 2.3 Animal treatment

In some experiment, 1 h after DZ injection, animals were injected with 4 U of a rapid-acting insulin (Humulin R, Eli Lilly Canada Inc) through the tail vein. Blood glucose was monitored every 30 min up to 3 h, animals were killed and hearts removed for determination of coronary LPL activity and RhoA activation. In another experiment, 2 h before and after diazoxide injection, DZ animals were given 7.5 mg/rat heparanase inhibitor SST0001 subcutaneously[117, 118].

## 2.4 Isolated heart perfusion

Hearts were isolated and perfused retrogradely[119]. To measure coronary LPL, perfusion solution was changed to buffer containing heparin (5 U/ml). Coronary effluents were collected (for 10 s) at different time points over 5 min. LPL activity in each fraction was determined, plotted against time, and coronary LPL activity was presented as area under the curve over 5 min or peak activity. Subsequent to LPL displacement, hearts were used for heparin-sepharose chromatography. To evaluate the effect of Angptl-4 on LPL at the vascular lumen, hearts from control and D55 animals were perfused with or without 1 ng/ml purified Angptl-4 for 1 h in a re-circulating mode. Perfusates were collected and run on a heparin-sepharose column. Following Angptl-4 perfusion, the hearts were perfused with heparin to release LPL activity remaining at the vascular lumen. A modified Langendorff retrograde perfusion was used to isolate active and latent heparanase in the interstitial effluent[75]. Briefly, the hearts were taken out with the aorta, inferior vena cava, lungs still attached and perfused retrogradely through the aorta by Langendorff technique. The left and right superior venae cava as well as the inferior vena cava were ligated close to the atrium. The left and right pulmonary veins were tied off close to the lungs, and the lungs were removed. The pulmonary artery was cannulated. Fluid that drips down to the apex of the heart (interstitial transudate) were collected.

## 2.5 Isolation of cardiac myocytes

Ventricular calcium-tolerant myocytes were prepared by a previously described procedure[120]. Following isolation, cardiomyocytes were plated on laminin-coated culture dishes and allowed to settle down for 3 h. Unattached cells were washed away using medium 199 before treatment. Myocytes from both control and DZ hearts were isolated, and

intracellular LPL protein in these cells determined by Western blot. Gene expression of LPL was measured using Taqman assay (Invitrogen). Gene expression was normalized to β-actin.

### 2.6 Endothelial cell culture

bCAECs and RAOEC were cultured at 37ºC in a 5% $CO_2$ humidified incubator alone or co-cultured with adult rat cardiomyocytes[75]. bCAECs from the 5$^{th}$ to the 8$^{th}$ passage were used.

### 2.7 Endothelial cell conditioned medium (ECCM)

bCAECs were incubated with high glucose (25 mM) DMEM for 30 min. This medium was collected as ECCM.

### 2.8 *In vitro* treatments

The glucosidase inhibitor castanospermine (Cs, 50 mM, 2 h) was used to interrupt the association between LPL and calnexin. Colocalization of LPL and calnexin was observed using immunofluorescence. LPL activity released into the medium and remaining in the myocytes was also measured. Myocytes were also exposed to 25 mM glucose (HG, high glucose) and 1.0 mM palmitic acid (PA) bound to 1% BSA (HG+PA) for 2 h, cells lysed, and run on a heparin-sepharose column. To evaluate the impact of HG+PA on processing of newly synthesized LPL, cells were pre-incubated with 50 μM cyclohexamide (CHX, 1 h) to inhibit protein synthesis. Subsequently, cells were washed, treated with HG+PA for another 1 h, and LPL activity released into the media was determined. Calnexin and LPL colocalization was also visualized at the indicated times. To study the effect of FA on Angptl-4 expression, isolated myocytes were treated with 1.0 mM palmitic acid (PA) for 4-24 h, and Angptl-4 mRNA determined using real-time PCR. To study the direct effect of Angptl-4 on cardiomyocytes, isolated cardiomyocytes from control animals were incubated

with Angptl-4 for the indicated times, and LPL activity in the media and on the cell surface (by incubating cardiomyocytes with media containing 8 U/ml heparin for 1 min) determined. In a separate experiment, at the end of treatment, cell lysates were loaded onto a heparin-sepharose column, and dimeric LPL determined. To study the effect of RhoA activation on LPL secretion, control myocytes were incubated with lysophosphatidic acid (LPA, 100 nM-1 μM) in the presence or absence of 1 μM cytochalasin D (Cy, an actin polymerization inhibitor). To rule out the effect of protein synthesis on LPL secretion, 50 μM of the protein synthesis inhibitor cyclohexamide (CHX) was applied to myocytes 1 h before and during treatment with LPA, and LPL secretion into the medium determined. RhoA activation was tested in myocytes treated with ECCM, or 1 μg/ml purified latent or active heparanase at the indicated times. To study the role of HSPGs and PKCα in RhoA activation, 10 IU/L heparinase III and 5 μM Gö6976 was used to digest heparan sulfate of HSPGs and inhibit PKCα/β in cardiomyocytes, respectively. To study the specific effect of PKCα and β on RhoA activation in the presence of latent heparanase, siRNAs specific for PKCα were designed and synthesized by Invitrogen (5'-UGAAGAAGCGGGCGAUGAAUUUGUG-3'). Lipofectamine RNAi/MAX (Invitrogen) were used to transfect siRNAs for PKCα or control unrelated siRNA into cardiomyocytes (at a final concentration of 50 nM). 24 h after transfection, medium was changed to Media 199 and following an additional 24 h, cells were incubated with 1 μg/ml latent heparanase for 15 min and RhoA activation in myocytes measured. In another experiment, myocytes were pre-incubated with 200 nM PKCβ inhibitor, 1 h before and during latent heparanase treatment, and RhoA activation in myocytes measured. To investigate the role of RhoA in ECCM-mediated actin

polymerization, 10 μM Y-27632 was used to block ROCK, the downstream effector of RhoA.

Following treatment of bCAECs with 5 or 25 mM glucose DMEM for 30 min, cells were collected and intracellular latent and active heparanase measured using Western blot. To test whether consecutive exposure to high glucose can eventually deplete heparanase secretion, bCAECs were treated with 25 mM glucose DMEM for 30 min, medium removed ($1^{st}$ release), and the cells exposed to a second 30 min incubation with 25 mM glucose DMEM ($2^{nd}$ release). Medium from both $1^{st}$ and $2^{nd}$ release were concentrated to detect latent and active heparanase. In a separate experiment, bCAECs that were pre-treated with 25 mM glucose DMEM for 30 min ($1^{st}$ release) were placed in the upper chamber of a co-culture system with isolated cardiomyocytes at the bottom. These cardiomyocytes had themselves been pre-incubated with purified LPL to saturate surface binding sites. 25 mM glucose DMEM ($2^{nd}$ release) was then applied to the co-culture system, and medium collected from the bottom chamber after 30 min to test LPL activity released from cardiomyocytes. Results were compared to a co-culture system in which bCAECs was not pre-treated with high glucose.

To test whether exogenous heparanase can bind and be taken up by cardiomyocytes, isolated myocytes were treated with 500 ng/ml recombinant latent heparanase for different time intervals at 37 °C. This experiment was also conducted at 15 °C to inhibit heparanase binding and uptake. In the presence of 10 IU/ml of heparin to compete for HSPGs binding sites, or 10 IU/L heparitinase III to digest heparan sulfate side chains (2 h), the contribution of myocyte surface HSPGs in heparanase uptake was determined. For studying the mechanism of internalization, 350 mM sucrose or 1 μg/ml filipin was applied to myocytes

for 15 min before latent heparanase, to block clathrin-coated pits and caveolae-dependent internalization, respectively. We also used 0-25 μM dynasore or 0-100 μM genistein for 1 h to inhibit dynamin and tyrosine kinase activity which could be involved in internalization of exogenous heparanase. To inhibit lysosomal enzymes, 200 μM chloroquine was used and myocytes incubated for 2 h.

### 2.9 LPL activity

LPL catalytic activity was determined by measuring the *in vitro* hydrolysis of a sonicated [$^3$H]triolein substrate emulsion[64]. The standard assay conditions were 0.6 mM glycerol tri[9,10-$^3$H]oleate (1 mCi/mmol; 1 Ci=37 GBq), 25 mM piperazine-N,N'-bis(2-ethanesulfonic acid) (pH 7.5), 0.05% (wt/v) albumin, 50 mM $MgCl_2$, 2% (v/v) heat-inactivated chicken serum as a source of apo-CII. The reaction mix was incubated at 30 ºC for 30 min. Reaction product, sodium [$^3$H]oleate, was extracted and determined by liquid scintillation counting. Results are expressed as nmol/h/ml (perfusate, elution fraction or media) or nmol/h/mg protein (cell lysate).

### 2.10 Heparin-sepharose chromatography

Heparin-sepharose chromatography was carried out as described previously to separate dimeric LPL from monomers[47, 102]. Heart perfusates or equal amounts (total protein) of tissue homogenates or cell lysates were loaded onto a HiTrap™ HP Column and sequentially eluted with 0.25, 0.75, 1.0, and 1.5 M NaCl at 0.2 ml/min. Fractions (1 ml each) collected were used to detect LPL activity and protein by ELISA (USCNLIFE) or Western blot following TCA precipitation. To determine total amount of monomeric or dimeric LPL, fractions from 0.75 or 1.0 M NaCl were combined before TCA precipitation. To determine the processing stage of dimeric LPL, aliquots from the 1.0 M NaCl fractions were subjected

to endoglycosidase H (endo H) digestion. Digested products of LPL were visualized by Western blotting following TCA precipitation.

### 2.11 Real time quantitative PCR and Taqman gene assay

LMF1 and Angptl-4 mRNA levels were determined using SYBR Green real-time quantitative PCR (Roche). Primer sequences for LMF1 were: forward, 5'-TGATCCTGCAGGGCACA -3'; reverse: 5'- GTCCAGGCGGTAGTGGTA -3'[121]; for Angptl-4, forward, 5'- CTCTGGGATCTCCACCATTT -3'; reverse: 5'-TTGGGGATCTCCGAAGCCAT -3'[122]. All values obtained were normalized to 18S-ribosomal RNA.

Myocytes from both control and DZ hearts were isolated, gene expression of LPL was measured using Taqman assay (Invitrogen). Gene expression was normalized to β-actin.

### 2.12 RT-PCR

Total RNA was extracted from isolated myocytes or RAOEC using Trizol reagent (invitrogen), and 1 μg total RNA was used for RT-PCR. PCR primers were as follow[123, 124]:

Heparanase (forward, 5'-CAAGAACAGCACCTACTCACGAAGC-3'; reverse, 5'-CCACATAAAGCCAGCTGCAAAGG-3'; 616 bp product)

MMP-9 (forward, 5'-CCCCACTTACTTTGGAAACGC-3'; reverse, 5'-ACCCACGACGATACAGATGCTG-3'; 686 bp product)

18S rRNA (forward, 5'-CGGCTACCACATCCAAGGAA-3'; reverse, 5'-GCTGGAATTACCGCGGCT-3'; 187 bp product)

### 2.13 Immunofluorescence

Following the indicated treatments, cells were double stained with Alexa635 and Alexa488 to colocalize LPL (red), and calnexin (green), respectively. Isolated

cardiomyocytes were also treated with 1 μg/ml active or latent heparanase for 30 min, and cells probed with anti-syndecan-4 antibody (H-140, Santa Cruz) to visualize syndecan-4 (green) stained by Alexa488. To induce syndecan-4 clustering, an antibody against the extracellular domain of syndecan-4 (H-17, Santa Cruz) was used as a positive control[125, 126]. 4,6-Diamidino-2-phenylindole (DAPI) was used to stain nuclei. Slides were visualized using a Confocal microscope.

### 2.14 In vitro inhibitory effect of Angtpl-4 on LPL activity

LPL from vascular lumen was obtained by perfusing hearts from D55 animals with heparin. Purified human Angptl-4 was incubated with perfusates containing peak LPL activity at a final concentration of 1 ng/ml, 0.1 μg/ml, and 1 μg/ml. The reaction mix was incubated at 37°C, and at the indicated times, 100 μl reaction solution was removed for measuring LPL activity.

### 2.15 Isolation of particulate fraction

To determine RhoA activation *in vivo*, particulate fraction from ventricles were prepared as described previously[127].

### 2.16 G-LISA assay

G-LISA assay was performed according to manufacturer's instruction (Cytoskeleton). The active GTP-RhoA was detected by reading the absorbance at 490 nm.

### 2.17 Actin polymerization

Actin polymerization was evaluated by measuring the filamentous to globular actin (F-actin/G-actin ratio) using an assay kit from Cytoskeleton.

### 2.18 Uptake of exogenous heparanase

Following incubation with 500 ng/ml purified latent heparanase, myocytes were washed three times with cold PBS. To determine binding and uptake of heparanase by myocytes, total cell lysis were collected to detect heparanase by Western blot. For measuring internalization of heparanase, plasma membrane was removed by a procedure described previously. Briefly, myocytes were lysed in 50 mM Tris-HCl, pH 7.5, 150 mM NaCl, 0.2 M sucrose, 2 mM EDTA, 2 mM EGTA and protease inhibitor cocktail (Roche), and centrifuged at 10, 000 g at 4 °C for 10 min. Supernatant was further centrifuged at 100,000 at 4°C for 1 h to spin down the plasma membrane. The resulting supernatant (-PM) containing cytosolic fraction was used to monitor heparanase internalization.

### 2.19 Serum measurements

Blood samples were collected from the tail vein before termination, and serum isolated. Concentrations of nonesterified fatty acid (NEFA) and triglyceride were determined using diagnostic kits (Wako and Stanbio). Angptl-4 was analyzed using an ELISA kit from Raybiotech.

### 2.20 Isolation of lysosomes and nuclear fractions

Lysosomes enriched fractions were isolated using a kit from Sigma. Nuclear and cytosolic fractions were separated using a kit from Pierce. To validate the purity of proteins, we used cytosolic (GAPDH) and nuclear (Histone H3) protein marker to detect their presence in cytosolic and nuclear fractions.

### 2.21 Western blot

Western blot was carried out as described previously[127]. In some experiments, samples were concentrated by TCA precipitation, or Amicon centrifuge filter (Millipore) before detection of heparanase or LPL.

### 2.22 Statistical analysis

Values are means ± SE. Wherever appropriate, one-way ANOVA followed by the Bonferroni test was used to determine differences between group mean values. The level of statistical significance was set at $P<0.05$.

# Chapter 3: Results

## 3.1 LPL maturation and disassembly is affected by diabetes

### 3.1.1 General characteristics of the experimental animals

Injection of DZ resulted in stable hyperglycemia within 4 h. These animals also exhibited an increase in circulating levels of NEFA. Although administration of STZ at both doses produced hyperglycemia of equal intensity as that seen with DZ, only D100 animals showed a robust elevation in circulating FA and TG levels (Table 1).

**Table 1** General characteristic of experimental animals

| | **Blood Glucose** (mM) | **NEFA** (mM) | **TG** (mM) |
|---|---|---|---|
| **Control** | 6.2±0.9 | 0.3±0.1 | 0.5±0.1 |
| **Diazoxide (4 h)** | 26.2±2.5** | 1.0±0.2** | 0.5±0.2 |
| **D55 (4 d)** | 24.6±2.0** | 0.4±0.1 | 0.5±0.3 |
| **D100 (4 d)** | 28.0±1.8** | 1.0±0.3** | 2.3±0.5** |

Blood samples were collected from the tail vein before termination, and serum isolated by centrifugation. Serum concentrations of nonesterified fatty acid (NEFA) and triglyceride (TG) were determined using diagnostic kits. Results are the mean±SE of 3 animals in each group. *Significantly different from control, $P<0.05$. **Significantly different from control, $P<0.01$.

### 3.1.2 Processing of LPL into an active dimeric enzyme is increased following DZ

LPL is an enzyme present in two forms based on its affinity to a heparin-sepharose column. Monomeric LPL has low affinity to the column, is predominantly eluted in 0.4-0.75 M NaCl fractions, and has no catalytic activity. Active LPL is a homodimer eluted at higher

concentrations of NaCl (1.0-1.5 M)[47, 102]. We found that the majority of LPL in the heart is monomeric (eluted at 0.75 M NaCl), with only ~30% of the enzyme in the form of dimers (eluted in 1.0 M NaCl fractions) accounting for all of the LPL activity (Figure 2). Consistent with our previous studies, total LPL protein remained unchanged following acute hyperglycemia induced by DZ (Figure 3*A*). However, when equal amounts of homogenate protein were loaded onto a heparin-sepharose column, the 1.0 M fractions from DZ hearts demonstrated higher LPL activity (Figure 3*B*) and protein (Figure. 3*C*), suggesting the presence of more dimeric LPL in these hearts.

Dimeric LPL could be located either at the vascular lumen, or within cardiomyocytes. To determine vascular LPL, hearts were perfused with heparin and LPL activity measured in the perfusate. DZ hearts possessed increased LPL activity at this site (Figure 4*A*). Following stripping of the dimeric enzyme from the vascular lumen with heparin, hearts with predominantly myocyte LPL were then subjected to a heparin-sepharose column. Interestingly, in addition to the vascular lumen, DZ hearts also harbored increased dimeric LPL in cardiomyocytes (Figure 4*B*, lane 1 *vs.* 3). Maturation of LPL including dimerization occurs within the endoplasmic reticulum (ER) of cardiomyocytes. To further localize myocyte LPL dimers, we used endo H to digest dimeric LPL. Endo H cleaves the glycan chains of LPL based on their processing stages in different cellular organelles; the 57 and 55 kDa products represent LPL that has either passed or is present within Golgi apparatus respectively, whereas the 52 kDa band refers to LPL undergoing processing inside the ER[47, 128]. Interestingly, DZ hearts had a higher proportion of dimeric LPL at a post-ER processing stage (Figure 4*B*, lane 2 *vs.* 4), implicating augmented maturation of LPL following DZ. To examine whether this is due to acute exposure to a hyperglycemic and hyperlipidemic

environment seen in DZ animals, isolated cardiomyocytes were incubated with HG+PA for 2 h. Using the same conditions, we have previously found an accelerated LPL trafficking from Golgi to the myocyte surface. HG+PA also increased dimerization of LPL (Figure 4*C*), indicating that processing of LPL could be a pre-requisite for trafficking.

### 3.1.3 Calnexin is required for LPL processing and is enhanced following diabetes

LPL is a glycan protein whose processing into active dimers requires its association with ER resident chaperones like calnexin/calreticulin to allow proper folding. Using immunofluorescence, LPL and calnexin were found to be intensively colocalized at the perinuclear region (Figure 5*A*). LPL association with this chaperone was further confirmed by immunoprecipitation (Figure 5*A*, inset). Castanospermine (Cs) is a glucosidase inhibitor that blocks trimming of LPL glycan chains, such that it cannot be recognized by calnexin[49]. Using Cs, we were able to inhibit the association between LPL and calnexin; a complete absence of the perinuclear colocalization of these proteins was observed (Figure 5*B*, inset). This hindered LPL secretion and processing-both secreted (Figure 5*B*) and intracellular (Figure 5*C*) LPL activity declined in the presence of Cs, likely due to reduced LPL dimerization (Figure 5*C*, inset). To determine whether HG+PA augmented LPL processing by affecting the association between calnexin and newly synthesized LPL, cardiomyocytes were pre-treated with the protein synthesis inhibitor cyclohexamide (CHX). After 1 h, as a result of no newly synthesized LPL entry into the ER, CHX abolished the association between LPL and calnexin (Figure 5*D*, inset 2). Upon removal of CHX and renewal of protein synthesis, association between newly synthesized LPL and calnexin was visualized in the presence or absence of HG+PA. 1 h after re-entry of LPL into the ER, newly synthesized LPL was observed colocalized with calnexin at the perinuclear region (Figure 5*D*, inset 3).

However, in contrast to Cs, even though HG+PA attenuated this colocalization (Figure 5*D*, inset 4), more LPL were observed present at the cell surface, suggesting that more enzyme had completed processing under these conditions. Increased LPL processing was also reflected in more active LPL being released into the media (Figure 5*D*).

To examine LPL processing subsequent to chronic diabetes, 55 mg/kg of STZ was administered to generate "moderate diabetes". Similar to D*Z*, although chronic diabetes did not increase total LPL protein (data not shown), D55 hearts also demonstrated higher amounts of dimeric LPL (Figure 6*A*). The importance of calnexin in LPL processing is also suggested in D55 hearts; augmented LPL dimerization in these hearts was accompanied by increased calnexin expression (Figure 6*B*). However, we did not observe the same increase in calnexin when cardiomyocytes were acutely exposed to HG+PA (data not shown). Another crucial factor for LPL dimerization, LMF1, was found to be unchanged following D55 (Figure 7). Overall, our data suggests that following diabetes, more LPL is processed into its active dimeric form, which appears to involve the ER chaperone calnexin.

### 3.1.4 Severe diabetes reduces dimeric LPL in the heart with increased expression of Angptl-4

Increasing the dose of STZ to 100 mg/kg (D100) produced hyperglycemia similar to that observed in D55 animals. However, unlike D55, D100 animals developed severe hyperlipidemia (Table 1). Additionally, in contrast to D55, D100 animals showed a decline in dimeric LPL, both in the whole heart (Figure 8*A*) and at the vascular lumen (Figure 8*B*). This effect on LPL was not a result of decreased calnexin expression in D100 (Figure 8*C*), but was accompanied by a robust increase in Angptl-4 serum concentrations (Figure 8*D*).

Furthermore, cardiac expression of Angptl-4 protein (Figure 8*E*) and mRNA (Figure 8*E*, inset) were also found to be higher in D100 animals.

### 3.1.5 Angptl-4 is capable of inhibiting LPL activity and its expression is stimulated by fatty acid

To test the direct inhibitory effect of Angptl-4 on LPL, dimeric LPL collected from the vascular lumen of D55 animals was incubated with purified Angptl-4 *in vitro*. The inhibition of LPL activity by Angptl-4 was fast (within 15 min) and dose-dependent with 1 μg/ml Angptl-4 inhibiting about 85% of the enzyme activity at 2 h (Figure 9*A*). It should be noted that the serum concentration of Angptl-4 in D100 animals (1 ng/ml) was effective in inhibiting approximately 20% of LPL activity *in vitro* (Figure 9*A*). When this concentration of Angptl-4 was perfused through D55 hearts for 1 h, LPL activity remaining at the vascular lumen was reduced (Figure 9*C*). Interestingly, this reduction in LPL activity correlated with an increased appearance of monomeric LPL in the perfusion buffer (Figure 9*B*), and a decline in dimeric LPL remaining at the coronary lumen (Figure 9*C*, inset), suggesting that the inhibitory action of Angptl-4 on LPL is through the conversion of dimeric LPL into monomers, which in turn reduces its affinity to the binding sites at the vascular lumen. This inhibitory effect of Angptl-4 was also observed in isolated hearts (Figure 10*A*) and cardiomyocytes (Figure 10*B* and *C*) from control animals. To duplicate the elevated serum NEFA level seen in D100 animals, isolated cardiomyocytes were treated with 1.0 mM PA for 4-24 h. Within 4 h of exposure to PA, Angptl-4 mRNA did not change significantly. However, at 12 h, increase in Angptl-4 mRNA was observed, an effect that was even more dramatic following a 24 h exposure to PA (Figure 9*D*).

## 3.2 Endothelial cells regulate LPL secretion from cardiomyocytes through heparanase

### 3.2.1 RhoA activation is involved in increasing cardiomyocyte LPL secretion

In consistent with our previous observation, DZ animals with hyperglycemia (CON, 6.5 ± 0.6; DZ, 19.2 ± 2.7 mM, $P<0.01$) had increased coronary LPL activity[129] (Figure 11*A*). Within 30 min, 4 U insulin effectively inhibited the development of hyperglycemia in DZ animals (DZ + In, 7.6 ± 1.4; DZ, 21.5 ± 4.2, mM, $P<0.01$), and normal glycemia remained until the animals were killed. Insulin attenuated the increase of coronary LPL activity in these DZ hyperglycemic animals (Figure 11*A*). As RhoA has been reported to regulate actin cytoskeleton remodeling, an event that could affect LPL secretion[127], we tested RhoA activation in diabetic hearts. Upon activation, RhoA shifts from the cytosolic to the particulate fraction, and binds to GTP[130]. In DZ hearts, an increased RhoA in the particulate fraction was observed, which was inhibited by insulin treatment (Figure 11*B*). As DZ animals are hyperglycemic for only a short period, a more chronic model of hyperglycemia was induced by injecting rats with 55 mg/kg streptozotocin (D55), and animals kept for 4 days. Similar to DZ animals, D55 animals also have higher coronary LPL activity, which was accompanied by RhoA activation in these hearts (Figure 12). To determine whether RhoA activation can induce LPL secretion from myocytes *in vitro*, cells were incubated with LPA. After 2 h of LPA, an increased amount of LPL was released into the medium (Figure 11*C*). RhoA activation by LPA was confirmed in cardiomyocyte as GTP-RhoA increased immediately 1 min following LPA, and declined with time (Figure 11*C*, inset). One effect of RhoA activation is actin cytoskeleton polymerization, which we observed as an increase in the formation of F actin in the presence of LPA (Figure. 11*D*). Given that LPL secretion

relies on stress fibers to move from an intracellular pool to the myocyte surface[131, 132], we inhibited actin cytoskeleton polymerization using Cy, and found that the impact of LPA on LPL secretion was abolished (Figure 11*E*). As the effect of LPA on LPL secretion was reproducible in mycoytes in which protein synthesis was inhibited (Figure 11*E*, inset, right panel), our data suggest that the increased LPL secretion observed with LPA is not a consequence of augmented protein synthesis, but likely due to increased LPL trafficking. Thus, RhoA activation could contribute towards augmented LPL secretion, possibly via actin cytoskeleton remodeling.

### 3.2.2 ECCM stimulates LPL secretion from cardiomyocytes

Following diabetes, endothelial cells are the first cells exposed to hyperglycemia, and could potentially release multiple factors affecting cardiomyocyte metabolism. For this reason, we incubated myocytes with high glucose treated endothelial cell conditioned medium (ECCM). Interestingly, ECCM released myocyte LPL within 30 min, an effect that was more significant after 1 h. High glucose itself had no impact on LPL (Figure 13*A*). As this increase in medium LPL was accompanied by a reciprocal decrease in LPL activity remaining at the myocyte surface (Figure 13*A*, inset, upper panel), we concluded that ECCM is capable of releasing myocyte surface LPL. Importantly, this ECCM-released LPL was catalytically active and able to breakdown exogenous VLDL-TG to FA (Figure 13*A*, inset, bottom panel). In addition to its ability to release LPL, we also tested whether ECCM could stimulate the replenishment of LPL when the enzyme at the myocyte surface is depleted. Myocytes were pre-treated with ECCM or heparin (10 mU/ml), followed by a bolus dose of heparin (8 U/ml) to deplete surface LPL, as confirmed in Figure 13*B* (left panel). Following a 2 h recovery, myocytes pre-treated with ECCM were able to recruit significantly more LPL

activity to the surface (Figure 13*B*, right panel), an effect not observed with 10 mU/ml heparin. Considering that RhoA is involved in augmented LPL secretion from myocytes, we tested the effect of ECCM on RhoA activation. An increase in GTP-bound RhoA was observed within 5 min in response to ECCM, reaching a peak at 15 min, and declined to basal levels after 30 min (Figure 14*A*). We did not see a similar effect with 25 mM glucose or 10 mU/ml heparin (data not shown). The down-stream effect of RhoA activation, actin cytoskeleton polymerization, was also augmented with ECCM, an effect that was abolished in the presence of the ROCK inhibitor Y-27632 (Figure 14*B*). Hence, our data suggested that ECCM can stimulate both the release, and likely through RhoA-mediated actin cytoskeleton polymerization, replenishment of LPL at the myocyte surface.

### 3.2.3 The effect of ECCM on LPL is related to the presence of heparanase

As LPL at the cardiomyocyte surface resides on HSPGs, its release by ECCM could be a consequence of cleavage of these binding sites by heparanase. As anticipated, ECCM contained a higher amount of both latent (65 kDa) and active (50 kDa) heparanase (Figure 15*A*), with a reciprocal decrease in the intracellular content of this enzyme (Figure 17*C*). The increase in active heparanase protein mirrored the higher heparanase activity in this medium (Figure 16). *In vivo*, both latent and active heparanase also increased in the interstitial space of hearts from DZ animals (Figure 15*B*), where coronary endothelial cells are exposed to high glucose. When heparanase in the ECCM was immunoprecipitated by an anti-heparanase antibody, thereby reducing the amount of both latent and active heparanase (Figure 15*C*, inset), the LPL releasing effect of ECCM was compromised (Figure 15*C*). When bCAECs were exposed to high glucose for two consecutive periods of 30 min, the amount of heparanase released into the medium diminished during the second incubation

(Figure 17*A*). In addition, the ability of this ECCM from the second incubation to release myocyte surface LPL also decreased (Figure 17*B*).

### 3.2.4 Latent and active heparanase play different roles in LPL secretion

Since high glucose stimulates the release of both latent and active heparanase from EC, we tested the roles of these two forms on LPL secretion using purified heparanase. Active, but not latent heparanase caused the release of LPL (Figure 15*D*), and this effect of active heparanase was dose-dependent (Figure 18). When heparin was added to remove LPL from the myocyte surface, active heparanase was unable to release LPL (Figure 15*E*), suggesting that LPL released by active heparanase is from the myocyte surface. Unexpectedly, RhoA activation was not observed with active heparanase, which only responded to the latent form of the enzyme (Figure 15*F*). Our data imply that active heparanase releases LPL from the myocyte surface, whereas latent heparanase may move LPL from an intracellular store to the surface.

### 3.2.5 Activation of RhoA by latent heparanase depends on HSPGs and PKC alpha

To examine the mechanism of RhoA activation by latent heparanase, we considered whether the integrity of the myocyte surface HSPGs is required for this signal mechanotransduction. As expected, removal of HS by heparinase III blocked RhoA activation by latent heparanase (Figure 19*A*). Interestingly, the effect of latent heparanase on RhoA activation and cytoskeleton polymerization was abolished by the PKCα/β inhibitor Gö6976 (Figure 19*B* and *C*), whereas PMA, a conventional PKC activator had effects similar to that seen with latent heparanase (Figure 20). Furthermore, the RhoA activation effect observed with latent heparanase was only attenuated in myocytes with reduced PKCα expression, but not in cells in which PKCβ was specifically inhibited (Figure 21). In normal

myocytes, syndecan-4 is distributed on myocyte surface in a dispersed manner. Upon addition of latent heparanase and anti-syndecan-4 antibody, syndecan-4 appeared clustered on the surface (Figure 19*D*, arrow), an effect not seen with active heparanase.

### 3.2.6 Secretion is increased when myocytes are co-cultured with endothelial cells exposed to high glucose

To simulate diabetes *in vitro*, myocytes were co-cultured with EC. As a limited number of myocytes can be seeded in the co-culture system, the intrinsic LPL activity at the surface of these myocyte is low. Hence, we used purified LPL added exogenously to amplify this surface pool. 200 µg of purified LPL was sufficient to saturate HSPGs binding sites on the myocyte surface (Figure 22*A*, inset). Using this amount of LPL, we exposed the co-culture system to normal and high glucose. A significantly higher medium LPL activity was detected from the lower chamber in the presence of high glucose (Figure 22*A*). To examine whether the released LPL from myocytes is ultimately recruited onto the apical side of EC, we tested LPL activity on the EC surface after 2 and 4 h with high glucose. In the normal glucose co-culture, we did not observe any change in EC surface LPL activity at 2 or 4 h. With high glucose, a robust increase in EC surface LPL activity was evident after 4 h (Figure 22*B*). Notably, high glucose co-culture also caused actin polymerization (within 1 h) (Figure 22*C*, inset), that was preceded by RhoA activation (within 30 min) in myocytes (Figure 22*C*).

## 3.3 Cardiomyocyte gene expression is affected by taking up latent heparanase from EC

### 3.3.1 Exogenous latent heparanase can be taken up by cardiomyocytes

In the heart, heparanase is expressed by the endothelial cells and cardiomyocytes do not synthesize this enzyme. To confirm this, we used RT-PCR, and were unable to detect the

presence of the heparanase gene in freshly isolated cardiomyocytes, even though this gene was highly expressed in RAOEC (Figure 23*A*, right inset). In the absence of gene expression, heparanase protein, both the 65 kDa latent and the 50 kDa active forms were detected in isolated myocytes (Figure 23*A*, left inset). As we failed to detect the EC marker CD31, our results indicated that these isolated myocytes were not contaminated by EC (Figure 23*A*, left inset). Interestingly, unlike RAOEC, the dominant form present in cardiomyocytes was the active heparanase (Figure 23*A*, left inset). Culturing cardiomyocytes for 36 h reduced the content of both heparanase forms, suggesting that the protein cannot be synthesized *de novo* when being turned over (Figure 23*B*). Introducing latent heparanase into the culture medium rapidly increased the level of latent heparanase in myocytes (within 5 min), which continued to accumulate over time. This increase was inhibited when temperature was lowered to 15°C. Unlike latent heparanase, the increase of active heparanase was gradual, and only significantly increased after 4 h (Figure 23*C*), suggesting intracellular conversion of latent to active heparanase in cardiomycoytes.

### 3.3.2 Internalization of latent heparanase is through a caveolae-dependent pathway that requires HSPGs, dynamin and tyrosine kinase activation

Heparanase in the total cell lysates could consist of two parts: heparanase bound to the myocyte surface or that which has been internalized. When plasma membrane was removed by ultracentrifugation, as validated by the absence of membrane protein $Na^+$-$K^+$ ATPase (Figure 24*A*, right inset), heparanase was still observed in the cytosolic fraction of myocytes, indicating that it had been internalized (Figure 24*A*). Using heparin to competitively inhibit the binding of latent heparanase to HSPGs, we were able to reduce the amount of heparanase that was internalized (Figure 24*A*). As similar results were seen with heparitinase III, that

digests the heparan sulfate chain of HSPGs (Figure 24*B*), our data implies that heparanase may be taken up by myocytes via binding to the HS heparin binding domain of HSPGs. As this internalization of heparanase was blocked by filipin, but was insensitive to sucrose (Figure 25*A*), it is likely that HSPGs-mediated endocytosis of heparanase is a caveolae-dependent rather than a clathrin-mediated event. It should be noted that at the concentration of sucrose used, the endocytosis of epidermal growth factor receptor (EGFR) that is typically internalized through formation of clathrin-coated pits, was blocked (Figure 25*A*, right inset). The involvement of dynamin and tyrosine kinase in this endocytotic process was apparent as dynasore (Figure 25*B*) and genistein (Figure 25*C*) reduced the amount of heparanase internalized.

### 3.3.3 Internalized latent heparanase is activated in lysosomes and enters the nucleus

On incubation of cardiomyocytes with latent heparanase, we were able to detect this enzyme in lysosomal fractions within 30 min. With time, latent heparanase in this lysosomal fraction progressively increased. Unlike latent heparanase, lysosomal active heparanase only increased at a later time point (after 3 h) (Figure 26*A*). As this increase in lysosomal active heparanase was prevented by chloroquine, which inhibit lysosomal proteases, our data suggests lysosomal conversion of latent to active heparanase in cardiomyocytes (Figure 26*B*).

### 3.3.4 Nuclear entry of heparanase is accompanied by increased matrix metalloproteinase 9 (MMP-9) expression

Assuming that conversion of latent to active heparanase in the lysosomes is to fulfill a biological function, we determined the nuclear content of heparanase, and observed the presence of active heparanase in this organelle even in the absence of exogenous heparanase. Following addition of latent heparanase into culture medium, there was a dramatic increase

of both latent and active heparanase in the nucleus after 4 h (Figure 27*A*). This entry was followed by an increase in MMP-9 expression 18 h after heparanase treatment (Figure 27*B*). *In vivo* studies using D55 cardiomyocytes demonstrated a 1.5 fold increase in the amount of active heparanase inside the nucleus (Figure 27*C*). MMP-9 expression in these myocytes was also significantly higher compared to control (Figure 27*D*). However, we did not detect any change in LPL expression in both latent heparanase treated myocytes or D55 myocytes (data not shown).

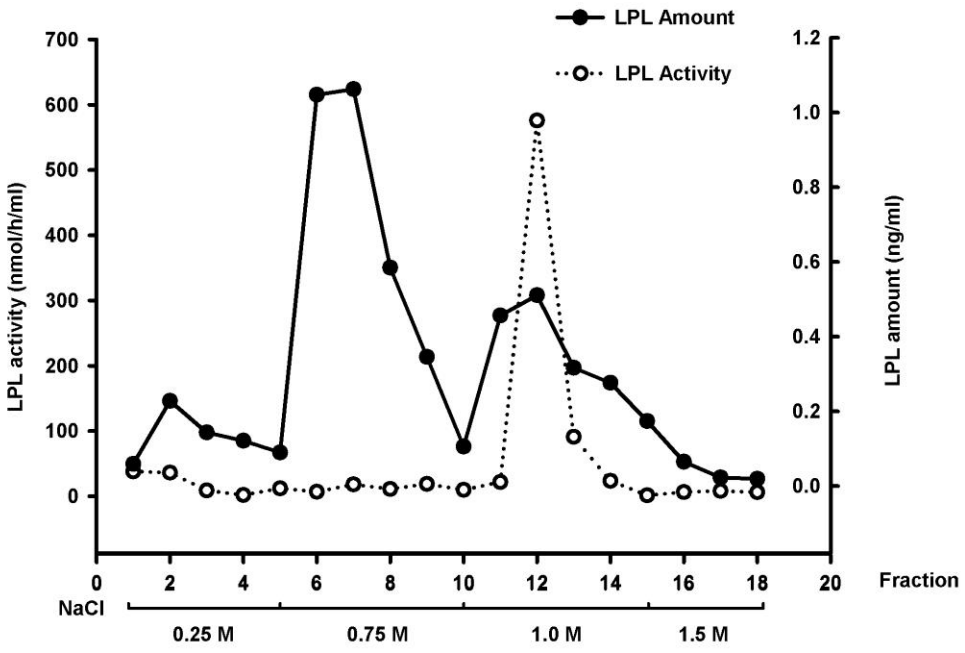
LPL Amount
LPL Activity
LPL activity (nmol/h/ml)
LPL amount (ng/ml)
700
600
500
400
300
200
100
0
1.2
1.0
0.8
0.6
0.4
0.2
0.0
0
2
4
6
8
10
12
14
16
18
20
Fraction
NaCl
0.25 M
0.75 M
1.0 M
1.5 M

**Figure 2 Monomeric and dimeric LPL are present in the heart.**

Whole heart homogenate was loaded onto a heparin-sepharose column followed by washing with increasing concentrations of NaCl (0.25, 0.75, 1.0, and 1.5 M, lower bar) at a flow rate of 0.2 ml/min. Both LPL amount (right axis) and activity (left axis) in each fraction were determined using ELISA and in vitro hydrolysis of a sonicated [$^{3}$H]triolein substrate emulsion, respectively.

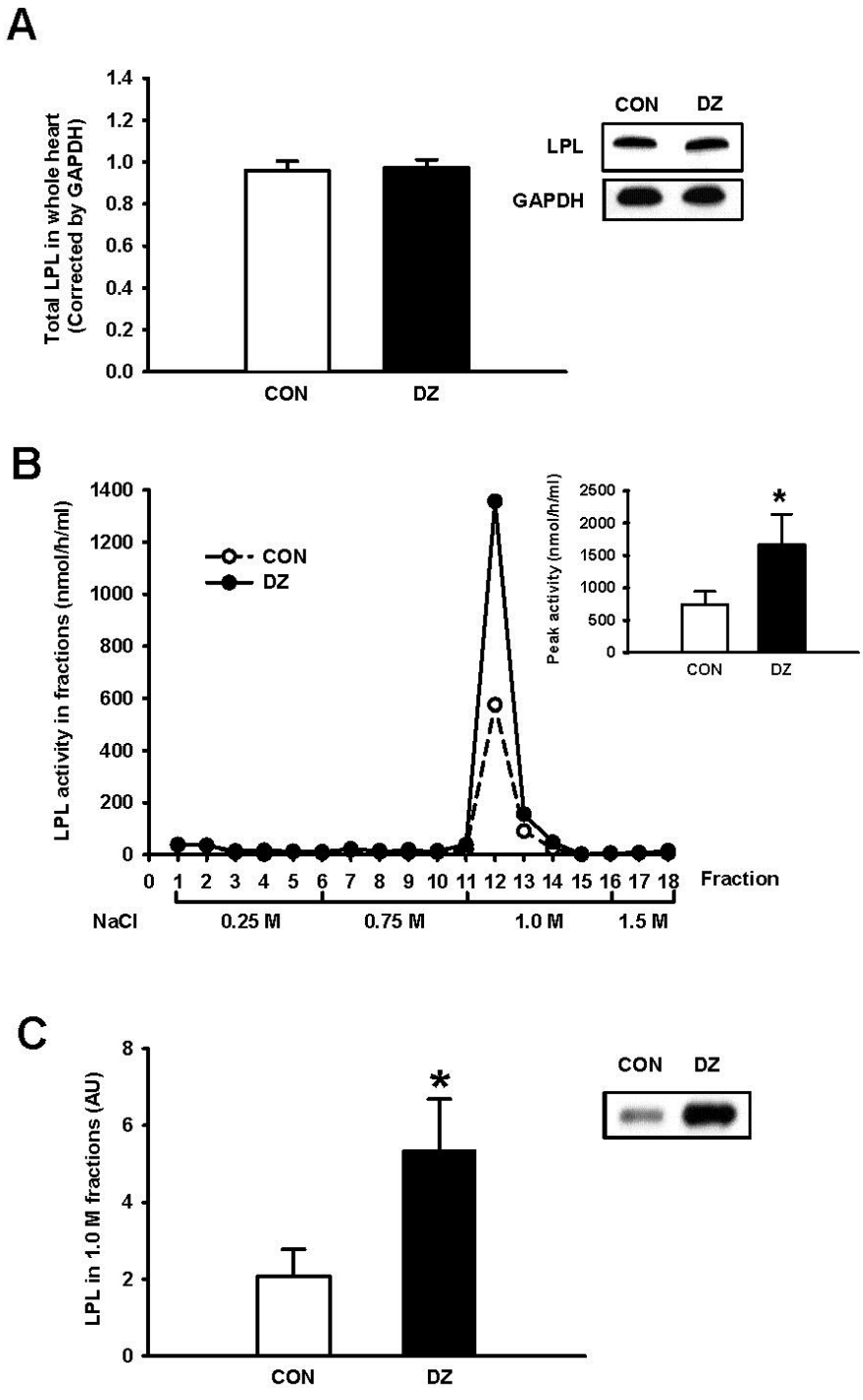
A
Total LPL in whole heart (Corrected by GAPDH)
1.4
1.2
1.0
0.8
0.6
0.4
0.2
0.0
CON
DZ
CON
DZ
LPL
GAPDH
B
LPL activity in fractions (nmol/h/ml)
1400
1200
1000
800
600
400
200
0
CON
DZ
0 1 2 3 4 5 6 7 8 9 10 11 12 13 14 15 16 17 18
Fraction
NaCl
0.25 M
0.75 M
1.0 M
1.5 M
Peak activity (nmol/h/ml)
2500
2000
1500
1000
500
0
*
CON
DZ
C
LPL in 1.0 M fractions (AU)
8
6
4
2
0
*
CON
DZ
CON
DZ

**Figure 3 Acute hyperglycemia increases cardiac LPL dimerization.**

Male Wistar rats were made hyperglycemic by injecting 100 mg/kg diazoxide (DZ) i.p. 4 h after injection, animals were killed and hearts removed. Total LPL protein expression was determined using Western blot normalized to GAPDH. Results are the mean±SE of 6 animals in each group (A). Ventricles were lysed with 25 mM ammonia buffer, pH 8.2, containing 1% Triton X-100, 0.1% SDS, 10 U heparin/ml, and protease inhibitor. Equal amounts of total protein from control (CON) and DZ heart homogenates were loaded onto a heparin-sepharose column, and eluted with increasing concentrations of NaCl (0.25, 0.75, 1.0 and 1.5 M). 1 ml fractions were collected and examined for LPL activity. Before the activity assay, aliquots of each fraction were diluted with equilibration buffer containing BSA to adjust NaCl concentration to 0.25 M and BSA to 1 mg/ml. Elution was repeated with samples from 6 animals in each group, but only a representative heparin-sepharose chromatography is illustrated (B). Peak LPL activity is presented as mean±SE from 6 animals in each group (B, inset). Fractions with LPL activity (1.0 M) were combined and precipitated by TCA before Western blot for LPL was carried out (C). Results are the mean±SE of 6 animals in each group. *Significantly different from control, $P<0.05$. AU: arbitrary units.

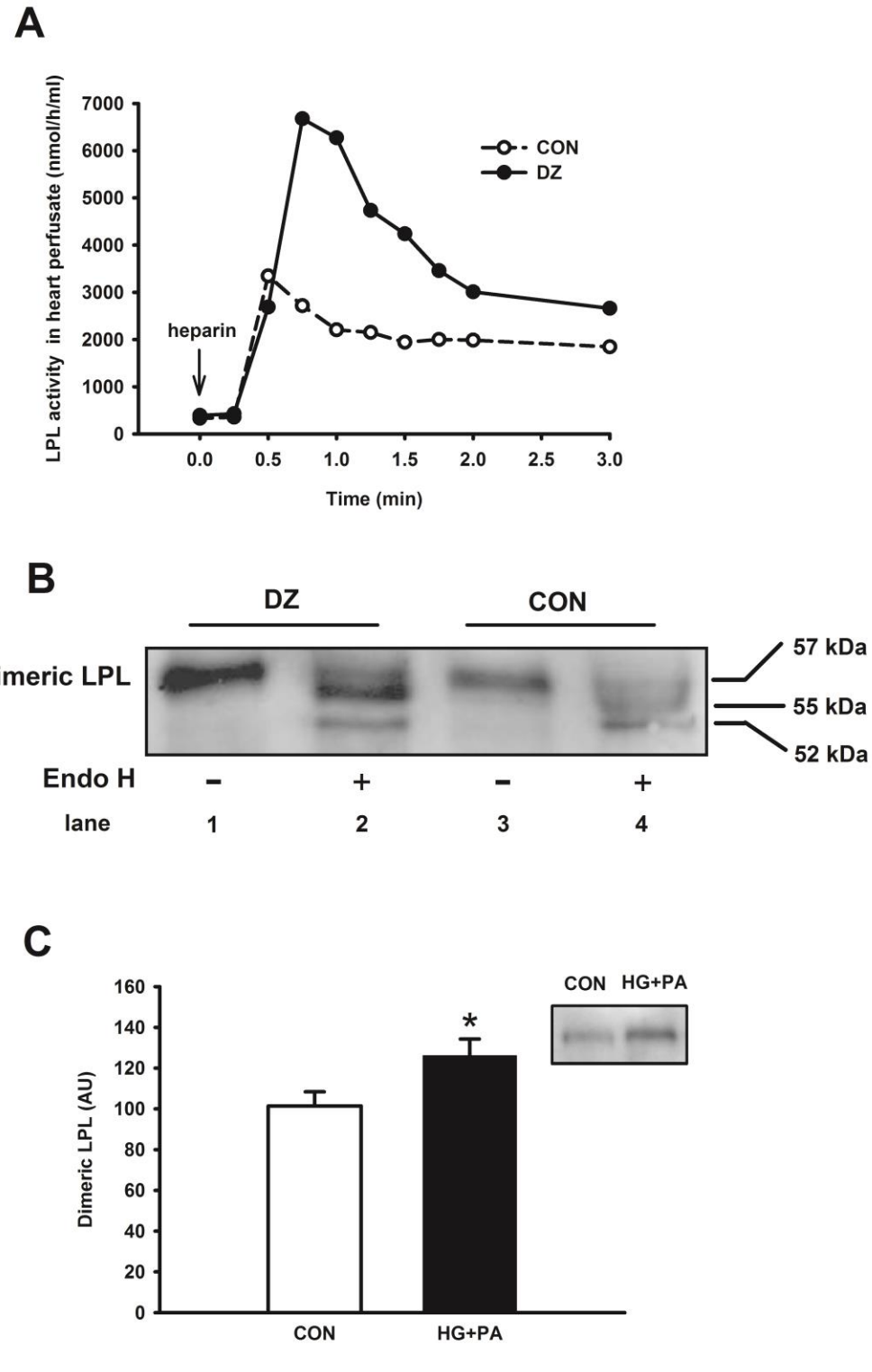
A
LPL activity in heart perfusate (nmol/h/ml)
7000
6000
5000
4000
3000
2000
1000
0
heparin
CON
DZ
0.0
0.5
1.0
1.5
2.0
2.5
3.0
Time (min)
B
DZ
CON
Dimeric LPL
57 kDa
55 kDa
52 kDa
Endo H
-
+
-
+
lane
1
2
3
4
C
CON
HG+PA
160
140
120
100
80
60
40
20
0
Dimeric LPL (AU)
*
CON
HG+PA

**Figure 4 Increased LPL dimers are present in cardiomyocytes from DZ animals and cells acutely exposed to high glucose and palmitic acid.**

4 h after injection of DZ, hearts were isolated, perfused with heparin (5 U/ml), and fractions of perfusate at the indicated times were analyzed for LPL activity (A). Subsequent to heparin perfusion and detachment of vascular LPL, heart homogenates were subjected to heparin-sepharose elution to isolate LPL dimers (in the 1.0 M NaCl elutions). These fractions were combined and digested with (+) or without (-) endo H for 20 h, concentrated by TCA precipitation, and LPL protein determined by Western blot (B). Isolated cardiac myocytes were plated on laminin-coated 60 × 15 mm tissue culture dishes and treated with palmitic acid (1 mM bound to 1 % BSA) and 25 mM glucose (HG+PA) for 2 h. Media containing 1% BSA were used as control (CON). Cellular dimeric LPL was determined by running cell lysates onto a heparin-sepharose column and fractions eluted at 1.0 M NaCl were used to determine LPL protein by Western blot (C). Results are the mean±SE of 5 repeated experiments using different animals. *Significantly different from control, $P<0.05$. AU: arbitrary units.

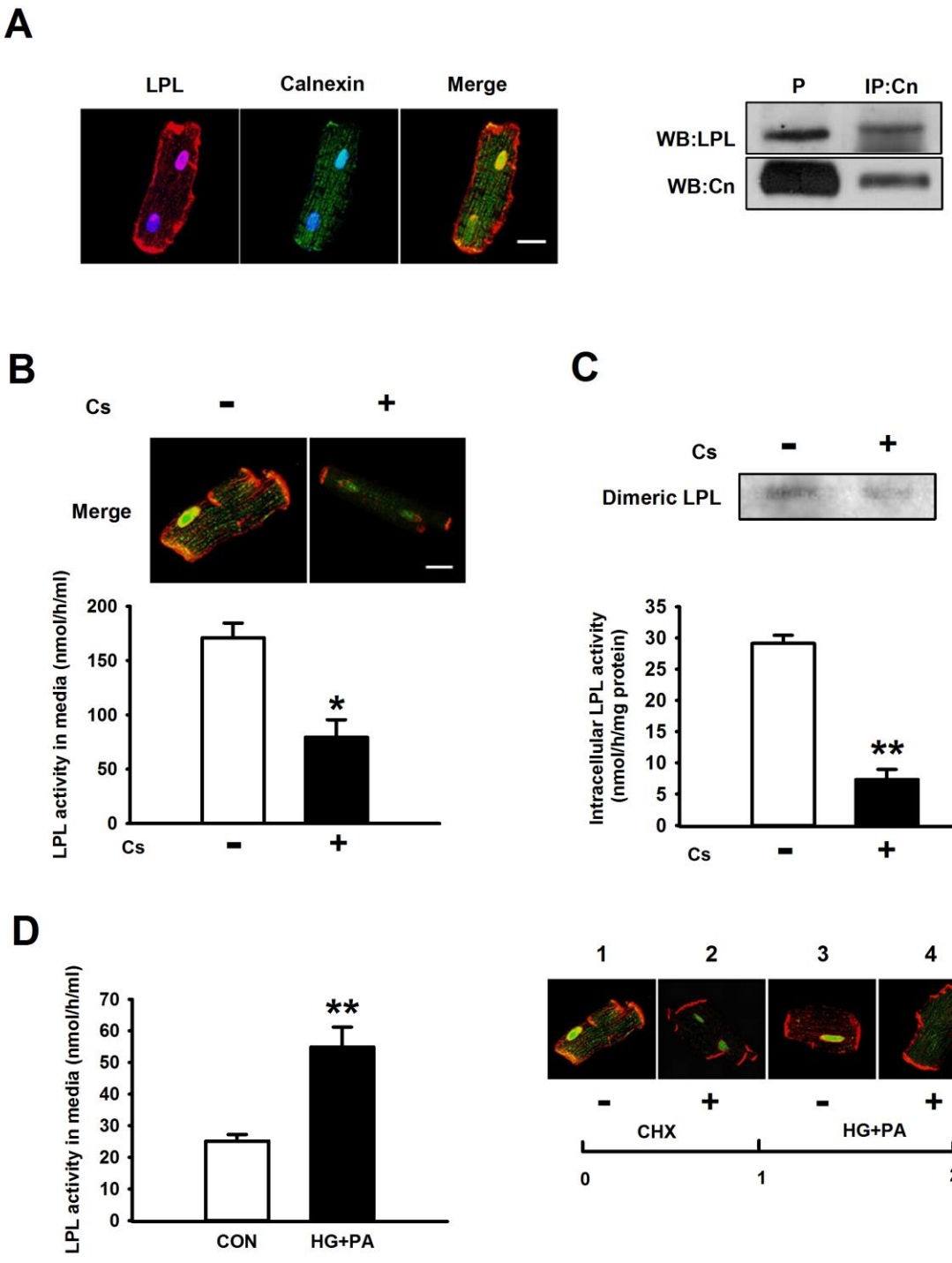
A
LPL
Calnexin
Merge
P
IP:Cn
WB:LPL
WB:Cn
B
Cs
-
+
Merge
LPL activity in media (nmol/h/ml)
200
150
100
50
0
*
Cs
-
+
C
Cs
-
+
Dimeric LPL
Intracellular LPL activity (nmol/h/mg protein)
35
30
25
20
15
10
5
0
**
Cs
-
+
D
LPL activity in media (nmol/h/ml)
70
60
50
40
30
20
10
0
**
CON
HG+PA
1
2
3
4
-
+
-
+
CHX
HG+PA
0
1
2 h

**Figure 5 LPL maturation requires calnexin and is enhanced by high glucose and palmitic acid.**

Plated myocytes from CON were immunostained with LPL (red) and calnexin (green). DAPI was used to stain the nuclei (blue), and colocalization of LPL and calnexin was visualized (Merge, yellow) (A). Cells were lysed with CHAPS lysis buffer (50 mM HEPES buffer, pH 7.5, containing 1% CHAPS, 200 mM NaCl, and protease inhibitor). Cell lysate of cardiomyocytes from control animals were immunoprecipitated using anti-calnexin (IP:Cn) antibody overnight at 4°C. The immunocomplex was captured by anti-rabbit Ig IP beads and immunoblotted for LPL. Direct Western blot of cell lysate was carried out as a positive control (P) (A, insert). Isolated myocytes were incubated in the presence or absence of castanospermine (Cs) for 2 h. At the end of treatment, colocalization of LPL and calnexin was visualized (B, inset). LPL activity released into the medium (B) and remaining in the myocytes (C) were measured. Treated cardiomyocytes were also loaded onto a heparin-sepharose column to determine the amount of dimeric LPL (C, inset). Results are the mean±SE of 3 repeated experiments using different animals. *Significantly different from control, $P<0.05$. **Significantly different from control, $P<0.01$. Isolated myocytes were pre-incubated with 50 μM cycloheximide (CHX) for 1 h. After sufficient washing to remove CHX, cells were treated with HG+PA or BSA only (CON) for another 1 h. LPL activity released into the media within this 1 h was measured (D). Results are the mean±SE of 3 repeated experiments using different animals. *Significantly different from control, $P<0.05$. Cells were also fixed with 4% paraformaldehyde before (D, inset 1) or after (D, inset 2) pre-incubation with CHX, and also following treatment with (D, inset 3) or without (D, inset 4)

HG+PA. Colocalization of LPL and calnexin (yellow) in these conditions were visualized by immunofluorescence. Scale bar=25 μm.

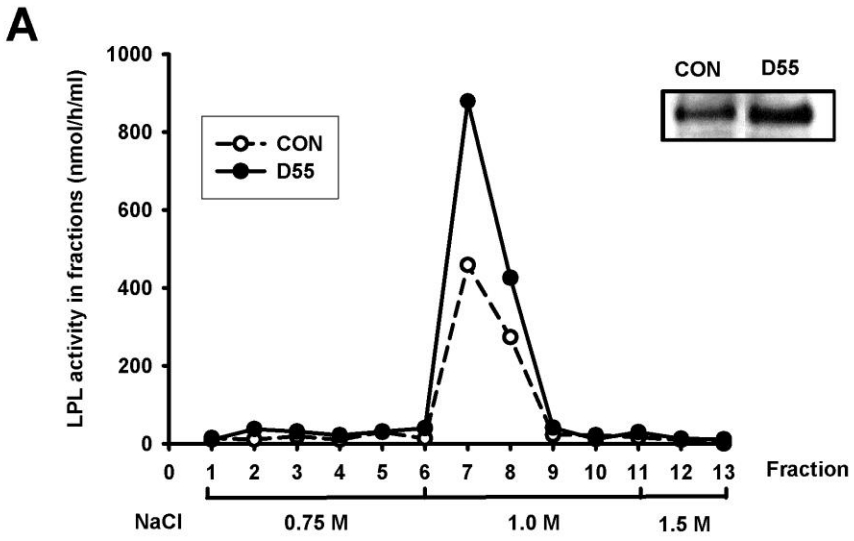
A
1000
800
600
400
200
0
LPL activity in fractions (nmol/h/ml)
CON
D55
CON
D55
0 1 2 3 4 5 6 7 8 9 10 11 12 13
Fraction
NaCl
0.75 M
1.0 M
1.5 M

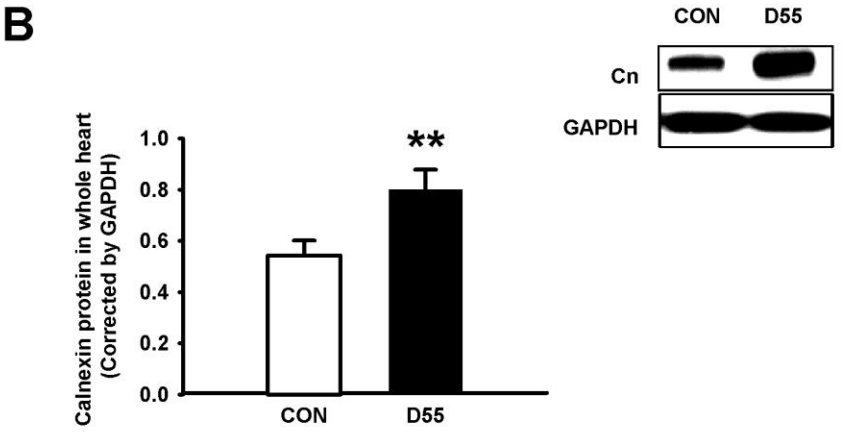
B
CON
D55
Cn
GAPDH
Calnexin protein in whole heart
(Corrected by GAPDH)
1.0
0.8
0.6
0.4
0.2
0.0
**
CON
D55

**Figure 6 Chronic diabetes also augments LPL processing with increased expression of calnexin.**

For chronic diabetes, animals were injected with 55 mg/kg STZ (D55), kept for 4 days and hearts removed. Equal amounts of total protein from CON and D55 heart homogenates were loaded onto a heparin-sepharose column, pre-washed with 0.25 M NaCl and eluted with 0.75, 1.0, and 1.5 M NaCl. LPL activity in each fraction was analyzed (A), and fractions from 1.0 M NaCl (containing LPL dimers) were combined to determine LPL amount by Western blot following TCA precipitation. Only a representative chromatography (A) and blot of LPL (A, insert) are shown from 5 repeated experiments. Calnexin protein expression (Cn) in CON and D55 hearts was determined by Western blot and normalized to GAPDH (B). Results are the mean±SE of 5 animals in each group. **Significantly different from control, $P<0.01$.

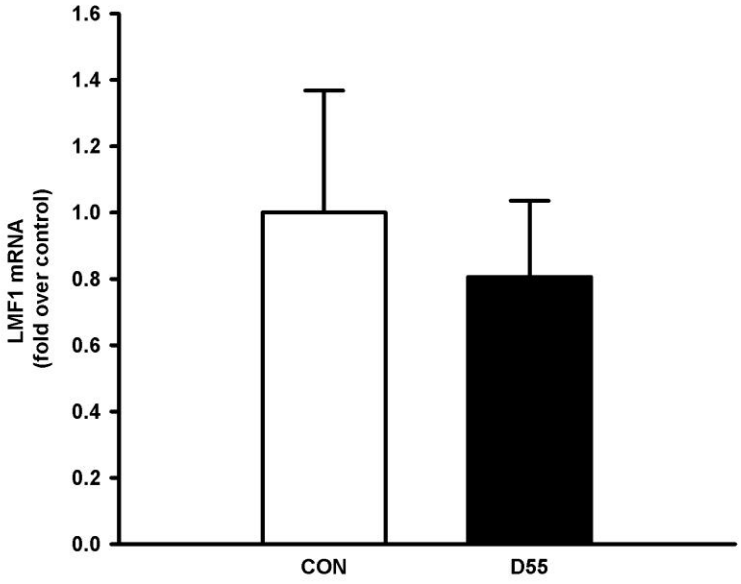
LMF1 mRNA
(fold over control)
1.6
1.4
1.2
1.0
0.8
0.6
0.4
0.2
0.0
CON
D55

**Figure 7 LMF1 mRNA expression in heart does not change following diabetes.**

LMF1 mRNA level from CON and D55 hearts was analyzed by real-time quantitative PCR and normalized to 18S-ribosomal RNA. Results were plotted as fold over control of mean±SE of 3 animals in each group.

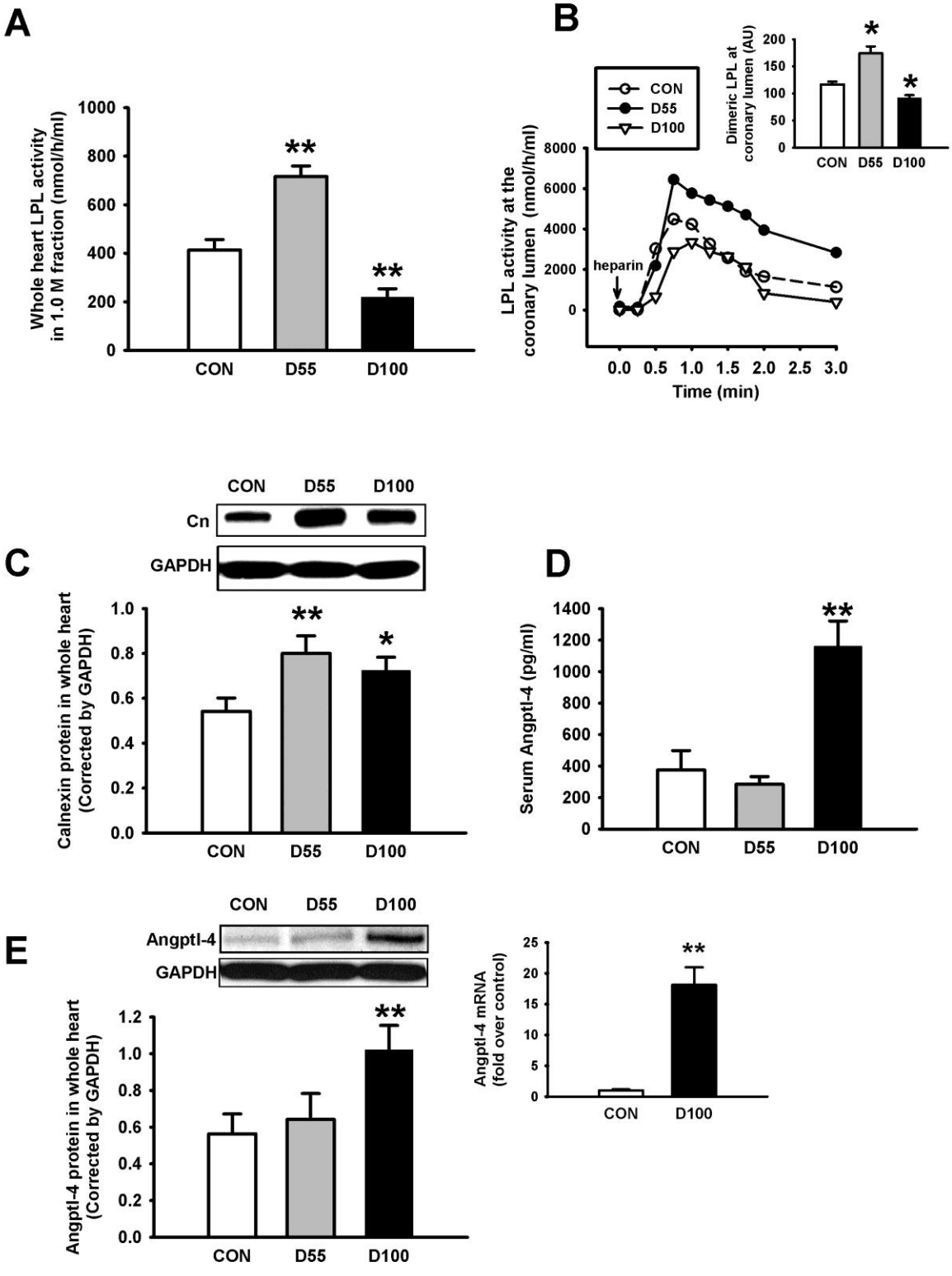
A
Whole heart LPL activity in 1.0 M fraction (nmol/h/ml)
1000
800
600
400
200
0
**
**
CON
D55
D100
B
CON
D55
D100
LPL activity at the coronary lumen (nmol/h/ml)
8000
6000
4000
2000
0
heparin
0.0 0.5 1.0 1.5 2.0 2.5 3.0
Time (min)
Dimeric LPL at coronary lumen (AU)
200
150
100
50
0
*
*
CON D55 D100
C
CON D55 D100
Cn
GAPDH
Calnexin protein in whole heart (Corrected by GAPDH)
1.0
0.8
0.6
0.4
0.2
0.0
**
*
CON
D55
D100
D
Serum Angptl-4 (pg/ml)
1400
1200
1000
800
600
400
200
0
**
CON
D55
D100
E
CON D55 D100
Angptl-4
GAPDH
Angptl-4 protein in whole heart (Corrected by GAPDH)
1.2
1.0
0.8
0.6
0.4
0.2
0.0
**
CON
D55
D100
Angptl-4 mRNA (fold over control)
25
20
15
10
5
0
**
CON
D100

**Figure 8 Severe diabetes reduces LPL dimers with an increase in Angptl-4.**

Animals were made moderate or severely diabetic by injecting STZ at a dose of 55 (D55) or 100 mg/kg (D100) respectively, and kept for 4 days. Hearts were isolated and equal amounts of homogenate protein from CON, D55, and D100 were loaded onto a heparin-sepharose column and eluted with increasing concentrations of NaCl. LPL activity in the 1.0 M fractions was measured and peak activity presented as mean±SE of 5 animals in each group (A). In a separate experiment, hearts from CON, D55, and D100 were perfused with heparin (5 U/ml), perfusates collected at the indicated times, and LPL activity determined (B, representative graph). These perfusates at the indicated times were pooled and loaded onto a heparin-sepharose column. Dimeric LPL in the 1.0 M fractions was determined using TCA precipitation followed by Western blot (B, inset). Results are the mean±SE of 3 animals in each group. *Significantly different from control, $P<0.05$. Heart homogenates from CON, D55, and D100 were also used for Western blot to detect calnexin (Cn, C) or Angptl-4 (E) protein expressions normalized by GAPDH. Serum samples were collected from the different groups to detect Angptl-4 using an ELISA assay (D). Angptl-4 mRNA expression from CON and D100 hearts was analyzed by real-time quantitative PCR. Gene expression was evaluated by normalizing to 18S-ribosomal RNA, and plotted as fold over control (E, inset). Results are the mean±SE of 5 animals in each group. *Significantly different from control, $P<0.05$. **Significantly different from control, $P<0.01$.

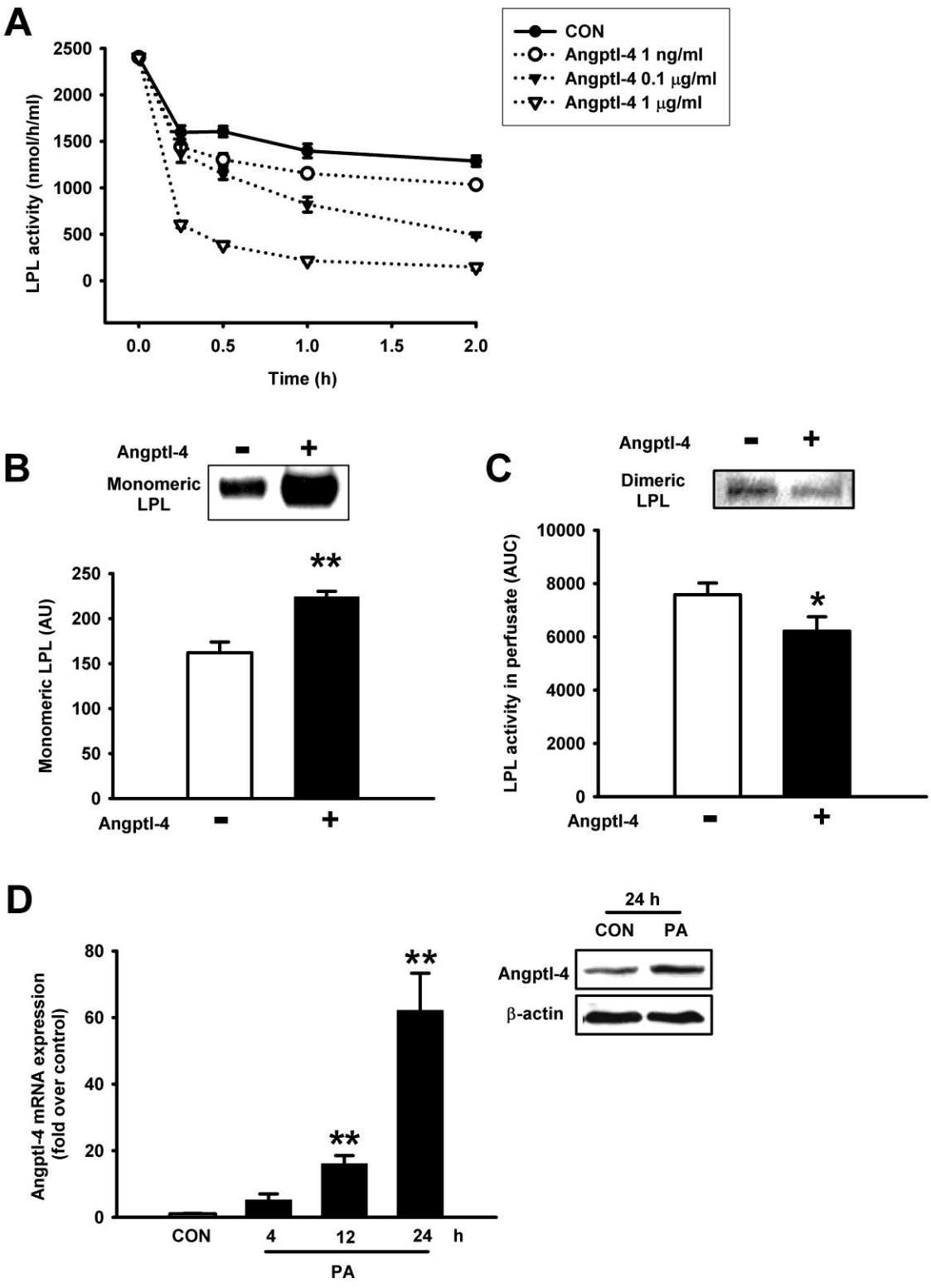
A
CON
Angptl-4 1 ng/ml
Angptl-4 0.1 μg/ml
Angptl-4 1 μg/ml
LPL activity (nmol/h/ml)
2500
2000
1500
1000
500
0
0.0
0.5
1.0
1.5
2.0
Time (h)
B
Angptl-4
-
+
Monomeric LPL
**
Monomeric LPL (AU)
250
200
150
100
50
0
Angptl-4
-
+
C
Angptl-4
-
+
Dimeric LPL
LPL activity in perfusate (AUC)
10000
8000
6000
4000
2000
0
*
Angptl-4
-
+
D
Angptl-4 mRNA expression (fold over control)
80
60
40
20
0
**
**
CON
4
12
24
h
PA
24 h
CON
PA
Angptl-4
β-actin

**Figure 9 Angptl-4 which reduces LPL activity is up-regulated by fatty acid.**

Hearts from D55 animals were perfused with heparin to release LPL at the vascular lumen. Fractions with peak LPL activity were then incubated with purified human Angptl-4 at a final concentration of 1 ng/ml, 0.1 μg/ml, and 1 μg/ml. Reaction mix was incubated at 37°C and LPL activity at the indicated times determined (A). Results are the mean±SE from 3 repeated experiments. Hearts from D55 animals were also directly perfused with or without 1 ng/ml purified Angptl-4 for 1 h. Perfusion buffer was collected at the end of this period. Monomeric LPL released into the perfusates were isolated by collecting the 0.75 M fractions from the heparin-sepharose column and quantified by Western blot (B). Following Angptl-4 perfusion, hearts were subsequently perfused with 5 U/ml heparin to release LPL activity remaining at the vascular lumen. LPL activity in the perfusate is expressed as area under curve over the 3 min perfusion (C). These perfusates over 3 min were pooled and loaded onto a heparin-sepharose column to visualize dimeric LPL in the 1.0 M fractions (C, inset). Results are the mean±SE of 3 animals in each group. *Significantly different from control, $P<0.05$. **Significantly different from control, $P<0.01$. Isolated cardiomyocytes were incubated with 1.0 mM palmitic acid (PA) for 4, 12 or 24 h. mRNA expression of Angptl-4 was quantified by real-time PCR and compared to control (CON) treated with 1% BSA (D). Protein expression of Angptl-4 after 24 h incubation with palmitic acid is illustrated in the inset. Results are the mean±SE of 5 repeated experiments using different animals. *Significantly different from control, $P<0.05$. AU: arbitrary units; AUC: area under curve.

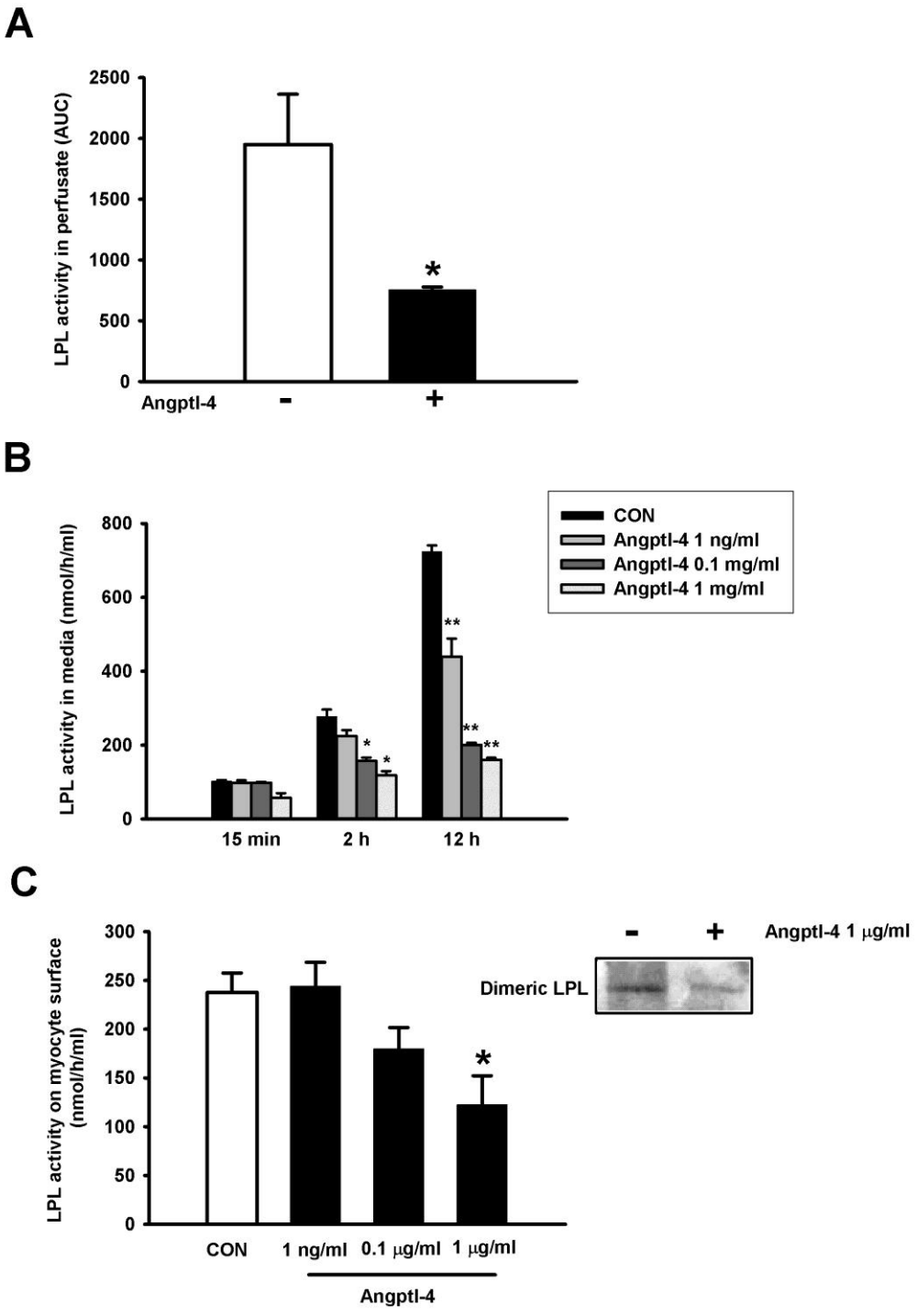
A
LPL activity in perfusate (AUC)
2500
2000
1500
1000
500
0
*
Angptl-4
-
+
B
LPL activity in media (nmol/h/ml)
800
600
400
200
0
CON
Angptl-4 1 ng/ml
Angptl-4 0.1 mg/ml
Angptl-4 1 mg/ml
**
*
15 min
2 h
12 h
C
LPL activity on myocyte surface (nmol/h/ml)
300
250
200
150
100
50
0
-
+
Angptl-4 1 μg/ml
Dimeric LPL
*
CON
1 ng/ml
0.1 μg/ml
1 μg/ml
Angptl-4

**Figure 10 Inhibitory effect of Angptl-4 on LPL at the vascular lumen and cardiomyocytes in control animals.**

Hearts from control animals were perfused with or without 1 ng/ml purified human Angptl-4 for 1 h. After Angptl-4 perfusion, hearts were subsequently perfused with 5 U/ml heparin to release LPL activity remaining at the vascular lumen. LPL activity in the perfusate is expressed as area under curve over the 3 min perfusion (A). Results are the mean±SE of 3 animals in each group. *Significantly different from control, $P<0.05$. Isolated cardiomyocytes from control animals were incubated with 1 ng/ml, 0.1 μg/ml, or 1 μg/ml Angptl-4 for the indicated times, incubation media collected, and LPL activity measured (B). In the 12 h groups, at the end of treatment, cells were washed with normal media, LPL on the cell surface released by incubation with media containing 8 U/ml heparin for 1 min, and LPL activity on the surface determined (C). Results are the mean±SE of 3 repeated experiments using different animals. *Significantly different from control, $P<0.05$. **Significantly different from control, $P<0.01$. In a separate experiment, isolated cardiomyocytes were plated on 60 × 15 mm tissue culture dishes and treated with or without 1 μg/ml angptl-4 for 12 h. Cells were washed with cold PBS and harvested. Cell lysates were loaded onto a heparin-sepharose column, and dimeric LPL visualized in the 1.0 M fractions by Western blot following TCA precipitation (C, inset). AUC: area under curve.

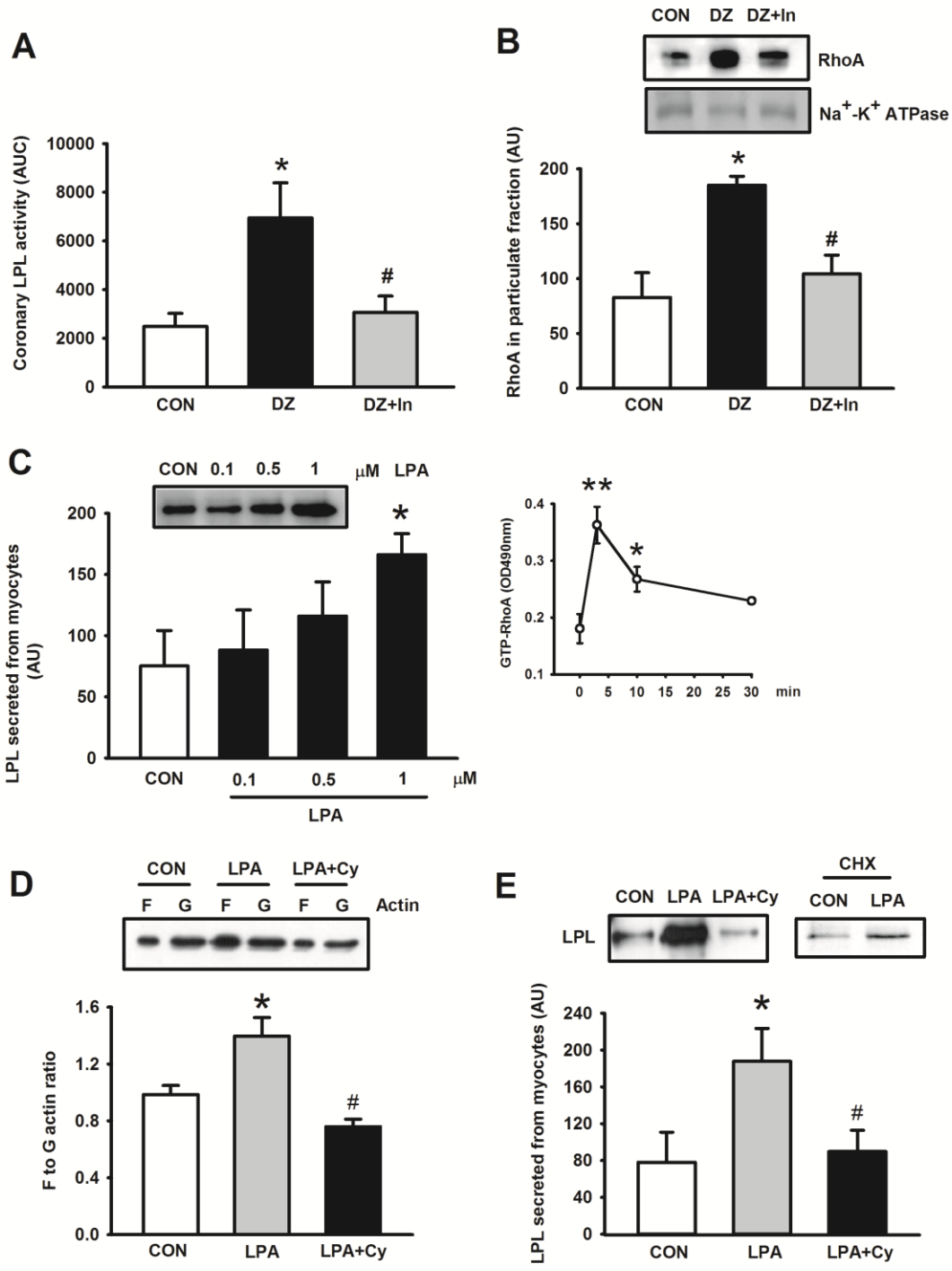
A
Coronary LPL activity (AUC)
10000
8000
6000
4000
2000
0
CON
DZ
DZ+In
B
CON DZ DZ+In
RhoA
Na+-K+ ATPase
RhoA in particulate fraction (AU)
200
150
100
50
0
C
CON 0.1 0.5 1 μM LPA
LPL secreted from myocytes (AU)
GTP-RhoA (OD490nm)
0.4
0.3
0.2
0.1
0 5 10 15 20 25 30 min
D
CON LPA LPA+Cy
F G F G F G Actin
F to G actin ratio
1.6
1.2
0.8
0.4
0.0
E
CON LPA LPA+Cy
CHX
CON LPA
LPL
LPL secreted from myocytes (AU)
240
200
160
120
80
40
0

**Figure 11 Increased LPL activity in diabetic hearts involves RhoA mediated actin cytoskeleton remodeling.**

Animals were made hyperglycemic with DZ, and kept for 4 h. 1 h after DZ injection, some animals were given 4 U of rapid-acting insulin i.v. (DZ+In), and kept for another 3 h. Animals were killed, hearts removed, and perfused with heparin (5 U/ml) to release coronary LPL. Coronary effluents were collected (for 10 s) at different time points over 5 min, and LPL activity in each fraction determined. The results are presented as area under the curve (AUC) for heparin-released LPL activity over 5 min (A). In a separate experiment, particulate fractions were also isolated from whole heart homogenates of control (CON), DZ and DZ+In animals, and RhoA recruitment to the particulate fraction determined by Western blot. A plasma membrane protein, $Na^+$-$K^+$-ATPase alpha subunit was used as a loading control (B). $^{*}P<0.05$, compared to CON, $^{\#}P<0.05$, compared to DZ, n= 3. Isolated cardiomyocytes from CON were incubated with increasing concentrations of LPA for 2 h, and LPL protein secreted into the medium measured by Western blot (C). Using 1 μM LPA, RhoA activation in cardiomyocytes was determined at the indicated times using G-LISA assay (C, inset). $^{*}P<0.05$, compared to CON, n=3. Myocytes were also pre-treated with 1 μM cytochalasin D for 30 min prior to incubation with 1 μM LPA (LPA+Cy). Actin cytoskeleton polymerization (D) and LPL secretion in these cells (E) were determined after 1 h and 2 h, respectively. In a different experiment, LPL secretion in the presence of LPA was tested in myocytes pre-incubated with 50 μM of the protein synthesis inhibitor cyclohexamide (CHX) (E, inset, right panel) $^{*}P<0.05$, $^{**}P<0.01$, compared to CON, $^{\#}P<0.05$, compared to LPA, n= 3-4.

A

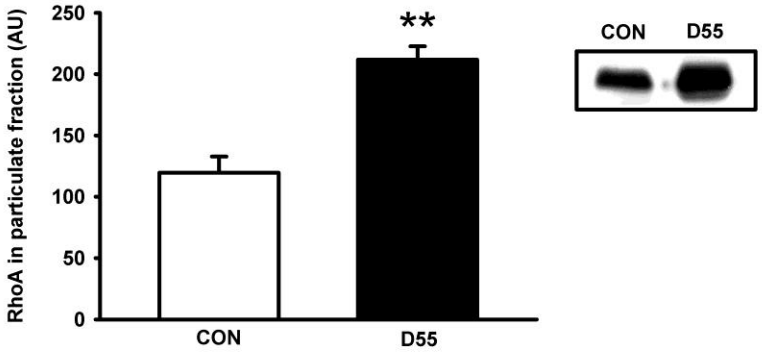
RhoA in particulate fraction (AU)
250
200
150
100
50
0
**
CON
D55
CON
D55

B

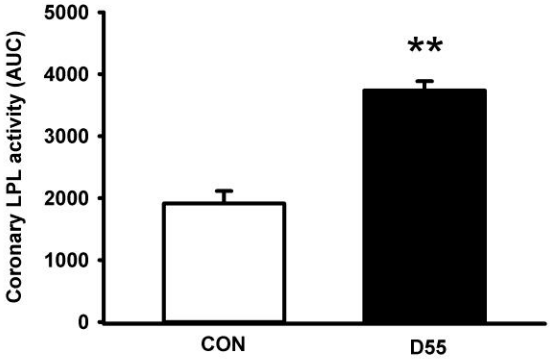
Coronary LPL activity (AUC)
5000
4000
3000
2000
1000
0
**
CON
D55

**Figure 12 Increased LPL activity in STZ-induced diabetic hearts is associated with RhoA activation.**

Male Wistar rats (250-320 g) were injected i.v. with 55 mg/kg STZ (D55), and animals kept for 4 days before hearts were removed. Particulate fractions were isolated from whole heart homogenates of control (CON) and D55 animals, and RhoA recruitment to the particulate fraction determined by Western blot (A). In a separate experiment, hearts were also perfused with heparin (5 U/ml) to release coronary LPL. Coronary effluents were collected (for 10 s) at different time points over 5 min, and LPL activity in each fraction determined. The results are presented as area under the curve for heparin-released LPL activity over 5 min (B). **P*<0.05, compared to CON, n= 3.

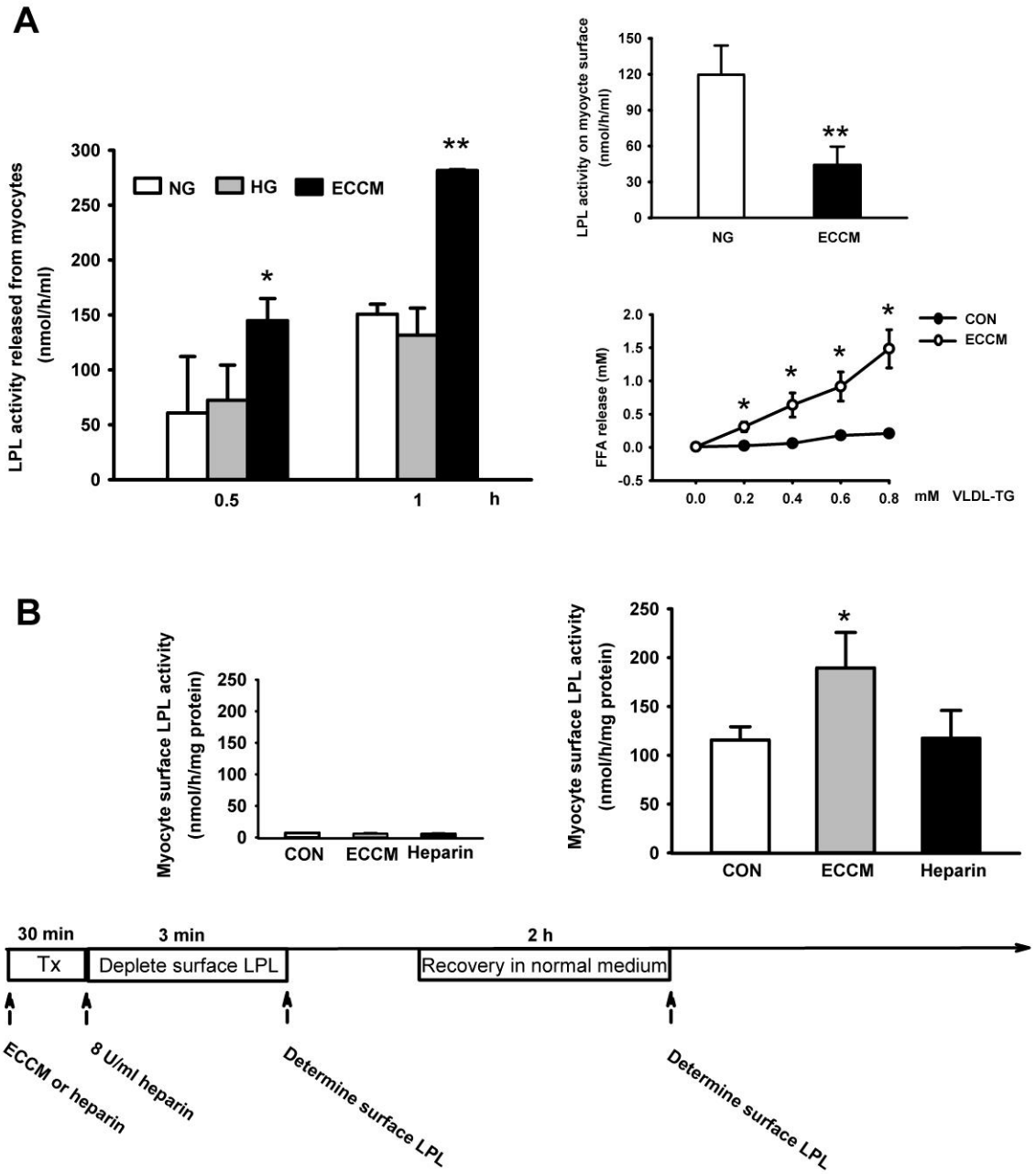
A
LPL activity released from myocytes (nmol/h/ml)
NG
HG
ECCM
0.5
1
h
LPL activity on myocyte surface (nmol/h/ml)
NG
ECCM
FFA release (mM)
CON
ECCM
mM VLDL-TG
B
Myocyte surface LPL activity (nmol/h/mg protein)
CON
ECCM
Heparin
30 min
3 min
2 h
Tx
Deplete surface LPL
Recovery in normal medium
ECCM or heparin
8 U/ml heparin
Determine surface LPL
Determine surface LPL

**Figure 13 Endothelial cell conditioned media increases LPL secretion from cardiomyocytes.**

ECCM was applied to cardiomyocytes, and at the indicated times, LPL activity released into the medium determined. Cardiomyocytes were also incubated with 5.5 mM glucose (NG) and 25 mM glucose (HG) as controls (A). After 30 min incubation with NG or ECCM, LPL remaining on the myocyte surface was released by incubating cells with 8 U/ml heparin for 3 min, and LPL activity determined (A, inset, upper panel). Cardiomyocytes were treated with 5.5 mM glucose DMEM (CON) or ECCM for 30 min, and the medium collected. This medium was then incubated with increasing concentrations of VLDL-TG (0-0.8 mM) and the concentration of released free fatty acids determined after 30 min (A, inset, bottom panel). $^{*}P<0.05$, $^{**}P<0.01$, compared to NG, n=3-5. Isolated cardiomyocytes were treated with 5.5 mM glucose (CON), ECCM, or 10 mU/ml heparin for 30 min. Following this, surface LPL was depleted by incubating these cells with 8 U/ml heparin for 3 min. To validate depletion of this surface LPL, 8 U/ml heparin was given and surface LPL activity determined (B, left panel). Following a wash with PBS, cells were allowed to recover in 5.5 mM glucose DMEM for 2 h. LPL activity recruited to the myocyte surface was then determined (B, right panel). $^{*}P<0.05$, compared to CON, n= 3.

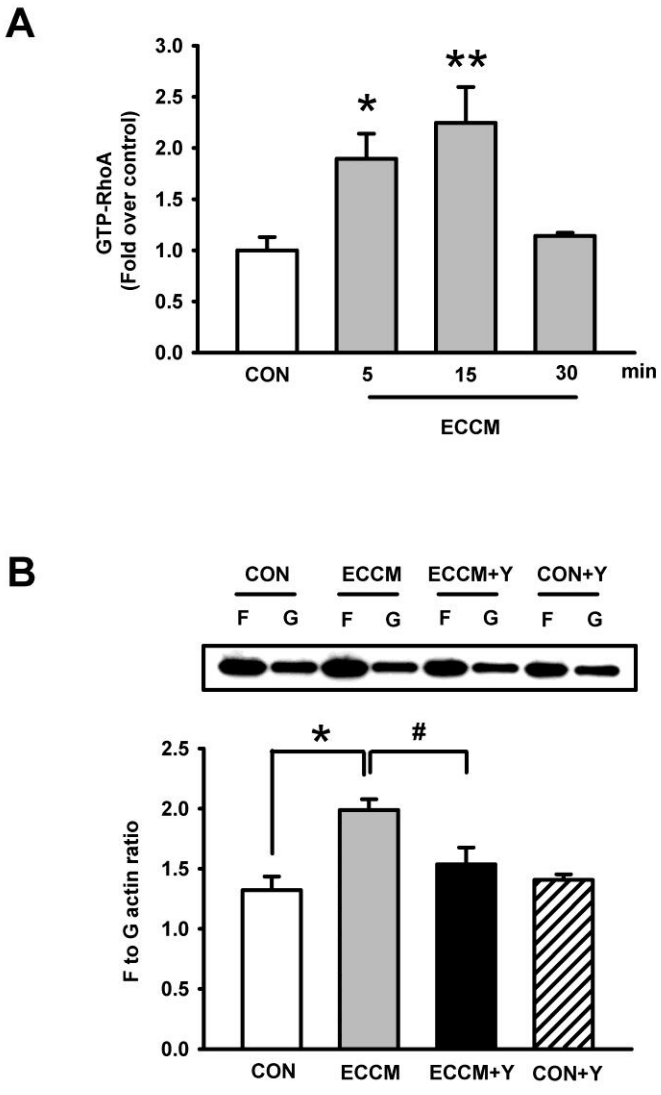
A
GTP-RhoA
(Fold over control)
3.0
2.5
2.0
1.5
1.0
0.5
0.0
*
**
CON
5
15
30
min
ECCM
B
CON
ECCM
ECCM+Y
CON+Y
F G F G F G F G
F to G actin ratio
2.5
2.0
1.5
1.0
0.5
0.0
*
#
CON
ECCM
ECCM+Y
CON+Y

**Figure 14 ECCM induces RhoA-mediated actin cytoskeleton polymerization.**

Myocytes were incubated with ECCM for 5, 15 or 30 min, and RhoA activation evaluated by measuring GTP-bound RhoA. Results were compared to myocytes incubated with 5.5 mM glucose DMEM (CON, A). In a different experiment, F to G actin ratio was measured 1 h following incubation with ECCM (B). 10 μM Y-27632 was also added to myocytes 30 min prior to ECCM (ECCM+Y), and actin cytoskeleton polymerization evaluated (B). $^{*}P<0.05$, $^{**}P<0.01$, compared to CON; $^{\#}P<0.05$, compared to ECCM, n=3-4.

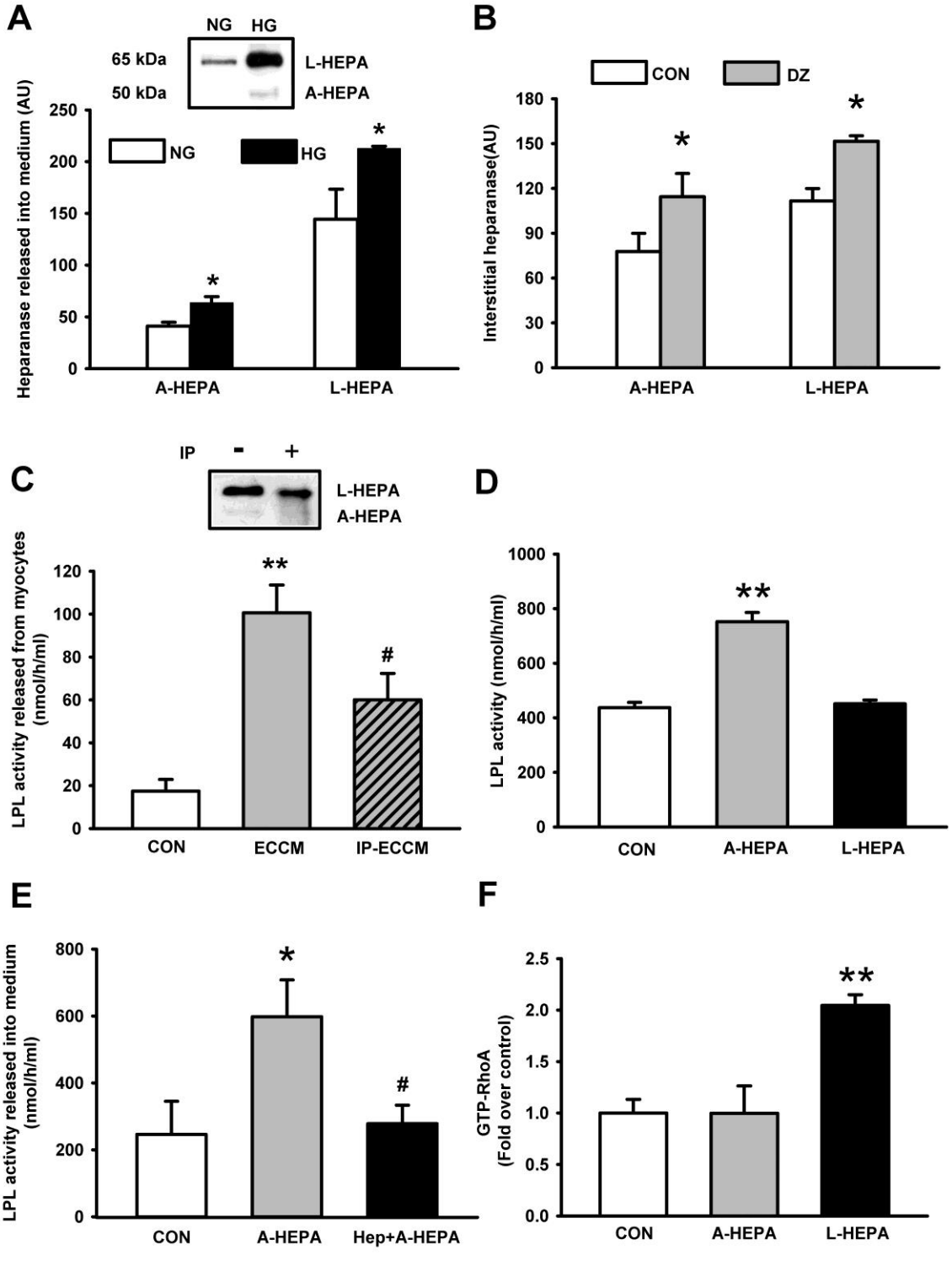
A
NG HG
65 kDa
50 kDa
L-HEPA
A-HEPA
NG
HG
Heparanase released into medium (AU)
250
200
150
100
50
0
*
*
A-HEPA
L-HEPA
B
CON
DZ
Interstitial heparanase(AU)
180
150
120
90
60
30
0
*
*
A-HEPA
L-HEPA
C
IP - +
L-HEPA
A-HEPA
LPL activity released from myocytes (nmol/h/ml)
120
100
80
60
40
20
0
**
#
CON
ECCM
IP-ECCM
D
LPL activity (nmol/h/ml)
1000
800
600
400
200
0
**
CON
A-HEPA
L-HEPA
E
LPL activity released into medium (nmol/h/ml)
800
600
400
200
0
*
#
CON
A-HEPA
Hep+A-HEPA
F
GTP-RhoA (Fold over control)
2.5
2.0
1.5
1.0
0.5
0.0
**
CON
A-HEPA
L-HEPA

**Figure 15 Latent and active heparanase have divergent effects on LPL secretion.**

bCAEC were incubated with 5.5 mM (NG), or 25 mM (HG) glucose DMEM for 30 min. The amount of latent and active heparanase released into the medium was determined by Western blot (A). Control and DZ hearts were perfused using a modified Langendorff perfusion technique to separate interstitial fluid from coronary perfusate. Latent (65 kDa) and active heparanase (50 kDa) were measured by Western blot in the interstitial fluid (B). Heparanase was immunoprecipitated from ECCM by an anti-heparanase antibody and the amount of latent and active heparanase remaining in this ECCM was determined and compared to the original ECCM using Western blot (C, inset). This immunoprecipitated ECCM (IP-ECCM) was applied to myocyte for 30 min, and LPL activity released into medium tested (C). $^{*}P<0.05$, compared to NG or CON; $^{\#}P<0.05$, compared to ECCM, n=3-4. Isolated cardiomyocytes were incubated with medium 199 (CON) and 1 μg/ml purified active (A-HEPA) or latent (L-HEPA) heparanase for 30 min, and LPL activity released into the medium determined (D). In a different experiment, myocytes were pre-incubated with 8 U/ml heparin for 3 min before 1 μg/ml purified active heparanase (Hep+A-HEPA), and LPL activity released after 30 min determined (E). Results were compared to CON and myocytes without heparin pre-incubation (A-HEPA). RhoA activation was measured in cardiomyocytes in the presence of 1 μg/ml active (A-HEPA) or latent (L-HEPA) heparanase for 15 min (F). $^{*}P<0.05$, $^{**}P<0.01$, compared to CON; $^{\#}P<0.05$, compared to A-HEPA, n=3.

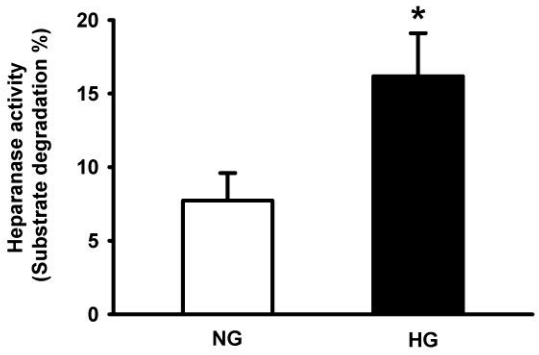
Heparanase activity
(Substrate degradation %)
20
15
10
5
0
*
NG
HG

**Figure 16 High glucose induced release of active heparanase.**

bCAECs were treated with 5.5 (NG) or 25 (HG) mM glucose DMEM for 30 min, and medium collected to measure heparanase activity with a kit (A). *$P$<0.05, compared to NG, n=4.

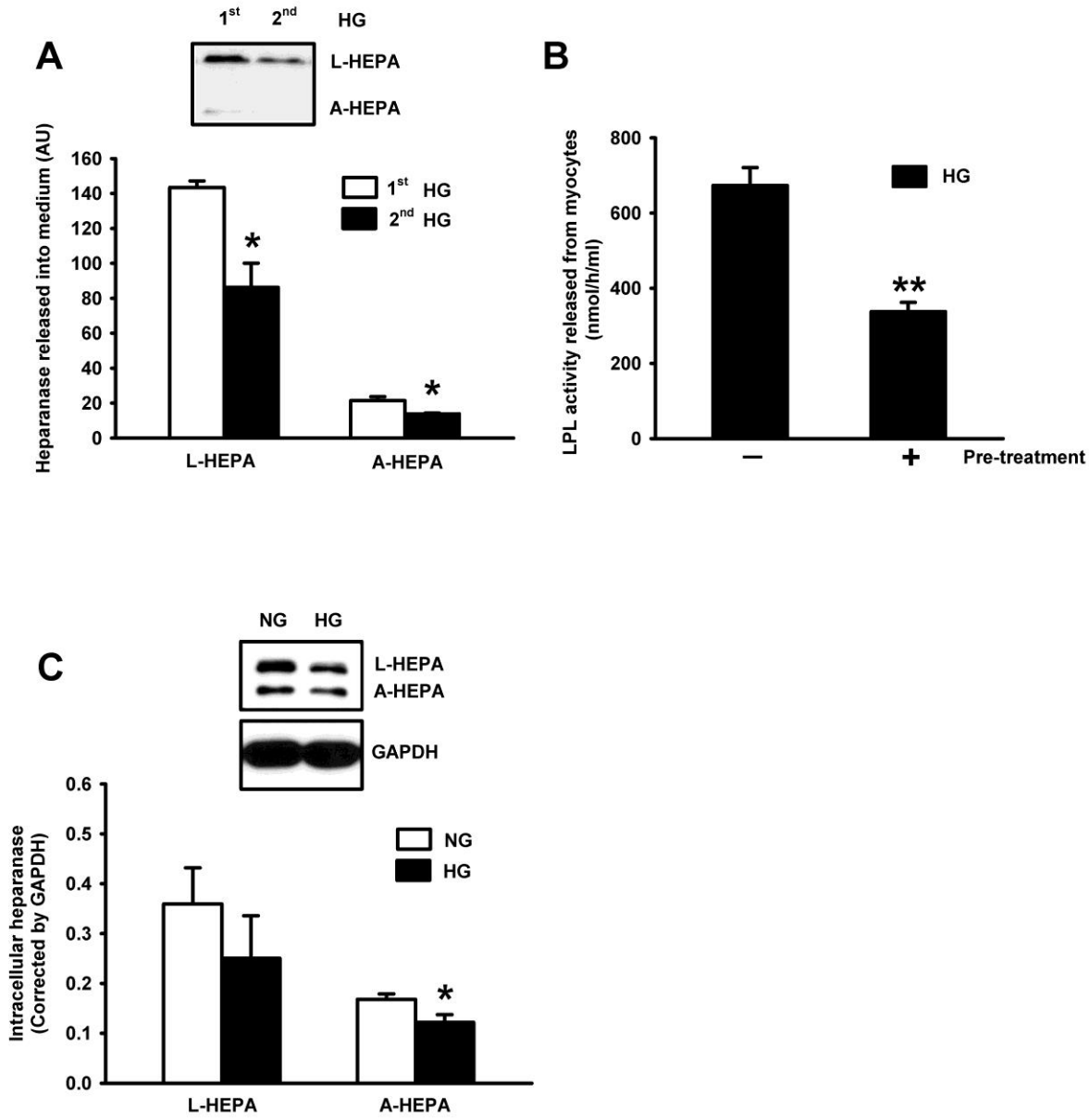
A
1st
2nd
HG
L-HEPA
A-HEPA
Heparanase released into medium (AU)
160
140
120
100
80
60
40
20
0
1st HG
2nd HG
*
*
L-HEPA
A-HEPA
B
LPL activity released from myocytes (nmol/h/ml)
800
600
400
200
0
HG
**
–
+
Pre-treatment
C
NG
HG
L-HEPA
A-HEPA
GAPDH
Intracellular heparanase (Corrected by GAPDH)
0.6
0.5
0.4
0.3
0.2
0.1
0.0
NG
HG
*
L-HEPA
A-HEPA

**Figure 17 High glucose affects heparanase secretion from endothelial cells.**

bCAECs were treated with 25 mM glucose DMEM for 30 min, medium removed (1$^{st}$ HG), and the cells exposed to a second 30 min incubation with 25 mM glucose DMEM (2$^{nd}$ HG). The amounts of latent and active heparanase in the medium of the 1$^{st}$ and 2$^{nd}$ HG treatment were measured by Western blot (A). **P*<0.05, compared to 1$^{st}$ HG release, n=3. In a co-culture system, cardiomyocytes placed in the bottom chamber were pre-incubated with 200 μg purified LPL for 30 min to saturate myocyte surface HSPGs. Cells were washed with PBS to remove unbound LPL. bCAECs that were pre-treated with 25 mM glucose DMEM for 30 min were then placed in the upper chamber of the co-culture system. 25 mM glucose DMEM was applied to the co-culture system, and the medium from the bottom chamber collected after 30 min to determine LPL activity released from cardiomyocytes. Results were compared to a co-culture system in which bCAECs was not pre-treated with high glucose. ***P*<0.01, n=3 (B). bCAECs were treated with either 5 (NG) or 25 (HG) mM glucose DMEM for 30 min, and intracellular heparanase determined by Western blot (C). **P*<0.05, compared to NG, n=3 (C).

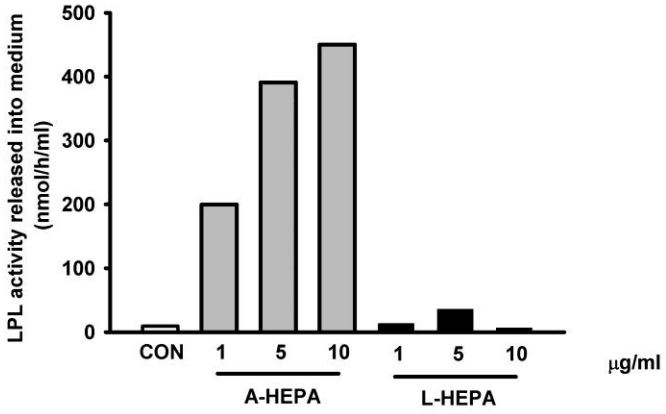
LPL activity released into medium
(nmol/h/ml)
500
400
300
200
100
0
CON
1
5
10
1
5
10
μg/ml
A-HEPA
L-HEPA

**Figure 18 Active heparanase releases myocyte surface LPL in a dose-dependent manner.**

Isolated myocytes were incubated with increasing concentrations of active (A-HEPA) or latent (L-HEPA) heparanase for 30 min, and LPL activity released into the medium determined. 5.5 mM glucose DMEM was used as control (CON).

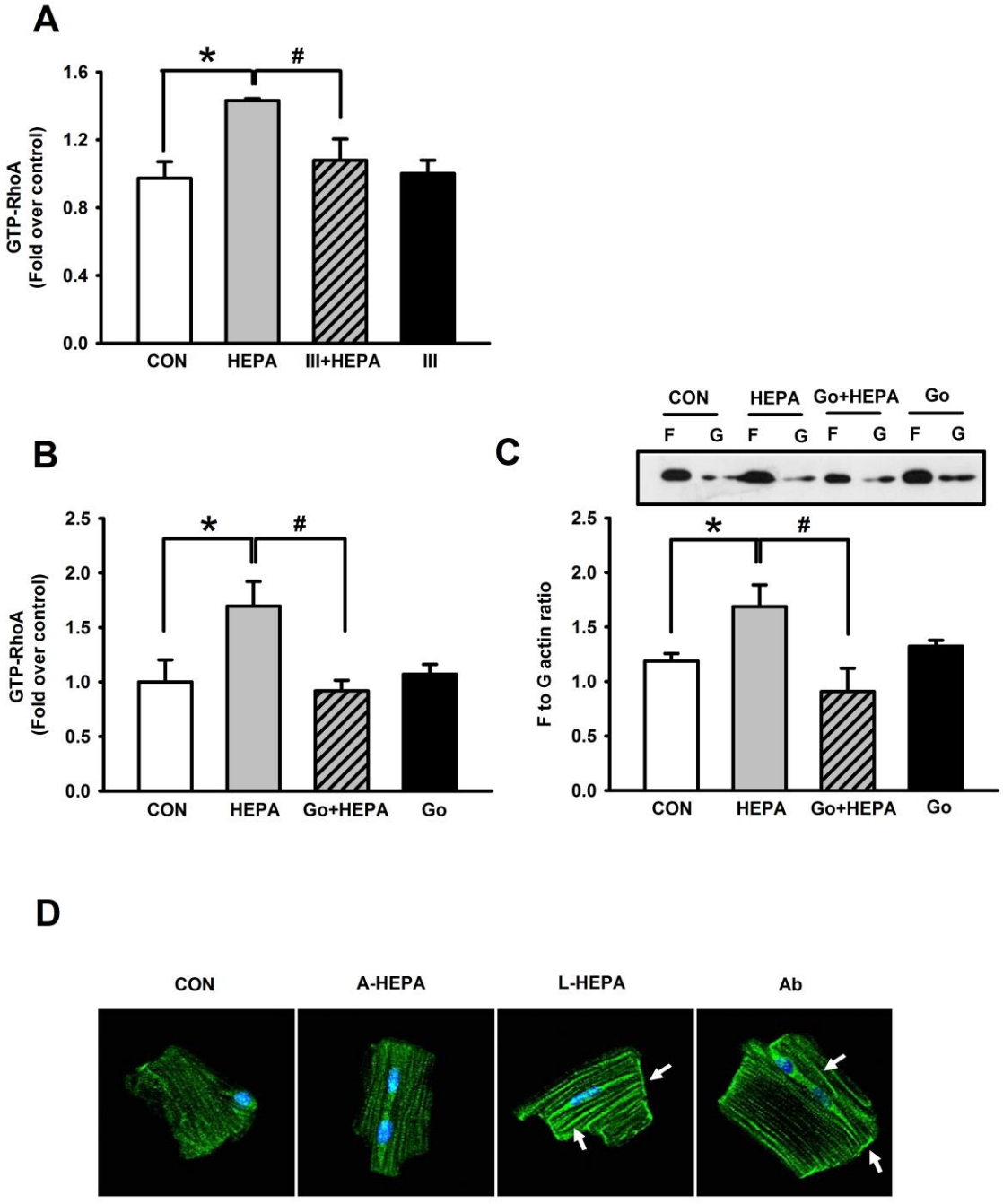
A
GTP-RhoA
(Fold over control)
1.6
1.2
0.8
0.4
0.0
*
#
CON
HEPA
III+HEPA
III
B
GTP-RhoA
(Fold over control)
2.5
2.0
1.5
1.0
0.5
0.0
*
#
CON
HEPA
Go+HEPA
Go
C
CON
HEPA
Go+HEPA
Go
F
G
F
G
F
G
F
G
F to G actin ratio
2.5
2.0
1.5
1.0
0.5
0.0
*
#
CON
HEPA
Go+HEPA
Go
D
CON
A-HEPA
L-HEPA
Ab

**Figure 19 Activation of RhoA by latent heparanase requires HSPGs and PKC.**

Myocytes were pre-treated with (III+HEPA) or without (HEPA) 10 IU/L heparinase III for 30 min, and RhoA activation determined 15 min following incubation with 1 µg/ml latent heparanase. The effect of heparinase III *per se* on RhoA activation was also evaluated (III) (A). A similar experiment was repeated, except that 5 µM Gö6976 was used to pre-treat the myocytes (B). In this experiment, F to G actin ratio was evaluated 1 h following addition of latent heparanase (C). Isolated cardiomyocytes were treated with 1 µg/ml active (A-HEPA) or latent (L-HEPA) heparanase, or 3 µg/ml anti-syndecan-4 antibody (Ab) for 30 min, and syndecan-4 distribution visualized by immunofluorenscence (D). $^{*}P<0.05$, compared to CON, n=3. $^{\#}P<0.05$, compared to HEPA, n=3.

A

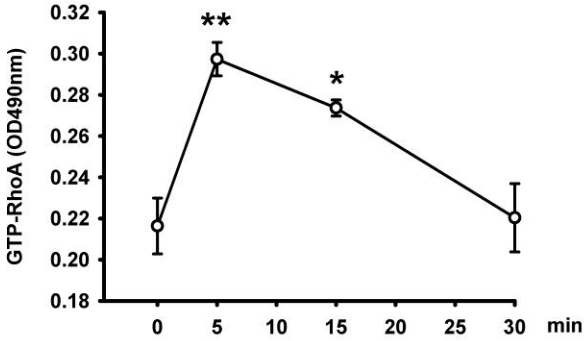
GTP-RhoA (OD490nm)
0.32
0.30
0.28
0.26
0.24
0.22
0.20
0.18
**
*
0
5
10
15
20
25
30
min

B

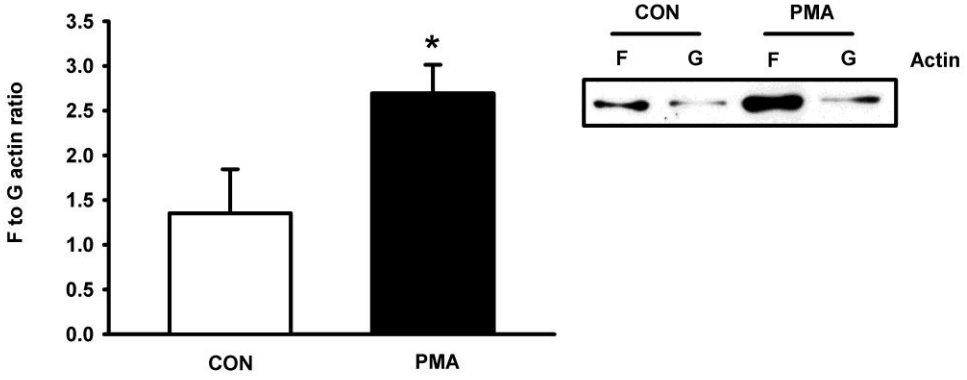
F to G actin ratio
3.5
3.0
2.5
2.0
1.5
1.0
0.5
0.0
*
CON
PMA
CON
PMA
F
G
F
G
Actin

**Figure 20 Activation of RhoA by PMA leads to actin cytoskeleton polymerization.**

Isolated myocytes were treated with 1 μM PMA for the indicated times, and RhoA activation determined using a G-LISA assay kit (A). Actin cytoskeleton polymerization in these cells was determined 1 h following PMA treatment (B). **P*<0.05, ***P*<0.01, compared to CON, n= 3.

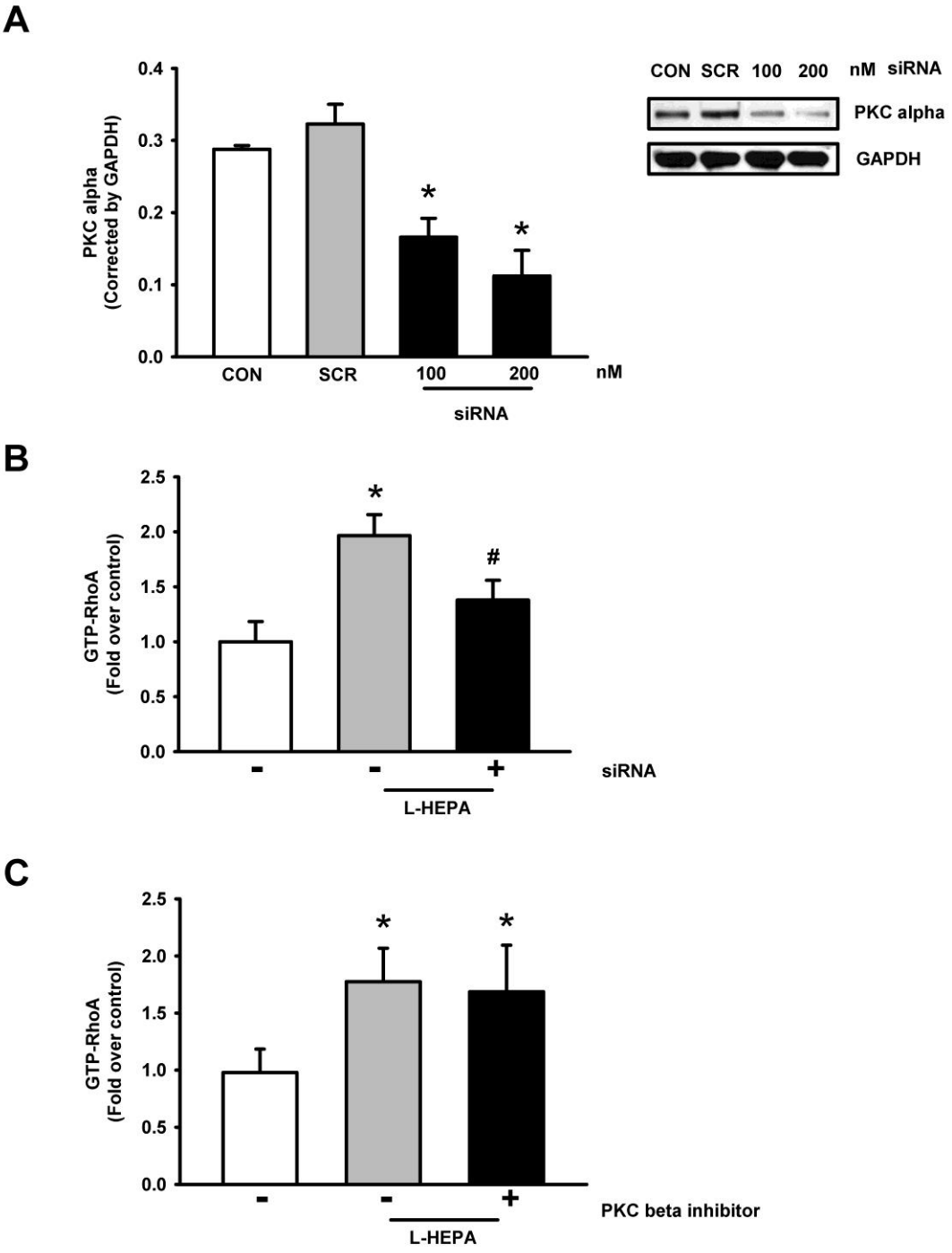
A
PKC alpha
(Corrected by GAPDH)
0.4
0.3
0.2
0.1
0.0
CON
SCR
100
200
nM
siRNA
*
*
CON SCR 100 200 nM siRNA
PKC alpha
GAPDH
B
GTP-RhoA
(Fold over control)
2.5
2.0
1.5
1.0
0.5
0.0
*
#
-
-
+
siRNA
L-HEPA
C
GTP-RhoA
(Fold over control)
2.5
2.0
1.5
1.0
0.5
0.0
*
*
-
-
+
PKC beta inhibitor
L-HEPA

**Figure 21 PKCα is important for RhoA activation by latent-heparanase.**

In a 6-well plate, isolated myocytes from control rats (CON) were transfected with siRNA specific for PKCα at 100 or 200 nM or control unrelated siRNA (SCR, 200 nM). 24 h following transfection, medium was changed to Media 199 and following an additional 24 h, cells were collected to Western Blot for PKCα (A). **P*<0.05, compared to SCR, n=3. In a separate experiment, myocytes were transfected with 200 nM siRNA for PKCα (+) or 200 nM control unrelated siRNA (-), before being exposed to 1 μg/ml latent heparanase for 15 min. GTP-bound RhoA in these myocytes were determined (B). 200 nM PKCβ inhibitor was given to mycoytes 1 h before and during incubation with latent heparanase for 15 min, and RhoA activation also determined in these myocytes (C). Results were from 3 experiments using different control animals. **P*<0.05, compared to control, #*P*<0.05, compared to control treated with L-HEPA.

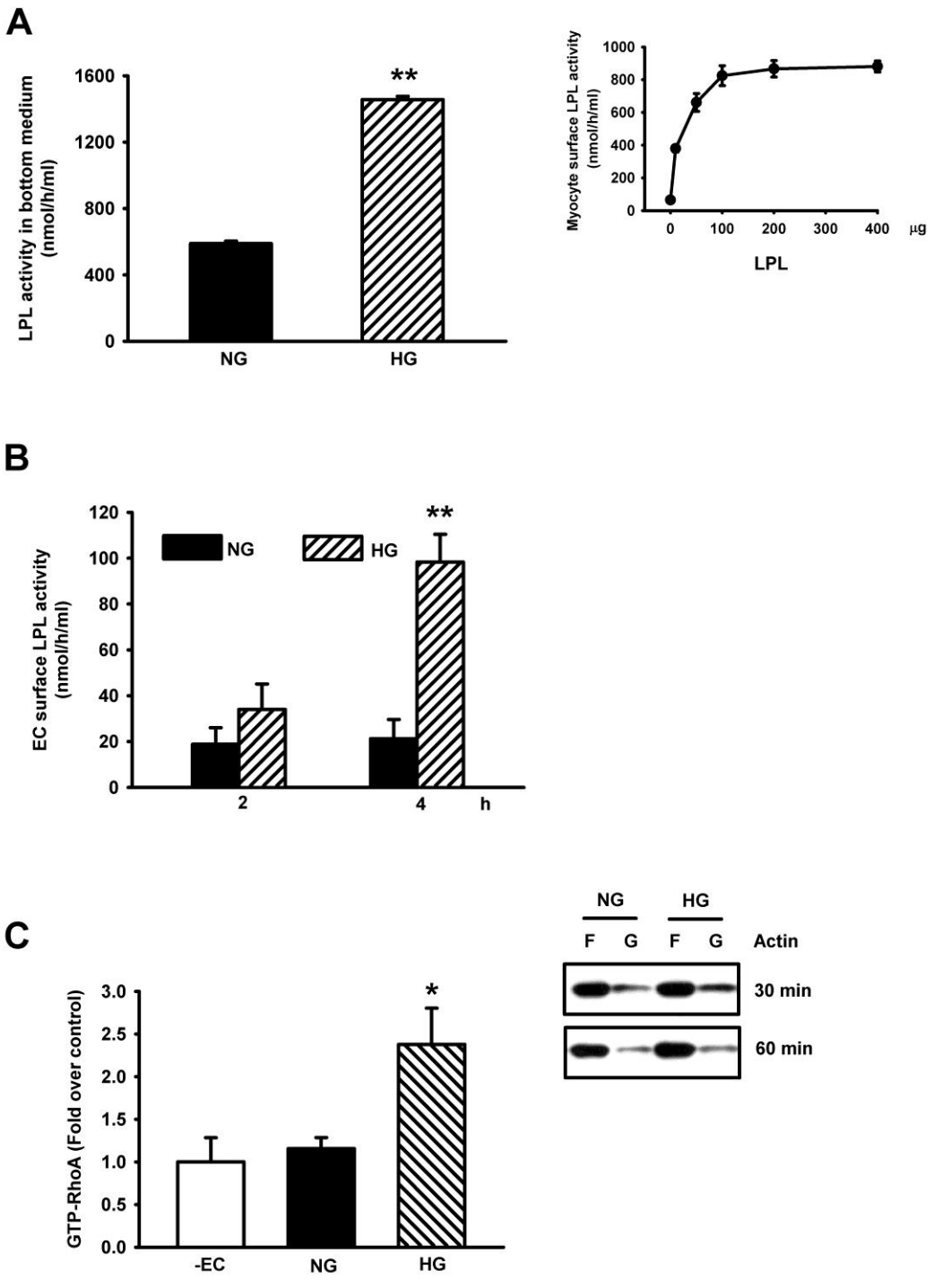
A
LPL activity in bottom medium (nmol/h/ml)
1600
1200
800
400
0
**
NG
HG
Myocyte surface LPL activity (nmol/h/ml)
1000
800
600
400
200
0
0
100
200
300
400
µg
LPL
B
EC surface LPL activity (nmol/h/ml)
120
100
80
60
40
20
0
NG
HG
**
2
4
h
C
GTP-RhoA (Fold over control)
3.0
2.5
2.0
1.5
1.0
0.5
0.0
*
-EC
NG
HG
NG
HG
F
G
F
G
Actin
30 min
60 min

**Figure 22 Co-culture with endothelial cells increased LPL secretion in the presence of high glucose.**

A co-culture was carried out using EC in the insert (top) and cardiomyocytes in the well (bottom). Cardiomyocytes were loaded with increasing amount of purified LPL for 30 min, and LPL activity bound to the myocyte surface was determined (A, inset). Myocytes were loaded with 200 μg purified LPL for 30 min, and washed with PBS to remove unbound LPL. Inserts with EC were placed on top, and the co-culture was exposed to normal glucose (NG, 5.5 mM) or high glucose (HG, 25 mM). Medium was collected from the lower chamber after 30 min, and LPL activity determined (A). After 2 and 4 h, LPL activity at the EC surface was also released and tested by incubating these cells with 8 U/ml heparin for 3 min (B). In this co-culture, activation of RhoA was measured in myocytes after 30 min, and compared to cells that did not have EC in the top chamber (-EC) (C). F to G actin ratio was also tested at 30 and 60 min (C, inset). *$P<0.05$, compared to NG, n=3.

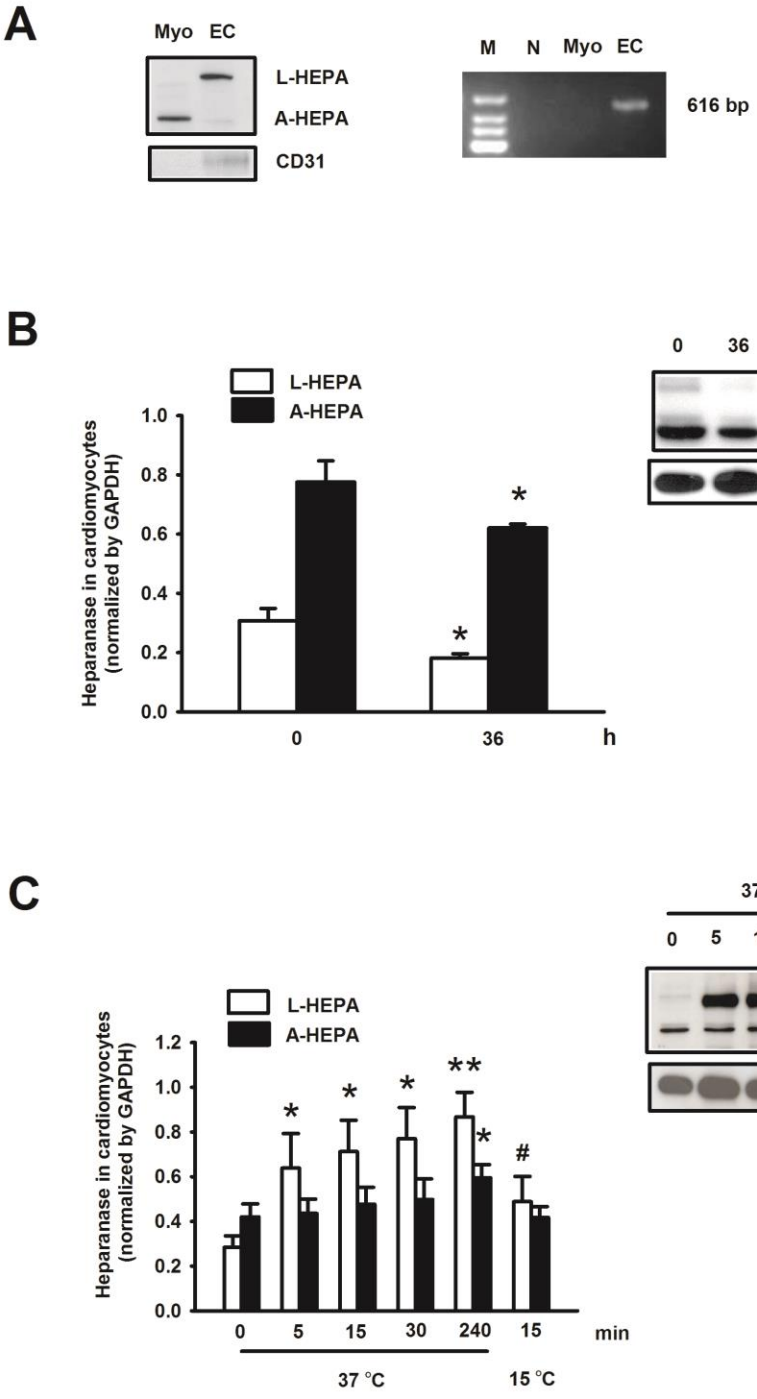
A
Myo EC
L-HEPA
A-HEPA
CD31
M N Myo EC
616 bp
B
0 36 h
L-HEPA
A-HEPA
GAPDH
L-HEPA
A-HEPA
Heparanase in cardiomyocytes (normalized by GAPDH)
1.0
0.8
0.6
0.4
0.2
0.0
*
*
0
36
h
C
37 °C
15 °C
0 5 15 30 240 15 min
L-HEPA
A-HEPA
GAPDH
L-HEPA
A-HEPA
Heparanase in cardiomyocytes (normalized by GAPDH)
1.2
1.0
0.8
0.6
0.4
0.2
0.0
*
*
*
**
*
#
0 5 15 30 240 15 min
37 °C
15 °C

**Figure 23 Heparanase is detected in cardiomyocytes.**

To validate the purity of cardiomyocytes, equal amounts of protein from cardiomyocytes (Myo) and RAOEC (EC) were used to determine the presence of CD31. Both cell lysates were also used to probe for latent (L-HEPA) and active heparanase (A-HEPA) by Western blot (A, left panel). 1 μg total RNA from cardiomyocytes and EC was used for RT-PCR. Amplified DNA products were run on an agrose gel in line with a DNA ladder (M), and a negative control (N, using water to replace PCR product) to detect heparanase gene expression (A, right panel). Cardiomyocytes from control rats were isolated, plated and allowed to settle down. Total cell lysates were then collected at 0 or 36 h, and probed for L-HEPA and A-HEPA using Western blot (B). 500 ng/ml purified latent heparanase was added to isolated myocytes and heparanase content in these cells was determined at the indicated times by Western blot. To inhibit internalization, myocytes were also incubated with heparanase at 15 ºC for 15 min (C). Results are the mean ± SE of 3 repeated experiments using different animals. *Significantly different from 0 time point, $P < 0.05$. **Significantly different from 0 time point, $P < 0.01$. $^{\#}$Significantly different from results at 15 min at 37 ºC for L-HEPA.

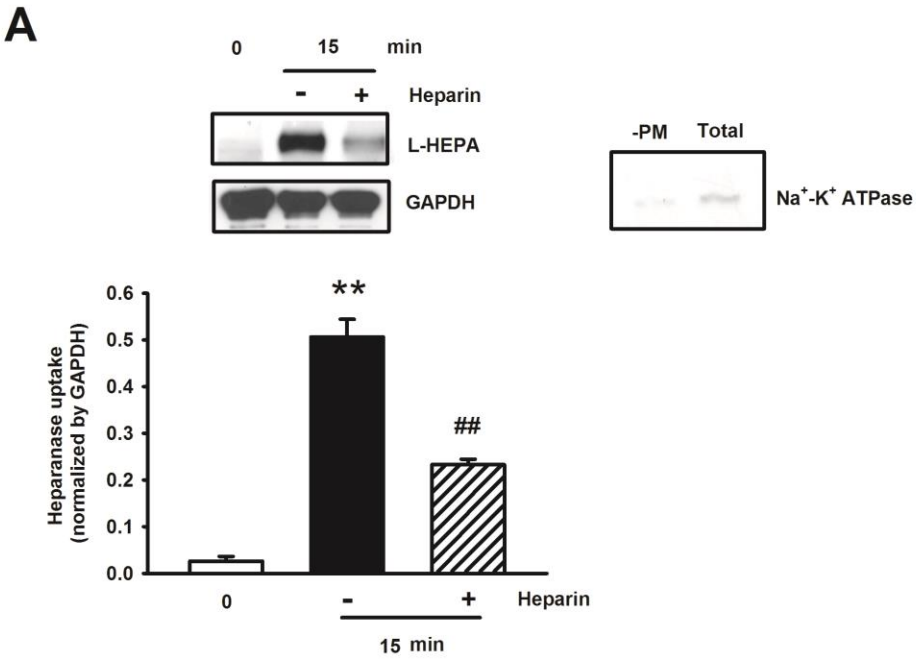
A
0
15
min
-
+
Heparin
L-HEPA
GAPDH
-PM
Total
Na+-K+ ATPase
Heparanase uptake
(normalized by GAPDH)
0.6
0.5
0.4
0.3
0.2
0.1
0.0
**
##
0
-
+
Heparin
15 min

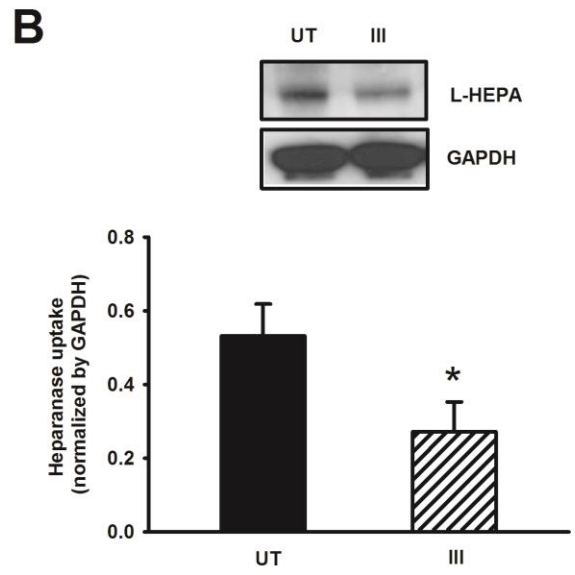
B
UT
III
L-HEPA
GAPDH
Heparanase uptake
(normalized by GAPDH)
0.8
0.6
0.4
0.2
0.0
*
UT
III

**Figure 24 Internalization of heparanase by cardiomyocytes is mediated by HSPGs.**

Isolated cardiomyocytes were treated with 500 ng/ml purified latent heparanase in the absence or presence of 10 IU/ml heparin for 15 min. Cell lysates devoid of plasma membrane (-PM) were used to monitor internalization of latent heparanase (A). To determine the purity of these cell lysates, 10 μg protein from –PM or total cell lysates (Total) was used to Western blot for the plasma membrane marker $Na^+$-$K^+$-ATPase (A, inset). Isolated myocytes were untreated (UT) or pre-treated with 10 IU/L heparitinase III for 2 h, and incubated with 500 ng/ml purified latent heparanase for 15 min. Internalization of latent heparanase was determined using –PM fraction (B). Results are the mean ± SE of 3 repeated experiments using different animals. **Significantly different from 0 time point, $P < 0.01$. ##Significantly different from 15 min without heparin. *Significantly different from untreated myocytes, $P < 0.05$.

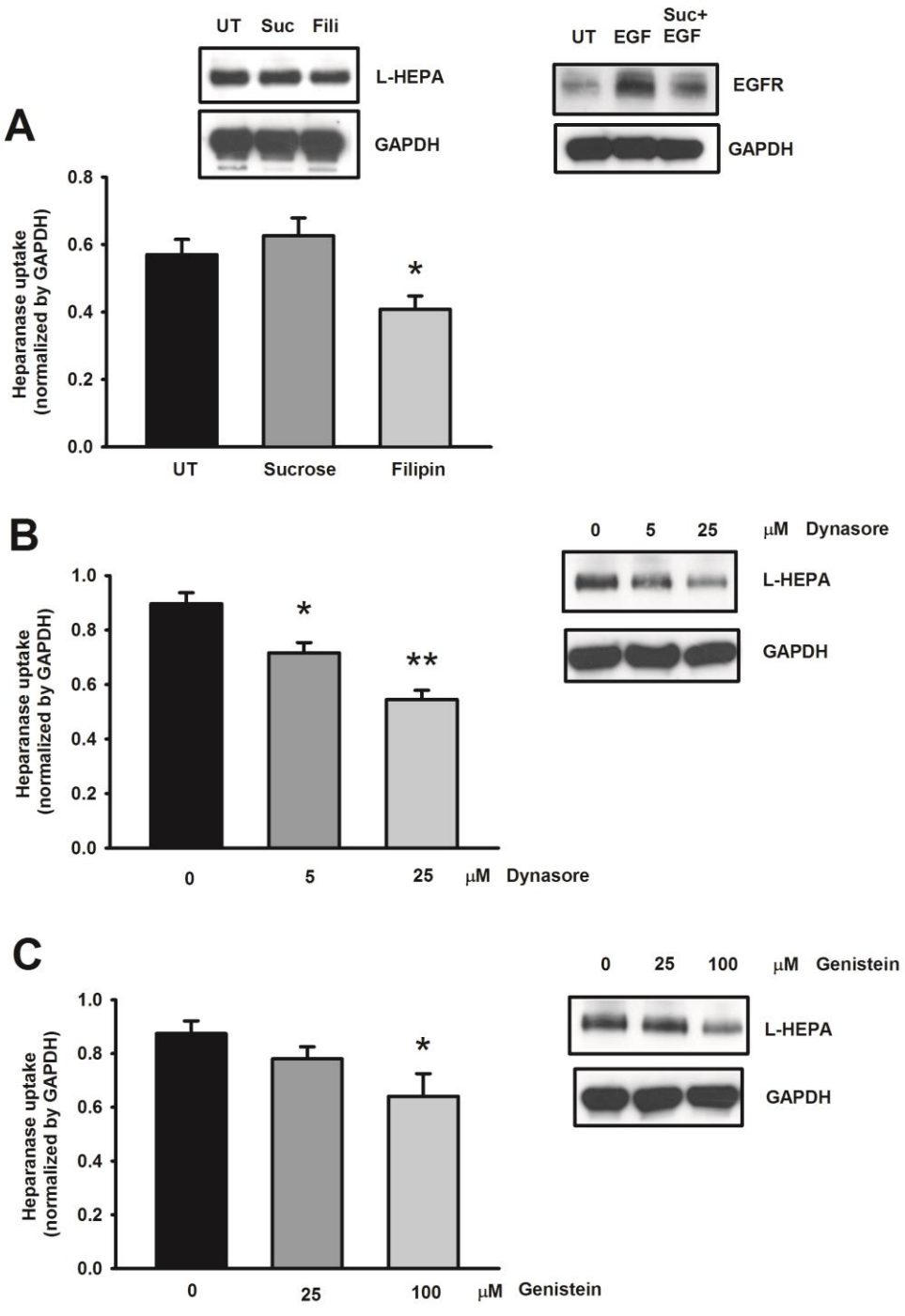
A
UT Suc Fili
L-HEPA
GAPDH
UT EGF Suc+ EGF
EGFR
GAPDH
Heparanase uptake (normalized by GAPDH)
0.8
0.6
0.4
0.2
0.0
*
UT
Sucrose
Filipin
B
0 5 25 μM Dynasore
L-HEPA
GAPDH
Heparanase uptake (normalized by GAPDH)
1.0
0.8
0.6
0.4
0.2
0.0
*
**
0
5
25 μM Dynasore
C
0 25 100 μM Genistein
L-HEPA
GAPDH
Heparanase uptake (normalized by GAPDH)
1.0
0.8
0.6
0.4
0.2
0.0
*
0
25
100 μM Genistein

**Figure 25 Internalization of latent heparanase is caveolae-dependent and requires dynamin and tyrosine kinase activity.**

Isolated cardiomyocytes were incubated with 350 mM sucrose (to inhibit clathrin-coated pit formation) or 1 μg/ml filipin (to inhibit caveolae-dependent internalization) for 15 min before 500 ng/ml purified latent heparanase was added into the medium. Internalization of latent heparanase was measured after 15 min using –PM fractions (A). The inhibitory effect of sucrose on clathrin-coated pit dependent internalization was validated by testing the internalization of epidermal growth factor receptor (EGFR) in myocytes treated with EGF in the presence or absence of sucrose (A, right inset). In a different experiment, isolated myocytes were pre-treated with either 0-25 μM dynasore (to inhibit dynamin activity, B) or 0-100 μM genistein (to inhibit tyrosine kinase activity, C) for 1 h, and internalization of latent heparanase after 15 min determined using Western blot. Results are the mean ± SE of 3 repeated experiments using different animals. *Significantly different from untreated myocytes, $P < 0.05$. **Significantly different from untreated myocytes, $P < 0.01$.

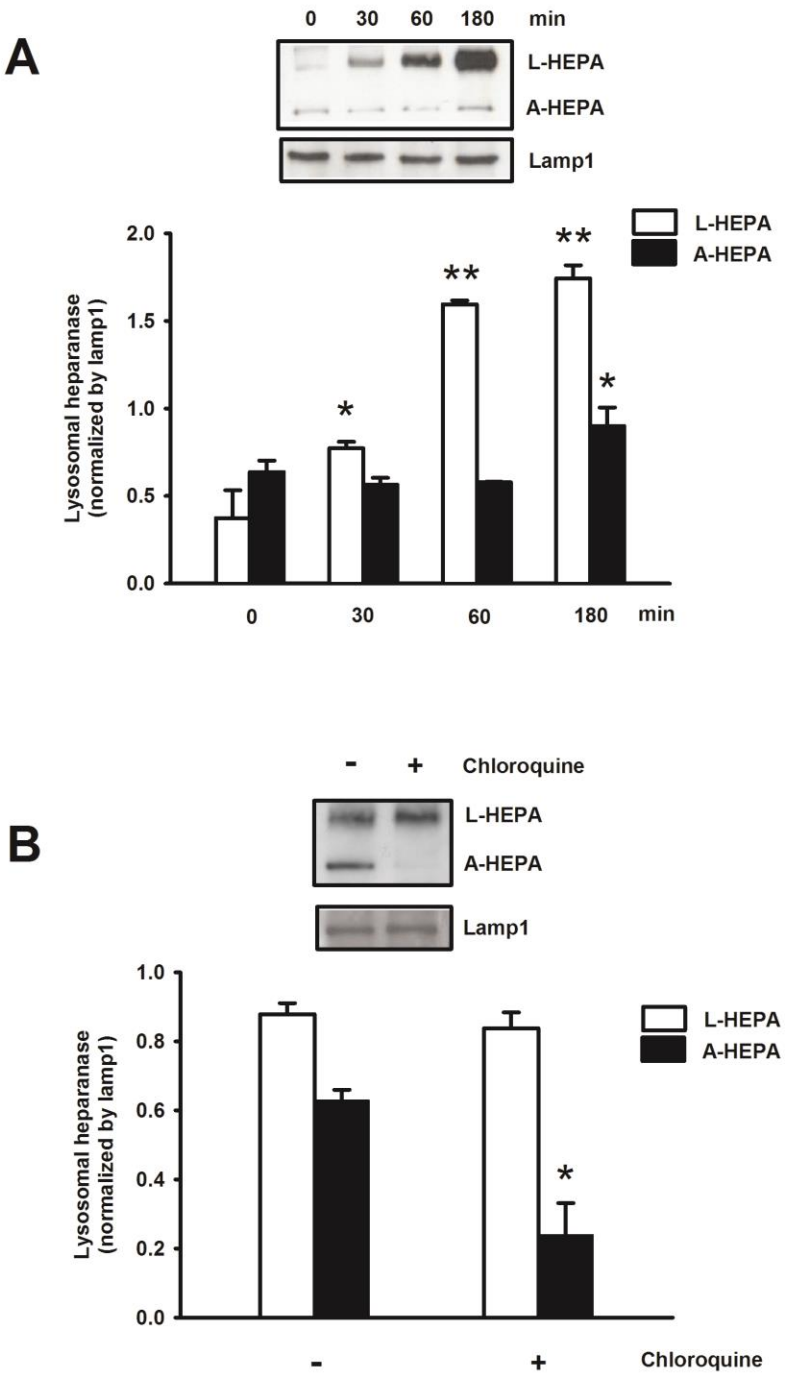
A
0
30
60
180
min
L-HEPA
A-HEPA
Lamp1
Lysosomal heparanase
(normalized by lamp1)
2.0
1.5
1.0
0.5
0.0
*
**
**
*
L-HEPA
A-HEPA
0
30
60
180
min
B
-
+
Chloroquine
L-HEPA
A-HEPA
Lamp1
Lysosomal heparanase
(normalized by lamp1)
1.0
0.8
0.6
0.4
0.2
0.0
*
L-HEPA
A-HEPA
-
+
Chloroquine

**Figure 26 Following uptake exogenous latent heparanase is activated in lysosomes.**

Isolated myocytes were incubated with 500 ng/ml purified latent heparanase for the indicated times. Fractions rich in lysosomes were isolated to detect heparanase by Western blot. Lysosomal-associated membrane protein 1 (Lamp1) was used as a marker to indicate equal loading of lysosomal protein (A). Myocytes were pre-incubated with 200 μM chloroquine before latent heparanase was added to the medium. Heparanase in the lysosomal fraction was measured after 3 h (B). Results are the mean ± SE of 3 repeated experiments using different animals. *Significantly different from 0 time point or untreated myocytes, $P < 0.05$. **Significantly different from 0 time point, $P < 0.01$.

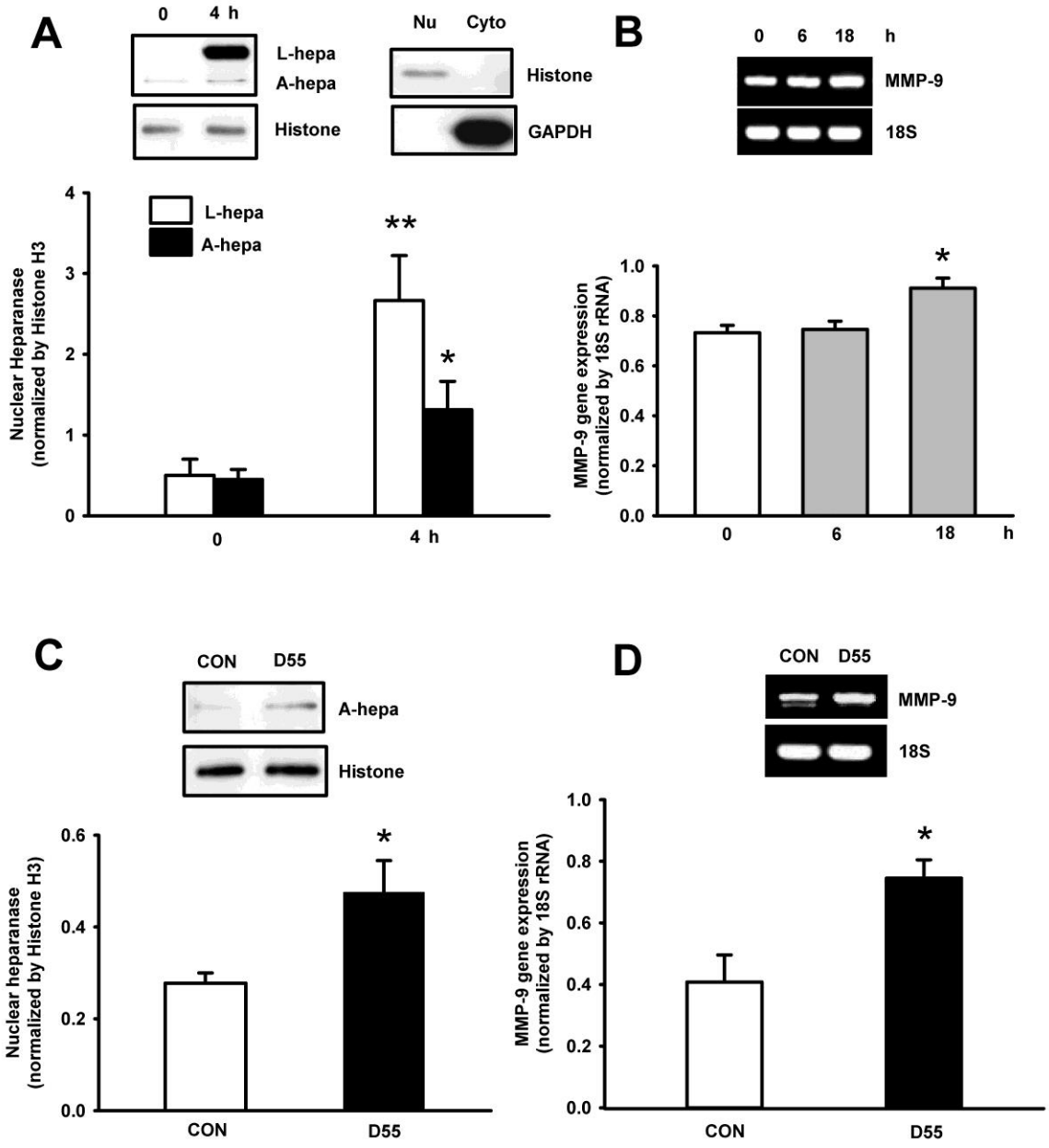
A
0
4 h
L-hepa
A-hepa
Histone
Nu
Cyto
Histone
GAPDH
B
0
6
18
h
MMP-9
18S
L-hepa
A-hepa
Nuclear Heparanase
(normalized by Histone H3
**
*
0
4 h
MMP-9 gene expression
(normalized by 18S rRNA)
*
0
6
18
h
C
CON
D55
A-hepa
Histone
Nuclear heparanase
(normalized by Histone H3)
*
CON
D55
D
CON
D55
MMP-9
18S
MMP-9 gene expression
(normalized by 18S rRNA)
*
CON
D55

**Figure 27 Nuclear entry of heparanase is accompanied by increased gene expression of MMP-9.**

Isolated myocytes were incubated with 500 ng/ml purified latent heparanase for the indicated times. Nuclear fraction was separated from cytosolic protein to detect heparanase by Western blot (A). To validate the purity of the nuclear fraction, equal amount of protein from both cytosolic and nuclear fractions were Western blotted for GAPDH and histone H3 (A, right inset). Total RNA was extracted from heparanase treated cardiomyoytes to measure gene expression of MMP-9 using RT-PCR (B). Animals were made diabetic by injecting 55 mg/kg i.p. STZ and kept for 4 days (D55). The amount of heparanase in the nuclear fractions of myocytes isolated from control and D55 heart was measured by Western blot (C). MMP-9 gene expression was also determined in isolated myocytes from these animals (D). Results are the mean ± SE of 3 repeated experiments using different animals. *Significantly different from 0 time point or control, $P < 0.05$. **Significantly different from 0 time point or control, $P < 0.01$.

# Chapter 4: Discussion

## 4.1 Calnexin augments LPL maturation after moderate diabetes

Majority of FA provided to the heart come from breakdown of circulating TG, a process catalyzed by LPL located at the vascular lumen[133]. In mice with cardiac overexpression of LPL, excess lipid uptake is evident, with development of dilated cardiomyopathy[134]. Paradoxically, chronic cardiac depletion of LPL is also associated with a decrease in cardiac ejection fraction[135]. Thus, cardiac LPL is of crucial importance for regulating lipid metabolism in hearts, and disturbing its innate function is sufficient to cause cardiomyopathy. Diabetes is a unique metabolic disorder during which either an increase (moderate T1D) or decrease (severe T1D) in vascular LPL activity is observed. Our data suggests that following acute hyperglycemia and moderate diabetes, more LPL is processed into an active dimeric form, whereas severe diabetes is associated with increased conversion of LPL into inactive monomers.

In T1D patients, insulin supplementation can never mimic the exquisite control of glucose by pancreatic insulin seen in normal individuals. Multiple finger pricks and insulin injections (3-4/day) means poor patient compliance, repeated exposure to bouts of inadequate glucose control (and a shift in cardiac metabolism), and cardiovascular disease in the long term. To imitate this poorly controlled T1D patient exposed to acute hyperglycemia, we used DZ. Measurement of LPL protein expression in the heart revealed no change following acute hyperglycemia. However, the drawback with this measurement is that it does not distinguish active LPL from its inactive monomeric form. Using the heparin-sepharose column, our data for the first time show that acute hyperglycemia can indeed increase the amount of dimeric LPL in the heart. We are unaware of a similar increase in dimeric LPL in other physiology

or pathology. In fact, the reverse is often seen with lipid metabolism disorders. In one case of human familial LPL deficiency, the Tyr262 --> His mutation of LPL gene results in shifting of dimeric LPL to monomers[136]. In addition, in cell lines derived from animals with a mutation (*cld*) which impairs post-translational processing of LPL, a significant amount of inactive LPL is produced as aggregated monomers[137]. The increased dimeric LPL in the whole heart following acute hyperglycemia correlated well with the elevated LPL activity at the vascular lumen. Our data suggest that following a rapid rise in circulating glucose, a unique augmentation in LPL dimerization contributes towards increased coronary enzyme, delivering more FA to the heart.

Following stripping of dimeric LPL from the vascular lumen, more LPL dimers were still evident in the myocytes from acute diabetic animals. These dimeric LPL could be located inside the ER, Golgi, secretion vesicles or at the myocyte surface. Interestingly, the majority of dimeric LPL displayed resistance to endo H digestion[47]. This suggested that following DZ, LPL processing is very efficient with more LPL completing its maturation in the ER before moving to the Golgi. Early processing of LPL into a conformation competent for dimerization is suggested to involve chaperones like calreticulin/calnexin. For example, in a transfected sf21 cell line, folding/dimerization of human LPL is only promoted when calreticulin is co-expressed[48]. In addition, the impaired LPL processing seen in *cld/cld* mice is related to a decreased expression of calnexin[138]. In our study, LPL in control cardiomyocytes was found associated with calnexin. As interruption of this association by Cs hindered LPL dimerization and secretion, our data imply that calnexin is important for LPL processing in the heart.

The Rodrigues' lab has previously found that HG+PA increased LPL trafficking from the Golgi to myocyte surface[58, 64]. The current data suggest that HG+PA are also responsible for enhanced LPL dimerization. To test whether the effect of an acute diabetic environment on LPL processing is not a transient response, we turned to a more chronic diabetic model using D55 animals. A significant increase in the amount of LPL dimers correlated to an increased expression of calnexin in D55 hearts. As no change in LMF1 gene expression was observed, our data suggest that chronic diabetes may have a profound impact on the early processing events of LPL dimerization. It is possible that the increased calnexin expression following chronic diabetes is related to the unfolded protein response (UPR), an adaptive mechanism that augments protein processing efficiency following ER stress[139]. One of the three well-defined arms of UPR includes up-regulation of ER chaperone expression through activation of inositol-requiring kinase 1 (IRE-1) on the ER membrane[140, 141]. It should be noted that acute exposure to HG+PA had no effect on calnexin expression. Nevertheless, this environment could still alter the processing efficiency of LPL by affecting chaperone activity and accessibility in the ER through calcium and extracellular signal-regulated kinase (ERK-1). Calcium is an important cofactor for protein folding in the ER, facilitating LPL dimerization, and can also impact the structural stability and substrate recognition of calnexin[142, 143]. ERK-1, activated in an IRE-dependent manner can directly phosphorylate calnexin at Ser563, resulting in its recruitment to ribosomes, potentially rendering it more accessible to newly synthesized proteins[144, 145]. The role of calcium and ERK-1 on LPL maturation, and how diabetes could potentially alter LPL processing through these pathways requires investigation.

### 4.2 Following severe diabetes Angptl-4 dissembles dimeric LPL

In contrast to D55, D100 animals have a more profound loss of pancreatic beta-cells and reduction in circulating insulin. Under these conditions, excessive lipolysis and hepatic lipoprotein secretion increases serum FA and TG, respectively. Thus, these doses of STZ represent a continuum of poor glycemic control, from moderate (D55) to severe (D100). To avoid lipid overload, LPL activity at the coronary lumen decreased in D100 hearts, and this could be due to enzyme inactivation by conversion from a dimeric to monomeric conformation[109]. Angptl-4, identified to bring about this conversion, is expressed in various tissues including white adipose tissue, liver, heart, and skeletal muscle[106]. This secreted protein can function in the circulation, breaking down vascular LPL[107]. Our data for the first time report a robust increase of Angptl-4 protein, both in the serum and heart tissue from D100 animals, an effect that was not seen in D55. Given that the serum concentration of Angptl-4 in D100 was capable of inhibiting the activity of vascular LPL released from D55 hearts *in vitro*, we assumed that introduction of Angptl-4 to D55 hearts would give these hearts a D100 phenotype. Indeed, a drop of LPL activity was observed at the vascular lumen in D55 hearts perfused with Angptl-4, an effect that correlated well with the inhibitory efficiency *in vitro*. The reduction of coronary LPL activity could be due to the increased conversion of dimeric LPL into monomers, with subsequent detachment from the vascular binding sites. This effect of Angptl-4 was also evident in control hearts. Long chain FA, through activation of PPAR δ, has been reported to increase the transcription of Angptl-4 in skeletal muscle cells[110]. In our study, as Angptl-4 expression in cardiomyocytes was also up-regulated following exposure to PA (more than 4 h), the decrease of LPL in D100 could be through a FA-Angptl-4 pathway. As this effect was absent in DZ which had short term

hyperlipidemia (less than 4 h), our data suggest that "turning off" LPL requires prolonged exposure to FA. Whether the increased expression of Angptl-4 seen in D100 hearts could contribute towards inhibition of LPL at the coronary lumen is currently unknown. Nevertheless, purified Angptl-4 was capable of directly inhibiting LPL in or on cardiomyocytes. In addition, in mice overexpressing Angptl-4 specifically in the heart, a reduced cardiac LPL activity was found without affecting this enzyme in other LPL expressing tissues, implying a tight link between tissue-specific Angptl-4 and local or proximal vascular LPL activity[106].

Overall, our data suggest that in moderate T1D, an exaggerated LPL processing to dimeric, catalytically active enzyme increases vascular LPL, delivering more FA to the heart when glucose utilization is compromised. In severe diabetes, conversion of LPL to inactive monomers at the coronary lumen would impede TG hydrolysis and FA supply.

### 4.3 Using heparanase, endothelial cells regulate LPL secretion from cardiomyocytes

LPL secretion requires trafficking from an intracellular pool to myocyte surface HSPGs, followed by translocation to the vascular lumen. Our previous studies have indicated that the trafficking component requires actin cytoskeleton polymerization, which can be achieved by RhoA activation[64, 127]. In fact, when isolated hearts were perfused with LPA, a RhoA activator, increased coronary LPL activity was detected[127]. RhoA is a small GTP-binding protein, with inactive RhoA associated with GDP and sequestered in the cytosol. Upon activation, GDP is replaced by GTP and GTP-RhoA shifts to the plasma membrane. Subsequently, through its downstream effector ROCK, activation of RhoA will ultimately induce actin cytoskeleton polymerization. We observed that the increase in LPL activity at the coronary lumen in hyperglycemic DZ and diabetic D55 hearts were both accompanied by

RhoA activation. As RhoA activation by LPA also promoted LPL secretion in cardiomyocytes through actin cytoskeleton polymerization, our data suggests that this GTP-binding protein is an important contributor to move LPL to the myocyte surface.

The mechanism by which LPL leaves the myocyte surface to move to the coronary lumen is not completely understood. At the myocyte surface, LPL is sequestered to HSPGs via an ionic interaction. Thus, its release is possible by negatively charged heparin. However, cleavage of HS, or shedding of the extracellular part of HSPGs is a more likely event for LPL to leave the surface *in vivo*. Interestingly, on exposure of cardiomyocytes to ECCM, LPL is released into the medium with a reciprocal decrease in surface LPL activity, suggesting that ECCM is likely releasing LPL from the myocyte surface. An additional observation noticed with ECCM was its ability to assist in LPL replenishment when the surface pool was depleted. We attributed this effect to its ability to activate RhoA in cardiomyocytes in a pattern similar to that seen with LPA. In both cases, after reaching a peak, the amount of GTP-RhoA declined as it is normally converted to a GDP-bound form following activation of downstream effectors[146]. Intriguingly, heparin had no effect on RhoA or LPL replenishment, implying that simple displacement of LPL is not sufficient to trigger the replenishment process, and that ECCM is likely altering the conformation of HSPGs.

An enzyme of special relevance that is known to cleave HS of HSPGs is heparanase. This enzyme is synthesized in the EC as a latent 65 kDa form, which possesses no catalytic activity. Following its secretion, it binds to EC surface HSPGs and is internalized into lysosomes[147]. There it is cleaved into a 50 kDa active form and stored until it is secreted in response to stimulation such as adenosine, ADP, and ATP[74, 148]. In the present study, increased secretion of both latent and active heparanase into the medium was also observed

when EC were exposed to high glucose. As both forms of heparanase were augmented in the interstitial space of hearts from DZ animals, it suggests that hyperglycemia is effective in triggering coronary endothelial heparanase release. The Rodrigues' lab has previously demonstrated that high glucose induced secretion of active heparanase from EC occurs through activation of P2Y receptors that initiates stress fiber formation (across which heparanase-containing cargos are transported) and disruption of cortical actin cytoskeleton (to allow heparanase to be released into the extracellular space)[149]. Whether the same mechanism applies to release of latent heparanase is unknown as we cannot rule out the possibility that high glucose could also block endocytosis of latent heparanase from the EC surface, or is capable of directly detaching the latent enzyme from surface HSPGs. Irrespective of the release mechanism, our study is the first to demonstrate that it is heparanase within ECCM which is responsible for detachment of LPL from the myocyte surface.

Although active heparanase is predicted to release surface LPL by cleaving HS, latent enzyme could also facilitate LPL release. As expected, only active heparanase initiated release of LPL from the myocyte surface. Surprisingly, this release was not accompanied by RhoA activation. In fact, it was latent heparanase that accounted for the RhoA activation seen with ECCM. Growing evidence has demonstrated that heparanase also possesses activity-independent effects, for example, activation of Src during cell adhesion[150]. Hence, our data suggests that active heparanase detaches LPL from the myocyte surface HSPGs, whereas latent heparanase activates RhoA to move intracellular LPL to replenish this released reservoir. Studies on HSPG-mediated signaling have focused on syndecan-4, a transmembrane HSPG with its cytoplasmic domain capable of activating and stabilizing

PKCα, and syndecan-4-dependent PKCα activation has been indicated in FGF signaling[151, 152]. Moreover, neuronal Thy-1 induced cell spreading requires RhoA-mediated actin cytoskeleton polymerization, a suggested downstream event following syndecan-4-dependent PKCα activation[153]. Our study also indicated that the RhoA activation induced by latent heparanase is mediated by PKCα. In U87 MG human glioma cells, clustering of syndecan-4 by latent heparanase or an anti-heparanase antibody was sufficient to induce cell spreading, a process involving PKC activation[154]. In addition, upon binding of phosphatidylinositol 4,5-bisphosphate (PtdIns(4,5P)(2)) to its cytoplasmic domain, oligomeriation of syndecan-4 was promoted with a subsequent up-regulation of PKCα[155, 156]. In this study, it is likely that clustering of syndecan-4 with latent heparanase triggers RhoA activation. It is possible that latent heparanase does this by acting as a bridging factor by binding to HS. This idea was supported by our results using heparinase III that eliminates HS and attenuated RhoA activation by latent heparanase. Altogether, results from our study suggest that active and latent heparanase work cooperatively to promote LPL secretion following diabetes (Figure 21*D*).

### 4.4 Heparanase from EC can be taken up by cardiomyocytes to affect gene expression

It was surprising that we could detect heparanase in cardiomyocytes in the absence of gene expression in these cells. Freshly isolated myocytes had a significant amount of active heparanase that decreased following 36 h *in vitro* culturing. As the half-life of active heparanase is approximately 30 h[147], this result suggests that the presence of heparanase in cardiomyocytes is not from *de novo* synthesis, but likely due to extracellular uptake. Indeed, on exposure of cardiomyocytes to exogenous latent heparanase, we demonstrated

its rapid and robust uptake. In CHO cells, endocytosis of exogenous latent heparanase involves low density lipoprotein receptor-related proteins, mannose 6-phosphate receptors, and HSPGs[157]. Although our data in cardiomyocytes strongly indicates an HSPG-dependent mechanism of internalization, we cannot rule out the contributive effects of other receptors in this uptake process. Regarding HSPGs, it is believed that their clustering leads to internalization of bound ligands, as observed in CHO cells, where latent heparanase triggers clustering of both syndecan-1 and -4 followed by rapid internalization of the heparanase-HSPGs complex[154]. As we have previously reported clustering of syndecan-4 when cardiomyocytes are exposed to latent heparanase[158], it is possible that a heparanase-HSPGs complex is also responsible for endocytosis of this enzyme in cardiomyocytes. Of the two novel endocytotic pathways, HSPGs are more involved in caveolae-dependent rather than clathrin-mediated endocytosis. For example, syndecan-1 has been shown to mediate apoE-VLDL uptake in the human fibroblast cell line (GM00701), a process that was clathrin-independent, but inhibited by nystatin, an inhibitor of the lipid raft-caveolae endocytosis pathway[159]. Our data demonstrated that internalization of latent heparanase by cardiomyocytes relies on caveolae to form endocytotic vesicles and dynamin for fission of these vesicles from the plasma membrane. The participation of tyrosine kinase in this process has also been seen in the syndecan family mediated endocytosis[160, 161]. It is believed that clustering would lead to redistribution of syndecans to lipid rafts, where their cytoplasmic domain could be phosphorylated by tyrosine kinase[126, 162]. Recruitment of cortactin to phosphorylated syndecans promotes actin polymerization at the actin cortex, thereby bringing HSPGs-mediated endocytotic vesicles into the cells[163]. Overall, it is

possible that in response to high glucose, the latent heparanase released from EC enters cardiomyocytes through an HSPG-dependent caveolae pathway.

It is interesting that cells like fibroblasts, which do not express heparanase can also take up latent heparanase[164], and this can be converted into active heparanase following lysosomal processing[74]. Our results also indicate that a similar mechanism applies to latent heparanase taken up by cardiomyocytes. In EC, active heparanase stored in lysosomes can be secreted in response to high glucose, or enters the nucleus in the presence of fatty acid[165]. Our data also demonstrated entry of both latent and active heparanase into the nucleus. Heat shock protein 90 (Hsp90) is a suggested chaperone for escorting active heparanase from lysosomes to nucleus in both HL-60 cells[166] and bCAECs[165], resulting in cell differentiation and upcoupling of glucose metabolism, respectively. As we were unable to detect an association between Hsp90 and heparanase (data not shown), the mechanism which drives the nuclear entry of heparanase in cardiomyocytes is currently unknown. Regardless, gene expression of MMP-9 increased significantly in heparanase treated myocytes. As similar results were also obtained in myocytes from D55 diabetic rats which showed accumulation of active heparanase in the nucleus together with a robust increase in MMP-9 expression, our data imply that gene expression in cardiomyocytes could be affected by heparanase secreted from EC. Interestingly, gene upregulation of MMP-9 has been observed in several cancer cell lines upon transfection of heparanase, transforming them to an aggressive phenotype[167]. As MMP-9 degrades components of the extracellular matrix such as collagens[168], upregulation of its expression, as shown in our D55 cardiomyocytes, could contribute to heart dysfunction in these diabetic animals in the long term. Other studies have reported a correlation between elevated level of MMP-9 and collagen accumulation in the hearts from STZ induced diabetic

rats[169]. In fact, in diabetic mice, deletion of MMP-9 gene effectively reduced cardiac fibrosis and increased survival of cardiac stem cells[170]. Further studies are required to investigate the relationship between EC derived heparanase and MMP-9 expression in cardiomyocytes.

In summary, heparanase is a key mediator of the cross-talk between EC and cardiomyocyte to increase LPL secretion following hyperglycemia. This idea was confirmed in DZ induced hyperglycemia and the high glucose co-culture system, with both experimental models exhibiting increased heparanase secretion together with LPL amplification at the apical side of EC. Additionally, it is possible that heparanase secreted from EC can be taken up by cardiomyocytes to modulate MMP-9 expression, driving the onset of fibrosis and development of diabetic cardiomyopathy.

# Chapter 5: Conclusions and future directions

## 5.1 Conclusions

In summary, following diabetes, recruitment of LPL to the vascular lumen could represent an immediate compensatory response to guarantee FA supply. In acute hyperglycemia and moderate diabetes, ER chaperone calnexin promoted LPL processing to dimeric, catalytically active enzyme, thereby increasing functional LPL to deliver more FA to the heart when glucose utilization is compromised. In severe chronic diabetes, to avoid lipid oversupply, FA-induced expression of angiopoietin-like protein 4 leads to conversion of LPL to inactive monomers at the coronary lumen to impede TG hydrolysis. However, both compensatory processes that alter the innate function of LPL at the vascular lumen would disturb heart metabolism, which could be the forerunner for cardiomyopathy seen with this disease (Figure 28).

Besides intrinsic factors from cardiomyocytes, endothelial heparanase is a key mediator to increase LPL secretion following hyperglycemia. Through cleaving HSPGs, active heparanase liberates LPL from myocytes surface *en route* for secretion, whereas latent heparanase stimulates replenishment of LPL by clustering of myocyte surface syndecan-4 to mediate RhoA-dependent actin cytoskeleton polymerization. The end result would be a continuous augmented secretion of LPL to the vascular lumen, which provides overwhelming amount of FA that could lead to lipotoxicity to the heart (Figure 29). Additionally, our data suggests that heparanase can be taken up by cardiomyocytes to modulate MMP-9 expression,

driving the onset of fibrosis and development of diabetic cardiomyopathy. Pharmaceutical manipulation of this process, for instance inhibition of heparanase secretion/activity, could potentially provide an additional strategy to limit FA delivery to the heart, and cardiomyopathy observed with chronic diabetes.

### 5.2 Future directions

To further investigate the relationship between endothelial heparanase and cardiomyocyte gene expression, the following studies are ongoing:

We demonstrated that cardiac MMP-9 expression increased following nuclear entry of active heparanase. To see whether the gene regulatory effect is a result of heparanase uptake, myocytes can be treated with latent heparanase in the presence of heparin or filipin which interfere with its uptake. *In vivo* studies can also be done using heparanase knock-out mice. They can be made diabetic by multiple, low-dose injection of STZ. Following hyperglycemia, levels of nuclear heparanase content and MMP-9 expression in the cardiomyocytes will be compared to those of their wild type counterparts.

Another question is the mechanism behind the gene regulatory effect. As mentioned before, cleavage of nuclear HSPGs and the subsequent increase in HAT activity is the first proposed pathway. Hence, multiple approaches could be used to block this pathway *in vitro*, including usage of: a) chloroquine that inhibits processing of latent to active heparanase, b) SST0001, a compound that inhibits heparanase activity, and c) anacardic acid, an inhibitor of HAT activity. Using another strategy, diabetic rats can be treated with heparanase inhibitor

SST0001 to determine whether the gene regulatory effect of heparanase is activity-dependent. In addition to that, ChIP-on-chip studies have revealed interaction of nuclear heparanase with promoter and transcribed regions of genes[167], modulating histone 3 lysine 4 (H3K4) methylation. Whether this newly found pathway could explain our results in cardiomyocytes remain to be investigated.

In our studies, we only focused on MMP-9 gene expression since it is a well-studied target gene of heparanase in tumor cell lines, which is also involved in diabetic cardiomyopathy. This study should be broadened using RNA-sequencing to explore more target gene in cardiomyocytes, and how they affect the pathogenesis of diabetic cardiomyopathy. For example, transforming growth factor β3, cardiac sarcoplasmatic reticulum $Ca^{2+}$ ATPase, cardiac $Na^{+}/Ca^{2+}$ exchanger 1, *etc.*.

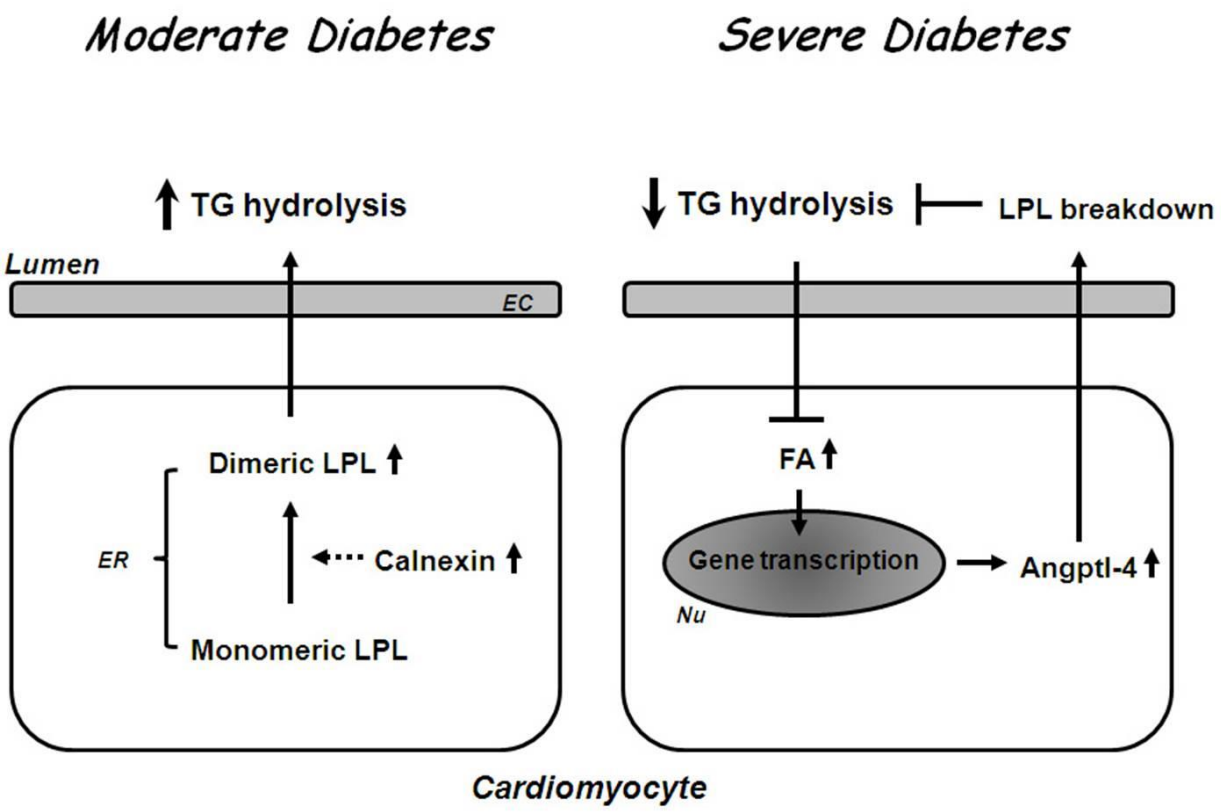


**Figure 28 Moderate and severe diabetes have a differential impact on LPL at the coronary lumen.**

In moderate diabetes, more monomeric LPL is processed into dimeric, catalytically active enzyme with the help of the ER chaperone calnexin. This increases LPL at the vascular lumen, breaking down more circulating TG to deliver increased FA to the heart when glucose utilization is compromised. In severe diabetes, when FA are excessive, a FA-induced expression of Angptl-4 leads to conversion of LPL to inactive monomers at the coronary lumen to impede TG hydrolysis. EC: endothelial cells; ER: endoplasmic reticulum; Nu: nucleus.

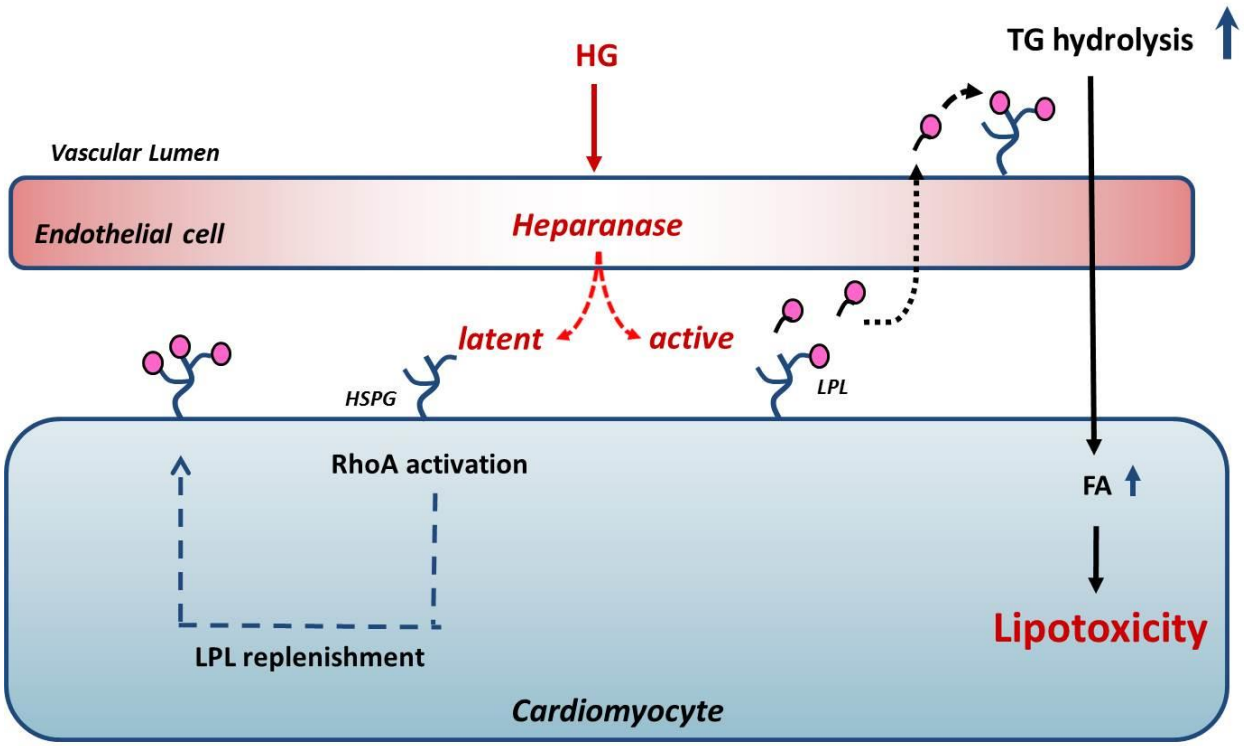


**Figure 29 Endothelial heparanase is a key mediator to increase LPL secretion following hyperglycemia.**

Two forms of heparanase are secreted when endothelial cells are exposed to high glucose. Through cleaving HSPGs, active heparanase liberates LPL from myocytes surface *en route* for secretion, whereas latent heparanase stimulates replenishment of LPL. This is achieved by clustering of myocyte surface syndecan-4 to mediate RhoA-dependent actin cytoskeleton polymerization. In this way, active and latent heparanase work cooperatively to facilitate continuous secretion of LPL to the vascular lumen, providing exaggerated amount of fatty acid that could lead up to lipotoxicity to the heart.

## References


1. Alberti KG, Zimmet P. Global burden of disease--where does diabetes mellitus fit in? *Nature reviews. Endocrinology*. 2013;9:258-260
2. Pelletier C, Dai S, Roberts KC, Bienek A, Onysko J, Pelletier L. Report summary. Diabetes in canada: Facts and figures from a public health perspective. *Chronic diseases and injuries in Canada*. 2012;33:53-54
3. Laing SP, Swerdlow AJ, Slater SD, Burden AC, Morris A, Waugh NR, Gatling W, Bingley PJ, Patterson CC. Mortality from heart disease in a cohort of 23,000 patients with insulin-treated diabetes. *Diabetologia*. 2003;46:760-765
4. Goyal BR, Mehta AA. Diabetic cardiomyopathy: Pathophysiological mechanisms and cardiac dysfuntion. *Human & experimental toxicology*. 2013;32:571-590
5. Avogaro A, Nosadini R, Doria A, Fioretto P, Velussi M, Vigorito C, Sacca L, Toffolo G, Cobelli C, Trevisan R, et al. Myocardial metabolism in insulin-deficient diabetic humans without coronary artery disease. *The American journal of physiology*. 1990;258:E606-618
6. Neely JR, Rovetto MJ, Oram JF. Myocardial utilization of carbohydrate and lipids. *Progress in cardiovascular diseases*. 1972;15:289-329
7. Ballard FB, Danforth WH, Naegle S, Bing RJ. Myocardial metabolism of fatty acids. *The Journal of clinical investigation*. 1960;39:717-723
8. Voshol PJ, Rensen PC, van Dijk KW, Romijn JA, Havekes LM. Effect of plasma triglyceride metabolism on lipid storage in adipose tissue: Studies using genetically engineered mouse models. *Biochimica et biophysica acta*. 2009;1791:479-485
9. Blanchette-Mackie EJ, Masuno H, Dwyer NK, Olivecrona T, Scow RO. Lipoprotein lipase in myocytes and capillary endothelium of heart: Immunocytochemical study. *The American journal of physiology*. 1989;256:E818-828
10. Niu YG, Evans RD. Metabolism of very-low-density lipoprotein and chylomicrons by streptozotocin-induced diabetic rat heart: Effects of diabetes and lipoprotein preference. *American journal of physiology. Endocrinology and metabolism*. 2008;295:E1106-1116
11. Pulinilkunnil T, Abrahani A, Varghese J, Chan N, Tang I, Ghosh S, Kulpa J, Allard M, Brownsey R, Rodrigues B. Evidence for rapid "metabolic switching" through lipoprotein lipase occupation of endothelial-binding sites. *Journal of molecular and cellular cardiology*. 2003;35:1093-1103
12. Pyper SR, Viswakarma N, Yu S, Reddy JK. Pparalpha: Energy combustion, hypolipidemia, inflammation and cancer. *Nuclear receptor signaling*. 2010;8:e002
13. Boudina S, Sena S, Theobald H, Sheng X, Wright JJ, Hu XX, Aziz S, Johnson JI, Bugger H, Zaha VG, Abel ED. Mitochondrial energetics in the heart in obesity-related diabetes: Direct evidence for increased uncoupled respiration and activation of uncoupling proteins. *Diabetes*. 2007;56:2457-2466

14. Battiprolu PK, Lopez-Crisosto C, Wang ZV, Nemchenko A, Lavandero S, Hill JA. Diabetic cardiomyopathy and metabolic remodeling of the heart. *Life sciences*. 2013;92:609-615
15. Davidson SM, Duchen MR. Effects of no on mitochondrial function in cardiomyocytes: Pathophysiological relevance. *Cardiovascular research*. 2006;71:10-21
16. Hickson-Bick DL, Buja LM, McMillin JB. Palmitate-mediated alterations in the fatty acid metabolism of rat neonatal cardiac myocytes. *Journal of molecular and cellular cardiology*. 2000;32:511-519
17. Park TS, Hu Y, Noh HL, Drosatos K, Okajima K, Buchanan J, Tuinei J, Homma S, Jiang XC, Abel ED, Goldberg IJ. Ceramide is a cardiotoxin in lipotoxic cardiomyopathy. *Journal of lipid research*. 2008;49:2101-2112
18. Hashimoto T. Peroxisomal beta-oxidation enzymes. *Neurochemical research*. 1999;24:551-563
19. Brandt JM, Djouadi F, Kelly DP. Fatty acids activate transcription of the muscle carnitine palmitoyltransferase i gene in cardiac myocytes via the peroxisome proliferator-activated receptor alpha. *The Journal of biological chemistry*. 1998;273:23786-23792
20. Murray AJ, Panagia M, Hauton D, Gibbons GF, Clarke K. Plasma free fatty acids and peroxisome proliferator-activated receptor alpha in the control of myocardial uncoupling protein levels. *Diabetes*. 2005;54:3496-3502
21. Gerber LK, Aronow BJ, Matlib MA. Activation of a novel long-chain free fatty acid generation and export system in mitochondria of diabetic rat hearts. *American journal of physiology. Cell physiology*. 2006;291:C1198-1207
22. Flarsheim CE, Grupp IL, Matlib MA. Mitochondrial dysfunction accompanies diastolic dysfunction in diabetic rat heart. *The American journal of physiology*. 1996;271:H192-202
23. Kratky D, Strauss JG, Zechner R. Tissue-specific activity of lipoprotein lipase in skeletal muscle regulates the expression of uncoupling protein 3 in transgenic mouse models. *The Biochemical journal*. 2001;355:647-652
24. Finck BN, Lehman JJ, Leone TC, Welch MJ, Bennett MJ, Kovacs A, Han X, Gross RW, Kozak R, Lopaschuk GD, Kelly DP. The cardiac phenotype induced by pparalpha overexpression mimics that caused by diabetes mellitus. *The Journal of clinical investigation*. 2002;109:121-130
25. Finck BN, Han X, Courtois M, Aimond F, Nerbonne JM, Kovacs A, Gross RW, Kelly DP. A critical role for pparalpha-mediated lipotoxicity in the pathogenesis of diabetic cardiomyopathy: Modulation by dietary fat content. *Proceedings of the National Academy of Sciences of the United States of America*. 2003;100:1226-1231
26. Duncan JG, Bharadwaj KG, Fong JL, Mitra R, Sambandam N, Courtois MR, Lavine KJ, Goldberg IJ, Kelly DP. Rescue of cardiomyopathy in peroxisome proliferator-

activated receptor-alpha transgenic mice by deletion of lipoprotein lipase identifies sources of cardiac lipids and peroxisome proliferator-activated receptor-alpha activators. *Circulation*. 2010;121:426-435

27. Sparkes RS, Zollman S, Klisak I, Kirchgessner TG, Komaromy MC, Mohandas T, Schotz MC, Lusis AJ. Human genes involved in lipolysis of plasma lipoproteins: Mapping of loci for lipoprotein lipase to 8p22 and hepatic lipase to 15q21. *Genomics*. 1987;1:138-144
28. Deeb SS, Peng RL. Structure of the human lipoprotein lipase gene. *Biochemistry*. 1989;28:4131-4135
29. Santamarina-Fojo S. The familial chylomicronemia syndrome. *Endocrinology and metabolism clinics of North America*. 1998;27:551-567, viii
30. Ameis D, Kobayashi J, Davis RC, Ben-Zeev O, Malloy MJ, Kane JP, Lee G, Wong H, Havel RJ, Schotz MC. Familial chylomicronemia (type i hyperlipoproteinemia) due to a single missense mutation in the lipoprotein lipase gene. *The Journal of clinical investigation*. 1991;87:1165-1170
31. Fojo SS, Beg O, Dichek H, Brewer HB, Jr. The molecular defects in lipoprotein lipase deficient patients. *European journal of epidemiology*. 1992;8 Suppl 1:59-63
32. Normand T, Bergeron J, Fernandez-Margallo T, Bharucha A, Ven Murthy MR, Julien P, Gagne C, Dionne C, De Braekeleer M, Ma R, et al. Geographic distribution and genealogy of mutation 207 of the lipoprotein lipase gene in the french canadian population of quebec. *Human genetics*. 1992;89:671-675
33. Chen Q, Razzaghi H, Demirci FY, Kamboh MI. Functional significance of lipoprotein lipase hindiii polymorphism associated with the risk of coronary artery disease. *Atherosclerosis*. 2008;200:102-108
34. Nakshatri H, Nakshatri P, Currie RA. Interaction of oct-1 with tfiib. Implications for a novel response elicited through the proximal octamer site of the lipoprotein lipase promoter. *The Journal of biological chemistry*. 1995;270:19613-19623
35. Currie RA, Eckel RH. Characterization of a high affinity octamer transcription factor binding site in the human lipoprotein lipase promoter. *Arch Biochem Biophys*. 1992;298:630-639
36. Schoonjans K, Gelman L, Haby C, Briggs M, Auwerx J. Induction of lpl gene expression by sterols is mediated by a sterol regulatory element and is independent of the presence of multiple e boxes. *Journal of molecular biology*. 2000;304:323-334
37. Homma H, Kurachi H, Nishio Y, Takeda T, Yamamoto T, Adachi K, Morishige K, Ohmichi M, Matsuzawa Y, Murata Y. Estrogen suppresses transcription of lipoprotein lipase gene. Existence of a unique estrogen response element on the lipoprotein lipase promoter. *The Journal of biological chemistry*. 2000;275:11404-11411
38. Harris SM, Harvey EJ, Hughes TR, Ramji DP. The interferon-gamma-mediated inhibition of lipoprotein lipase gene transcription in macrophages involves casein

kinase 2- and phosphoinositide-3-kinase-mediated regulation of transcription factors sp1 and sp3. *Cellular signalling*. 2008;20:2296-2301

39. Morin CL, Schlaepfer IR, Eckel RH. Tumor necrosis factor-alpha eliminates binding of nf-y and an octamer-binding protein to the lipoprotein lipase promoter in 3t3-l1 adipocytes. *The Journal of clinical investigation*. 1995;95:1684-1689
40. Staels B, Schoonjans K, Fruchart JC, Auwerx J. The effects of fibrates and thiazolidinediones on plasma triglyceride metabolism are mediated by distinct peroxisome proliferator activated receptors (ppars). *Biochimie*. 1997;79:95-99
41. Schoonjans K, Peinado-Onsurbe J, Lefebvre AM, Heyman RA, Briggs M, Deeb S, Staels B, Auwerx J. Pparalpha and ppargamma activators direct a distinct tissue-specific transcriptional response via a ppre in the lipoprotein lipase gene. *The EMBO journal*. 1996;15:5336-5348
42. Raynolds MV, Awald PD, Gordon DF, Gutierrez-Hartmann A, Rule DC, Wood WM, Eckel RH. Lipoprotein lipase gene expression in rat adipocytes is regulated by isoproterenol and insulin through different mechanisms. *Mol Endocrinol*. 1990;4:1416-1422
43. Ranganathan G, Phan D, Pokrovskaya ID, McEwen JE, Li C, Kern PA. The translational regulation of lipoprotein lipase by epinephrine involves an rna binding complex including the catalytic subunit of protein kinase a. *The Journal of biological chemistry*. 2002;277:43281-43287
44. Ranganathan G, Pokrovskaya I, Ranganathan S, Kern PA. Role of a kinase anchor proteins in the tissue-specific regulation of lipoprotein lipase. *Mol Endocrinol*. 2005;19:2527-2534
45. Camps L, Reina M, Llobera M, Vilaro S, Olivecrona T. Lipoprotein lipase: Cellular origin and functional distribution. *The American journal of physiology*. 1990;258:C673-681
46. Semenkovich CF, Luo CC, Nakanishi MK, Chen SH, Smith LC, Chan L. In vitro expression and site-specific mutagenesis of the cloned human lipoprotein lipase gene. Potential n-linked glycosylation site asparagine 43 is important for both enzyme activity and secretion. *The Journal of biological chemistry*. 1990;265:5429-5433
47. Ben-Zeev O, Mao HZ, Doolittle MH. Maturation of lipoprotein lipase in the endoplasmic reticulum. Concurrent formation of functional dimers and inactive aggregates. *The Journal of biological chemistry*. 2002;277:10727-10738
48. Zhang L, Wu G, Tate CG, Lookene A, Olivecrona G. Calreticulin promotes folding/dimerization of human lipoprotein lipase expressed in insect cells (sf21). *The Journal of biological chemistry*. 2003;278:29344-29351
49. Carroll R, Ben-Zeev O, Doolittle MH, Severson DL. Activation of lipoprotein lipase in cardiac myocytes by glycosylation requires trimming of glucose residues in the endoplasmic reticulum. *The Biochemical journal*. 1992;285 ( Pt 3):693-696

50. Garfinkel AS, Kempner ES, Ben-Zeev O, Nikazy J, James SJ, Schotz MC. Lipoprotein lipase: Size of the functional unit determined by radiation inactivation. *Journal of lipid research*. 1983;24:775-780
51. Peterson J, Fujimoto WY, Brunzell JD. Human lipoprotein lipase: Relationship of activity, heparin affinity, and conformation as studied with monoclonal antibodies. *Journal of lipid research*. 1992;33:1165-1170
52. Wong H, Yang D, Hill JS, Davis RC, Nikazy J, Schotz MC. A molecular biology-based approach to resolve the subunit orientation of lipoprotein lipase. *Proceedings of the National Academy of Sciences of the United States of America*. 1997;94:5594-5598
53. Dallinga-Thie GM, Franssen R, Mooij HL, Visser ME, Hassing HC, Peelman F, Kastelein JJ, Peterfy M, Nieuwdorp M. The metabolism of triglyceride-rich lipoproteins revisited: New players, new insight. *Atherosclerosis*. 2010;211:1-8
54. Doolittle MH, Ehrhardt N, Peterfy M. Lipase maturation factor 1: Structure and role in lipase folding and assembly. *Current opinion in lipidology*. 2010;21:198-203
55. Doolittle MH, Neher SB, Ben-Zeev O, Ling-Liao J, Gallagher CM, Hosseini M, Yin F, Wong H, Walter P, Peterfy M. Lipase maturation factor lmf1, membrane topology and interaction with lipase proteins in the endoplasmic reticulum. *The Journal of biological chemistry*. 2009;284:33623-33633
56. Peterfy M, Ben-Zeev O, Mao HZ, Weissglas-Volkov D, Aouizerat BE, Pullinger CR, Frost PH, Kane JP, Malloy MJ, Reue K, Pajukanta P, Doolittle MH. Mutations in lmf1 cause combined lipase deficiency and severe hypertriglyceridemia. *Nature genetics*. 2007;39:1483-1487
57. Busca R, Pujana MA, Pognonec P, Auwerx J, Deeb SS, Reina M, Vilaro S. Absence of n-glycosylation at asparagine 43 in human lipoprotein lipase induces its accumulation in the rough endoplasmic reticulum and alters this cellular compartment. *Journal of lipid research*. 1995;36:939-951
58. Kim MS, Wang F, Puthanveetil P, Kewalramani G, Hosseini-Beheshti E, Ng N, Wang Y, Kumar U, Innis S, Proud CG, Abrahani A, Rodrigues B. Protein kinase d is a key regulator of cardiomyocyte lipoprotein lipase secretion after diabetes. *Circ Res*. 2008;103:252-260
59. Hausser A, Storz P, Martens S, Link G, Toker A, Pfizenmaier K. Protein kinase d regulates vesicular transport by phosphorylating and activating phosphatidylinositol-4 kinase iiibeta at the golgi complex. *Nature cell biology*. 2005;7:880-886
60. Lu G, Chen J, Espinoza LA, Garfield S, Toshiyuki S, Akiko H, Huppler A, Wang QJ. Protein kinase d 3 is localized in vesicular structures and interacts with vesicle-associated membrane protein 2. *Cellular signalling*. 2007;19:867-879
61. Klinger SC, Glerup S, Raarup MK, Mari MC, Nyegaard M, Koster G, Prabakaran T, Nilsson SK, Kjaergaard MM, Bakke O, Nykjaer A, Olivecrona G, Petersen CM,

Nielsen MS. Sorla regulates the activity of lipoprotein lipase by intracellular trafficking. *Journal of cell science*. 2011;124:1095-1105

62. Vannier C, Ailhaud G. Biosynthesis of lipoprotein lipase in cultured mouse adipocytes. Ii. Processing, subunit assembly, and intracellular transport. *The Journal of biological chemistry*. 1989;264:13206-13216
63. Ewart HS, Severson DL. Insulin and dexamethasone stimulation of cardiac lipoprotein lipase activity involves the actin-based cytoskeleton. *The Biochemical journal*. 1999;340 ( Pt 2):485-490
64. Kim MS, Kewalramani G, Puthanveetil P, Lee V, Kumar U, An D, Abrahani A, Rodrigues B. Acute diabetes moderates trafficking of cardiac lipoprotein lipase through p38 mitogen-activated protein kinase-dependent actin cytoskeleton organization. *Diabetes*. 2008;57:64-76
65. Kewalramani G, An D, Kim MS, Ghosh S, Qi D, Abrahani A, Pulinilkunnil T, Sharma V, Wambolt RB, Allard MF, Innis SM, Rodrigues B. Ampk control of myocardial fatty acid metabolism fluctuates with the intensity of insulin-deficient diabetes. *Journal of molecular and cellular cardiology*. 2007;42:333-342
66. Filmus J, Capurro M, Rast J. Glypicans. *Genome biology*. 2008;9:224
67. Couchman JR. Transmembrane signaling proteoglycans. *Annual review of cell and developmental biology*. 2010;26:89-114
68. Nadanaka S, Kitagawa H. Heparan sulphate biosynthesis and disease. *Journal of biochemistry*. 2008;144:7-14
69. Kolset SO, Salmivirta M. Cell surface heparan sulfate proteoglycans and lipoprotein metabolism. *Cellular and molecular life sciences : CMLS*. 1999;56:857-870
70. Mertens G, Cassiman JJ, Van den Berghe H, Vermylen J, David G. Cell surface heparan sulfate proteoglycans from human vascular endothelial cells. Core protein characterization and antithrombin iii binding properties. *The Journal of biological chemistry*. 1992;267:20435-20443
71. Chuang CY, Lord MS, Melrose J, Rees MD, Knox SM, Freeman C, Iozzo RV, Whitelock JM. Heparan sulfate-dependent signaling of fibroblast growth factor 18 by chondrocyte-derived perlecan. *Biochemistry*. 2010;49:5524-5532
72. Berryman DE, Bensadoun A. Heparan sulfate proteoglycans are primarily responsible for the maintenance of enzyme activity, binding, and degradation of lipoprotein lipase in chinese hamster ovary cells. *The Journal of biological chemistry*. 1995;270:24525-24531
73. Pillarisetti S, Paka L, Sasaki A, Vanni-Reyes T, Yin B, Parthasarathy N, Wagner WD, Goldberg IJ. Endothelial cell heparanase modulation of lipoprotein lipase activity. Evidence that heparan sulfate oligosaccharide is an extracellular chaperone. *The Journal of biological chemistry*. 1997;272:15753-15759

74. Zetser A, Levy-Adam F, Kaplan V, Gingis-Velitski S, Bashenko Y, Schubert S, Flugelman MY, Vlodavsky I, Ilan N. Processing and activation of latent heparanase occurs in lysosomes. *Journal of cell science*. 2004;117:2249-2258
75. Wang F, Kim MS, Puthanveetil P, Kewalramani G, Deppe S, Ghosh S, Abrahani A, Rodrigues B. Endothelial heparanase secretion after acute hypoinsulinemia is regulated by glucose and fatty acid. *American journal of physiology. Heart and circulatory physiology*. 2009;296:H1108-1116
76. Yuan L, Hu J, Luo Y, Liu Q, Li T, Parish CR, Freeman C, Zhu X, Ma W, Hu X, Yu H, Tang S. Upregulation of heparanase in high-glucose-treated endothelial cells promotes endothelial cell migration and proliferation and correlates with akt and extracellular-signal-regulated kinase phosphorylation. *Molecular vision*. 2012;18:1684-1695
77. Han J, Woytowich AE, Mandal AK, Hiebert LM. Heparanase upregulation in high glucose-treated endothelial cells is prevented by insulin and heparin. *Exp Biol Med (Maywood)*. 2007;232:927-934
78. Shafat I, Ilan N, Zoabi S, Vlodavsky I, Nakhoul F. Heparanase levels are elevated in the urine and plasma of type 2 diabetes patients and associate with blood glucose levels. *PloS one*. 2011;6:e17312
79. Kobayashi M, Naomoto Y, Nobuhisa T, Okawa T, Takaoka M, Shirakawa Y, Yamatsuji T, Matsuoka J, Mizushima T, Matsuura H, Nakajima M, Nakagawa H, Rustgi A, Tanaka N. Heparanase regulates esophageal keratinocyte differentiation through nuclear translocation and heparan sulfate cleavage. *Differentiation; research in biological diversity*. 2006;74:235-243
80. Purushothaman A, Hurst DR, Pisano C, Mizumoto S, Sugahara K, Sanderson RD. Heparanase-mediated loss of nuclear syndecan-1 enhances histone acetyltransferase (hat) activity to promote expression of genes that drive an aggressive tumor phenotype. *The Journal of biological chemistry*. 2011;286:30377-30383
81. He YQ, Sutcliffe EL, Bunting KL, Li J, Goodall KJ, Poon IK, Hulett MD, Freeman C, Zafar A, McInnes RL, Taya T, Parish CR, Rao S. The endoglycosidase heparanase enters the nucleus of t lymphocytes and modulates h3 methylation at actively transcribed genes via the interplay with key chromatin modifying enzymes. *Transcription*. 2012;3:130-145
82. Bishop JR, Passos-Bueno MR, Fong L, Stanford KI, Gonzales JC, Yeh E, Young SG, Bensadoun A, Witztum JL, Esko JD, Moulton KS. Deletion of the basement membrane heparan sulfate proteoglycan type xviii collagen causes hypertriglyceridemia in mice and humans. *PloS one*. 2010;5:e13919
83. Obunike JC, Lutz EP, Li Z, Paka L, Katopodis T, Strickland DK, Kozarsky KF, Pillarisetti S, Goldberg IJ. Transcytosis of lipoprotein lipase across cultured endothelial cells requires both heparan sulfate proteoglycans and the very low density lipoprotein receptor. *The Journal of biological chemistry*. 2001;276:8934-8941

84. Saxena U, Klein MG, Goldberg IJ. Transport of lipoprotein lipase across endothelial cells. *Proceedings of the National Academy of Sciences of the United States of America*. 1991;88:2254-2258
85. Saxena U, Klein MG, Goldberg IJ. Metabolism of endothelial cell-bound lipoprotein lipase. Evidence for heparan sulfate proteoglycan-mediated internalization and recycling. *The Journal of biological chemistry*. 1990;265:12880-12886
86. Saxena U, Klein MG, Goldberg IJ. Identification and characterization of the endothelial cell surface lipoprotein lipase receptor. *The Journal of biological chemistry*. 1991;266:17516-17521
87. Beigneux AP, Davies BS, Gin P, Weinstein MM, Farber E, Qiao X, Peale F, Bunting S, Walzem RL, Wong JS, Blaner WS, Ding ZM, Melford K, Wongsiriroj N, Shu X, de Sauvage F, Ryan RO, Fong LG, Bensadoun A, Young SG. Glycosylphosphatidylinositol-anchored high-density lipoprotein-binding protein 1 plays a critical role in the lipolytic processing of chylomicrons. *Cell metabolism*. 2007;5:279-291
88. Gin P, Beigneux AP, Voss C, Davies BS, Beckstead JA, Ryan RO, Bensadoun A, Fong LG, Young SG. Binding preferences for gpihbp1, a glycosylphosphatidylinositol-anchored protein of capillary endothelial cells. *Arteriosclerosis, thrombosis, and vascular biology*. 2011;31:176-182
89. Davies BS, Goulbourne CN, Barnes RH, 2nd, Turlo KA, Gin P, Vaughan S, Vaux DJ, Bensadoun A, Beigneux AP, Fong LG, Young SG. Assessing mechanisms of gpihbp1 and lipoprotein lipase movement across endothelial cells. *Journal of lipid research*. 2012;53:2690-2697
90. Young SG, Davies BS, Voss CV, Gin P, Weinstein MM, Tontonoz P, Reue K, Bensadoun A, Fong LG, Beigneux AP. Gpihbp1, an endothelial cell transporter for lipoprotein lipase. *Journal of lipid research*. 2011;52:1869-1884
91. Beigneux AP, Davies BS, Bensadoun A, Fong LG, Young SG. Gpihbp1, a gpi-anchored protein required for the lipolytic processing of triglyceride-rich lipoproteins. *Journal of lipid research*. 2009;50 Suppl:S57-62
92. Gin P, Goulbourne CN, Adeyo O, Beigneux AP, Davies BS, Tat S, Voss CV, Bensadoun A, Fong LG, Young SG. Chylomicronemia mutations yield new insights into interactions between lipoprotein lipase and gpihbp1. *Human molecular genetics*. 2012;21:2961-2972
93. Beigneux AP, Davies BS, Tat S, Chen J, Gin P, Voss CV, Weinstein MM, Bensadoun A, Pullinger CR, Fong LG, Young SG. Assessing the role of the glycosylphosphatidylinositol-anchored high density lipoprotein-binding protein 1 (gpihbp1) three-finger domain in binding lipoprotein lipase. *The Journal of biological chemistry*. 2011;286:19735-19743
94. Franssen R, Young SG, Peelman F, Hertecant J, Sierts JA, Schimmel AW, Bensadoun A, Kastelein JJ, Fong LG, Dallinga-Thie GM, Beigneux AP.

Chylomicronemia with low postheparin lipoprotein lipase levels in the setting of gpihbp1 defects. *Circulation. Cardiovascular genetics*. 2010;3:169-178

95. Voss CV, Davies BS, Tat S, Gin P, Fong LG, Pelletier C, Mottler CD, Bensadoun A, Beigneux AP, Young SG. Mutations in lipoprotein lipase that block binding to the endothelial cell transporter gpihbp1. *Proceedings of the National Academy of Sciences of the United States of America*. 2011;108:7980-7984
96. Davies BS, Waki H, Beigneux AP, Farber E, Weinstein MM, Wilpitz DC, Tai LJ, Evans RM, Fong LG, Tontonoz P, Young SG. The expression of gpihbp1, an endothelial cell binding site for lipoprotein lipase and chylomicrons, is induced by peroxisome proliferator-activated receptor-gamma. *Mol Endocrinol*. 2008;22:2496-2504
97. Rodrigues B, Cam MC, Jian K, Lim F, Sambandam N, Shepherd G. Differential effects of streptozotocin-induced diabetes on cardiac lipoprotein lipase activity. *Diabetes*. 1997;46:1346-1353
98. Peterson J, Bihain BE, Bengtsson-Olivecrona G, Deckelbaum RJ, Carpentier YA, Olivecrona T. Fatty acid control of lipoprotein lipase: A link between energy metabolism and lipid transport. *Proceedings of the National Academy of Sciences of the United States of America*. 1990;87:909-913
99. Bengtsson G, Olivecrona T. Lipoprotein lipase. Mechanism of product inhibition. *European journal of biochemistry / FEBS*. 1980;106:557-562
100. Kim MS, Wang F, Puthanveetil P, Kewalramani G, Innis S, Marzban L, Steinberg SF, Webber TD, Kieffer TJ, Abrahani A, Rodrigues B. Cleavage of protein kinase d after acute hypoinsulinemia prevents excessive lipoprotein lipase-mediated cardiac triglyceride accumulation. *Diabetes*. 2009;58:2464-2475
101. Koster A, Chao YB, Mosior M, Ford A, Gonzalez-DeWhitt PA, Hale JE, Li D, Qiu Y, Fraser CC, Yang DD, Heuer JG, Jaskunas SR, Eacho P. Transgenic angiopoietin-like (angptl)4 overexpression and targeted disruption of angptl4 and angptl3: Regulation of triglyceride metabolism. *Endocrinology*. 2005;146:4943-4950
102. Yau MH, Wang Y, Lam KS, Zhang J, Wu D, Xu A. A highly conserved motif within the nh2-terminal coiled-coil domain of angiopoietin-like protein 4 confers its inhibitory effects on lipoprotein lipase by disrupting the enzyme dimerization. *The Journal of biological chemistry*. 2009;284:11942-11952
103. Liu J, Afroza H, Rader DJ, Jin W. Angiopoietin-like protein 3 inhibits lipoprotein lipase activity through enhancing its cleavage by proprotein convertases. *The Journal of biological chemistry*. 2010;285:27561-27570
104. Mattijssen F, Kersten S. Regulation of triglyceride metabolism by angiopoietin-like proteins. *Biochimica et biophysica acta*. 2012;1821:782-789
105. Nakajima K, Kobayashi J, Mabuchi H, Nakano T, Tokita Y, Nagamine T, Imamura S, Ai M, Otokozawa S, Schaefer EF. Association of angiopoietin-like protein 3 with

hepatic triglyceride lipase and lipoprotein lipase activities in human plasma. *Annals of clinical biochemistry*. 2010;47:423-431

106. Yu X, Burgess SC, Ge H, Wong KK, Nassem RH, Garry DJ, Sherry AD, Malloy CR, Berger JP, Li C. Inhibition of cardiac lipoprotein utilization by transgenic overexpression of angptl4 in the heart. *Proceedings of the National Academy of Sciences of the United States of America*. 2005;102:1767-1772
107. Ge H, Yang G, Huang L, Motola DL, Pourbahrami T, Li C. Oligomerization and regulated proteolytic processing of angiopoietin-like protein 4. *The Journal of biological chemistry*. 2004;279:2038-2045
108. Yin W, Romeo S, Chang S, Grishin NV, Hobbs HH, Cohen JC. Genetic variation in angptl4 provides insights into protein processing and function. *The Journal of biological chemistry*. 2009;284:13213-13222
109. Sukonina V, Lookene A, Olivecrona T, Olivecrona G. Angiopoietin-like protein 4 converts lipoprotein lipase to inactive monomers and modulates lipase activity in adipose tissue. *Proc Natl Acad Sci U S A*. 2006;103:17450-17455
110. Staiger H, Haas C, Machann J, Werner R, Weisser M, Schick F, Machicao F, Stefan N, Fritsche A, Haring HU. Muscle-derived angiopoietin-like protein 4 is induced by fatty acids via peroxisome proliferator-activated receptor (ppar)-delta and is of metabolic relevance in humans. *Diabetes*. 2009;58:579-589
111. Smart-Halajko MC, Kelley-Hedgepeth A, Montefusco MC, Cooper JA, Kopin A, McCaffrey JM, Balasubramanyam A, Pownall HJ, Nathan DM, Peter I, Talmud PJ, Huggins GS. Angptl4 variants e40k and t266m are associated with lower fasting triglyceride levels in non-hispanic white americans from the look ahead clinical trial. *BMC medical genetics*. 2011;12:89
112. Blich M, Golan A, Arvatz G, Sebbag A, Shafat I, Sabo E, Cohen-Kaplan V, Petcherski S, Avniel-Polak S, Eitan A, Hammerman H, Aronson D, Axelman E, Ilan N, Nussbaum G, Vlodavsky I. Macrophage activation by heparanase is mediated by tlr-2 and tlr-4 and associates with plaque progression. *Arteriosclerosis, thrombosis, and vascular biology*. 2013;33:e56-65
113. Chang SF, Reich B, Brunzell JD, Will H. Detailed characterization of the binding site of the lipoprotein lipase-specific monoclonal antibody 5d2. *J Lipid Res*. 1998;39:2350-2359
114. Pulinilkunnil T, Qi D, Ghosh S, Cheung C, Yip P, Varghese J, Abrahani A, Brownsey R, Rodrigues B. Circulating triglyceride lipolysis facilitates lipoprotein lipase translocation from cardiomyocyte to myocardial endothelial lining. *Cardiovasc Res*. 2003;59:788-797
115. Foy JM, Furman BL. Effect of single dose administration of diuretics on the blood sugar of alloxan-diabetic mice or mice made hyperglycaemic by the acute administration of diazoxide. *Br J Pharmacol*. 1973;47:124-132

116. Pratz J, Mondot S, Montier F, Cavero I. Effects of the k+ channel activators, rp 52891, cromakalim and diazoxide, on the plasma insulin level, plasma renin activity and blood pressure in rats. *The Journal of pharmacology and experimental therapeutics*. 1991;258:216-222
117. Gil N, Goldberg R, Neuman T, Garsen M, Zcharia E, Rubinstein AM, van Kuppevelt T, Meirovitz A, Pisano C, Li JP, van der Vlag J, Vlodavsky I, Elkin M. Heparanase is essential for the development of diabetic nephropathy in mice. *Diabetes*. 2012;61:208-216
118. Ritchie JP, Ramani VC, Ren Y, Naggi A, Torri G, Casu B, Penco S, Pisano C, Carminati P, Tortoreto M, Zunino F, Vlodavsky I, Sanderson RD, Yang Y. Sst0001, a chemically modified heparin, inhibits myeloma growth and angiogenesis via disruption of the heparanase/syndecan-1 axis. *Clinical cancer research : an official journal of the American Association for Cancer Research*. 2011;17:1382-1393
119. Sambandam N, Abrahani MA, St Pierre E, Al-Atar O, Cam MC, Rodrigues B. Localization of lipoprotein lipase in the diabetic heart: Regulation by acute changes in insulin. *Arterioscler Thromb Vasc Biol*. 1999;19:1526-1534
120. Rodrigues B, Spooner M, Severson DL. Free fatty acids do not release lipoprotein lipase from isolated cardiac myocytes or perfused hearts. *Am J Physiol*. 1992;262:E216-223
121. Forcheron F, Basset A, Del Carmine P, Beylot M. Lipase maturation factor 1: Its expression in zucker diabetic rats, and effects of metformin and fenofibrate. *Diabetes Metab*. 2009;35:452-457
122. Josephs T, Waugh H, Kokay I, Grattan D, Thompson M. Fasting-induced adipose factor identified as a key adipokine that is up-regulated in white adipose tissue during pregnancy and lactation in the rat. *J Endocrinol*. 2007;194:305-312
123. Mendes O, Kim HT, Stoica G. Expression of mmp2, mmp9 and mmp3 in breast cancer brain metastasis in a rat model. *Clinical & experimental metastasis*. 2005;22:237-246
124. Zhang Y, Yeung MN, Liu J, Chau CH, Chan YS, Shum DK. Mapping heparanase expression in the spinal cord of adult rats. *The Journal of comparative neurology*. 2006;494:345-357
125. Tkachenko E, Elfenbein A, Tirziu D, Simons M. Syndecan-4 clustering induces cell migration in a pdz-dependent manner. *Circ Res*. 2006;98:1398-1404
126. Tkachenko E, Simons M. Clustering induces redistribution of syndecan-4 core protein into raft membrane domains. *The Journal of biological chemistry*. 2002;277:19946-19951
127. Pulinilkunnil T, An D, Ghosh S, Qi D, Kewalramani G, Yuen G, Virk N, Abrahani A, Rodrigues B. Lysophosphatidic acid-mediated augmentation of cardiomyocyte lipoprotein lipase involves actin cytoskeleton reorganization. *Am J Physiol Heart Circ Physiol*. 2005;288:H2802-2810

128. Ben-Zeev O, Doolittle MH, Davis RC, Elovson J, Schotz MC. Maturation of lipoprotein lipase. Expression of full catalytic activity requires glucose trimming but not translocation to the cis-golgi compartment. *J Biol Chem*. 1992;267:6219-6227
129. Wang Y, Puthanveetil P, Wang F, Kim MS, Abrahani A, Rodrigues B. Severity of diabetes governs vascular lipoprotein lipase by affecting enzyme dimerization and disassembly. *Diabetes*. 2011;60:2041-2050
130. Hakoshima T, Shimizu T, Maesaki R. Structural basis of the rho gtpase signaling. *J Biochem*. 2003;134:327-331
131. Kim MS, Wang Y, Rodrigues B. Lipoprotein lipase mediated fatty acid delivery and its impact in diabetic cardiomyopathy. *Biochim Biophys Acta*. 2012;1821:800-808
132. An D, Rodrigues B. Role of changes in cardiac metabolism in development of diabetic cardiomyopathy. *Am J Physiol Heart Circ Physiol*. 2006;291:H1489-1506
133. Augustus AS, Kako Y, Yagyu H, Goldberg IJ. Routes of fa delivery to cardiac muscle: Modulation of lipoprotein lipolysis alters uptake of tg-derived fa. *American journal of physiology. Endocrinology and metabolism*. 2003;284:E331-339
134. Noh HL, Yamashita H, Goldberg IJ. Cardiac metabolism and mechanics are altered by genetic loss of lipoprotein triglyceride lipolysis. *Cardiovasc Drugs Ther*. 2006;20:441-444
135. Noh HL, Okajima K, Molkentin JD, Homma S, Goldberg IJ. Acute lipoprotein lipase deletion in adult mice leads to dyslipidemia and cardiac dysfunction. *Am J Physiol Endocrinol Metab*. 2006;291:E755-760
136. Rouis M, Lohse P, Dugi KA, Lohse P, Beg OU, Ronan R, Talley GD, Brunzell JD, Santamarina-Fojo S. Homozygosity for two point mutations in the lipoprotein lipase (lpl) gene in a patient with familial lpl deficiency: Lpl(asp9-->asn, tyr262-->his). *J Lipid Res*. 1996;37:651-661
137. Briquet-Laugier V, Ben-Zeev O, White A, Doolittle MH. Cld and lec23 are disparate mutations that affect maturation of lipoprotein lipase in the endoplasmic reticulum. *J Lipid Res*. 1999;40:2044-2058
138. Scow RO, Schultz CJ, Park JW, Blanchette-Mackie EJ. Combined lipase deficiency (cld/cld) in mice affects differently post-translational processing of lipoprotein lipase, hepatic lipase and pancreatic lipase. *Chem Phys Lipids*. 1998;93:149-155
139. Kennedy J, Katsuta H, Jung MH, Marselli L, Goldfine AB, Balis UJ, Sgroi D, Bonner-Weir S, Weir GC. Protective unfolded protein response in human pancreatic beta cells transplanted into mice. *PLoS One*.5:e11211
140. Eizirik DL, Cardozo AK, Cnop M. The role for endoplasmic reticulum stress in diabetes mellitus. *Endocr Rev*. 2008;29:42-61
141. Ma Y, Hendershot LM. Er chaperone functions during normal and stress conditions. *J Chem Neuroanat*. 2004;28:51-65
142. Zhang L, Lookene A, Wu G, Olivecrona G. Calcium triggers folding of lipoprotein lipase into active dimers. *J Biol Chem*. 2005;280:42580-42591

143. Thammavongsa V, Mancino L, Raghavan M. Polypeptide substrate recognition by calnexin requires specific conformations of the calnexin protein. *J Biol Chem*. 2005;280:33497-33505
144. Nguyen DT, Kebache S, Fazel A, Wong HN, Jenna S, Emadali A, Lee EH, Bergeron JJ, Kaufman RJ, Larose L, Chevet E. Nck-dependent activation of extracellular signal-regulated kinase-1 and regulation of cell survival during endoplasmic reticulum stress. *Mol Biol Cell*. 2004;15:4248-4260
145. Chevet E, Wong HN, Gerber D, Cochet C, Fazel A, Cameron PH, Gushue JN, Thomas DY, Bergeron JJ. Phosphorylation by ck2 and mapk enhances calnexin association with ribosomes. *Embo J*. 1999;18:3655-3666
146. Loirand G, Pacaud P. The role of rho protein signaling in hypertension. *Nat Rev Cardiol*. 2010;7:637-647
147. Gingis-Velitski S, Zetser A, Kaplan V, Ben-Zaken O, Cohen E, Levy-Adam F, Bashenko Y, Flugelman MY, Vlodavsky I, Ilan N. Heparanase uptake is mediated by cell membrane heparan sulfate proteoglycans. *J Biol Chem*. 2004;279:44084-44092
148. Shafat I, Vlodavsky I, Ilan N. Characterization of mechanisms involved in secretion of active heparanase. *J Biol Chem*. 2006;281:23804-23811
149. Wang F, Wang Y, Kim MS, Puthanveetil P, Ghosh S, Luciani DS, Johnson JD, Abrahani A, Rodrigues B. Glucose-induced endothelial heparanase secretion requires cortical and stress actin reorganization. *Cardiovasc Res*. 2010;87:127-136
150. Barash U, Cohen-Kaplan V, Dowek I, Sanderson RD, Ilan N, Vlodavsky I. Proteoglycans in health and disease: New concepts for heparanase function in tumor progression and metastasis. *FEBS J*. 2010;277:3890-3903
151. Keum E, Kim Y, Kim J, Kwon S, Lim Y, Han I, Oh ES. Syndecan-4 regulates localization, activity and stability of protein kinase c-alpha. *Biochem J*. 2004;378:1007-1014
152. Kuriyama S, Mayor R. A role for syndecan-4 in neural induction involving erk- and pkc-dependent pathways. *Development*. 2009;136:575-584
153. Avalos AM, Valdivia AD, Munoz N, Herrera-Molina R, Tapia JC, Lavandero S, Chiong M, Burridge K, Schneider P, Quest AF, Leyton L. Neuronal thy-1 induces astrocyte adhesion by engaging syndecan-4 in a cooperative interaction with alphavbeta3 integrin that activates pkcalpha and rhoa. *J Cell Sci*. 2009;122:3462-3471
154. Levy-Adam F, Feld S, Suss-Toby E, Vlodavsky I, Ilan N. Heparanase facilitates cell adhesion and spreading by clustering of cell surface heparan sulfate proteoglycans. *PloS one*. 2008;3:e2319
155. Oh ES, Woods A, Lim ST, Theibert AW, Couchman JR. Syndecan-4 proteoglycan cytoplasmic domain and phosphatidylinositol 4,5-bisphosphate coordinately regulate protein kinase c activity. *J Biol Chem*. 1998;273:10624-10629

156. Horowitz A, Murakami M, Gao Y, Simons M. Phosphatidylinositol-4,5-bisphosphate mediates the interaction of syndecan-4 with protein kinase c. *Biochemistry*. 1999;38:15871-15877
157. Vreys V, Delande N, Zhang Z, Coomans C, Roebroek A, Durr J, David G. Cellular uptake of mammalian heparanase precursor involves low density lipoprotein receptor-related proteins, mannose 6-phosphate receptors, and heparan sulfate proteoglycans. *The Journal of biological chemistry*. 2005;280:33141-33148
158. Wang Y, Zhang D, Chiu AP, Wan A, Neumaier K, Vlodavsky I, Rodrigues B. Endothelial heparanase regulates heart metabolism by stimulating lipoprotein lipase secretion from cardiomyocytes. *Arteriosclerosis, thrombosis, and vascular biology*. 2013;33:894-902
159. Wilsie LC, Gonzales AM, Orlando RA. Syndecan-1 mediates internalization of apoe-vldl through a low density lipoprotein receptor-related protein (lrp)-independent, non-clathrin-mediated pathway. *Lipids in health and disease*. 2006;5:23
160. Fuki IV, Kuhn KM, Lomazov IR, Rothman VL, Tuszynski GP, Iozzo RV, Swenson TL, Fisher EA, Williams KJ. The syndecan family of proteoglycans. Novel receptors mediating internalization of atherogenic lipoproteins in vitro. *The Journal of clinical investigation*. 1997;100:1611-1622
161. Fuki IV, Meyer ME, Williams KJ. Transmembrane and cytoplasmic domains of syndecan mediate a multi-step endocytic pathway involving detergent-insoluble membrane rafts. *The Biochemical journal*. 2000;351 Pt 3:607-612
162. Williams KJ, Fuki IV. Cell-surface heparan sulfate proteoglycans: Dynamic molecules mediating ligand catabolism. *Current opinion in lipidology*. 1997;8:253-262
163. Chen K, Williams KJ. Molecular mediators for raft-dependent endocytosis of syndecan-1, a highly conserved, multifunctional receptor. *The Journal of biological chemistry*. 2013;288:13988-13999
164. Nadav L, Eldor A, Yacoby-Zeevi O, Zamir E, Pecker I, Ilan N, Geiger B, Vlodavsky I, Katz BZ. Activation, processing and trafficking of extracellular heparanase by primary human fibroblasts. *Journal of cell science*. 2002;115:2179-2187
165. Wang F, Wang Y, Zhang D, Puthanveetil P, Johnson JD, Rodrigues B. Fatty acid-induced nuclear translocation of heparanase uncouples glucose metabolism in endothelial cells. *Arteriosclerosis, thrombosis, and vascular biology*. 2012;32:406-414
166. Nobuhisa T, Naomoto Y, Okawa T, Takaoka M, Gunduz M, Motoki T, Nagatsuka H, Tsujigiwa H, Shirakawa Y, Yamatsuji T, Haisa M, Matsuoka J, Kurebayashi J, Nakajima M, Taniguchi S, Sagara J, Dong J, Tanaka N. Translocation of heparanase into nucleus results in cell differentiation. *Cancer science*. 2007;98:535-540
167. Parish CR, Freeman C, Ziolkowski AF, He YQ, Sutcliffe EL, Zafar A, Rao S, Simeonovic CJ. Unexpected new roles for heparanase in type 1 diabetes and immune

gene regulation. *Matrix biology : journal of the International Society for Matrix Biology*. 2013;32:228-233

168. Van den Steen PE, Dubois B, Nelissen I, Rudd PM, Dwek RA, Opdenakker G. Biochemistry and molecular biology of gelatinase b or matrix metalloproteinase-9 (mmp-9). *Critical reviews in biochemistry and molecular biology*. 2002;37:375-536
169. Bhatt LK, Veeranjaneyulu A. A therapeutic approach to treat cardiovascular dysfunction of diabetes. *Experimental and toxicologic pathology : official journal of the Gesellschaft fur Toxikologische Pathologie*. 2012;64:847-853
170. Mishra PK, Chavali V, Metreveli N, Tyagi SC. Ablation of mmp9 induces survival and differentiation of cardiac stem cells into cardiomyocytes in the heart of diabetics: A role of extracellular matrix. *Canadian journal of physiology and pharmacology*. 2012;90:353-360